

# **Regulation of anti-viral CD8<sup>+</sup> T cells in the liver**

Peter D. Krueger  
Middleburg, Virginia

B.S., Molecular Biology, Fairfield University, May 2008

A Dissertation Presented to the Graduate Faculty of the University of Virginia in  
Candidacy for the Degree of Doctor of Philosophy

Department of Microbiology

University of Virginia  
March 2015

---

---

---

---

---

## **Abstract**

The liver is a unique organ in that its immune repertoire promotes a tolerogenic environment in response to continuous exposure to immunogenic material arriving in the intestinal blood. This hyporesponsive state leaves the liver vulnerable to chronic infections, such as HCV. Impaired T cell responses correlate strongly to HCV persistence; however, little is known about the cellular and molecular mechanisms contributing to T cell dysfunction. We demonstrate that during hepatotropic viral infection, liver-resident CD103<sup>+</sup> DCs upregulate costimulatory receptors and present Ag to induce effective anti-viral CD8<sup>+</sup> T cell responses. Furthermore, virally infected Batf3<sup>-/-</sup> mice, which lack CD103<sup>+</sup> DCs in the liver, exhibit a three-fold reduction in the proliferative response of Ag-specific CD8<sup>+</sup> T cells. Limiting DC migration out of the liver does not significantly alter CD8<sup>+</sup> T cell induction to viral infection, indicating that CD103<sup>+</sup> DCs initiate CD8<sup>+</sup> T cell responses *in situ*. Moreover, we examine local arbiters of CD103<sup>+</sup> DC activation during hepatotropic viral infection. The liver maintains two independent group 1 ILC subsets, CD49b<sup>+</sup> natural killer (NK) cells and CD49a<sup>+</sup> ILC1. Liver-resident CD49a<sup>+</sup> ILC1 constitutively express high levels of the inhibitory receptor NKG2A, suggesting they are contributing to liver immune tolerance. Viral infection in the NKG2A<sup>-/-</sup> mouse exhibits a sustained increase in the proliferative response of both adoptively transferred and endogenous anti-viral CD8<sup>+</sup> T cells. NKG2A<sup>-/-</sup> CD49a<sup>+</sup> ILC1 express elevated levels of IFN $\gamma$ , a proinflammatory mediator of DC maturation, and liver-resident CD103<sup>+</sup> DCs isolated from NKG2A<sup>-/-</sup> mice are capable of priming anti-viral CD8<sup>+</sup> T cells to a greater degree than their wild-type counterparts. In summary, we demonstrate for the first time that liver-resident CD103<sup>+</sup> DCs are the major APCs

supporting anti-viral CD8<sup>+</sup> T cell priming directly within the liver parenchyma, and that NKG2A<sup>+</sup>CD49a<sup>+</sup> ILC1 dampen DC activation by limiting IFN $\gamma$  production via NKG2A signaling. Taken together, these data help elucidate how the liver suppresses anti-viral immune responses and raises the possibility for an exciting therapeutic approach for developing next generation vaccines, i.e. targeting Ag to hepatic CD103<sup>+</sup> DCs while inhibiting ILC1 NKG2A signaling in order to induce a more robust and sustainable CD8<sup>+</sup> T cell response to hepatotropic viral infection.

## Acknowledgements

My time at the University of Virginia has been an incredible intellectual and personal journey. One could argue it started 20 years ago, in the summer of 1995, when I first set foot in a *Xenopus* research laboratory at Gilmer Hall. My brother-in-law Paul was finishing his own Ph.D., and I remember many late nights with young grad students conversing in spirited tones about the thrilling life of science. Looking back on my childhood, it is obvious that spending a few weeks every summer with my sister Liesel and her husband left a lasting impression on how I view education, and science. Their passion for honesty, truth, and humble skepticism has been inspirational in my development, and I look up to them as standards by which to imitate. It is my firm belief that without their continuing support throughout my life, I would be neither the individual, nor the scientist that I have become. For this, I am thankful.

If I have learned one thing during my doctoral studies, it is that growth takes time. I began my graduate career in Young Hahn's lab with ambitious motivation to work, and to discover. Indeed, like an untrained jockey, it was within a few yards of the gate that I quickly fell short. In looking back on those early years of graduate school I gracefully realize that it was only with the extraordinary help of so many people here in the Carter Center for which I have been able to accomplish this degree.

First and foremost, Young's unwavering patience allowed me to learn how to slow down, to grow into a scientist. I cannot ask for a more talented and supportive mentor, and for

her, I am eternally grateful. I am also thankful to those who gave their time and energy to my education, especially my committee members, all of whom have supported and guided me during the course of my studies. In addition, I want to express my gratitude for Tom Braciale's influence. It has been a privilege experiencing science with him, most particularly in our joint lab meetings, where his obvious joy for the scientific method has been motivational. I would also like to thank Taeg Kim, whose support over the years has been unlimited, and who undeniably taught me almost all of the immunology techniques I know today.

Over the years I have had the privilege of working alongside phenomenal graduate students, especially Rob Tacke and Sowmya Narayanan. Scientific research is hard, and without motivated and collaborative lab mates, it would be near impossible. Thank you all for making my time in the Hahn lab fun and intellectually stimulating.

Lastly, I would like to thank both my mother, whose charisma and overall passion for life has helped define who I am, and my wife, whose persevering support and generosity are gifts I will always consider more than I deserve.

*This thesis is dedicated to my parents, Tom and Trauti, who exemplify the value of hard work, and to my wife, Elsie, whose kindness has no limit*

## Table of Contents

Abstract.....	iii
Acknowledgements.....	v
Table of Contents.....	viii
List of figures.....	ix
Abbreviations.....	xi
 CHAPTER 1: Introduction.....	1
 CHAPTER 2: Statement of rationale and purpose.....	27
 CHAPTER 3: Liver-resident CD103 <sup>+</sup> dendritic cells prime anti-viral CD8 <sup>+</sup> T cells <i>in situ</i> .....	31
 CHAPTER 4: Liver-resident NKG2A <sup>+</sup> CD49a <sup>+</sup> ILC1 mediate anti-viral CD103 <sup>+</sup> DC activation.....	73
 CHAPTER 5: Conclusions and future directions.....	121
 Literature Cited.....	132

## **List of Figures**

**Fig. 3.1.** Liver-resident conventional dendritic cell (DC) subsets.

**Fig. 3.2.** Phenotype of naïve liver-resident conventional DCs.

**Fig. 3.3.** Hepatic resident CD103<sup>+</sup> exhibit enhanced priming capability *in vitro*.

**Fig. 3.4.** Batf3<sup>-/-</sup> livers lack CD103<sup>+</sup> and CD8α<sup>+</sup> DCs.

**Fig. 3.5.** Batf3<sup>-/-</sup> mice exhibit decreased antigen-specific CD8<sup>+</sup> T cell numbers during Ad-OVA infection.

**Fig. 3.6.** Antigen-specific T cells in the liver have similar CD25 and IFNγ expression in the absence of CD103<sup>+</sup> DCs.

**Fig. 3.7.** Batf3<sup>-/-</sup> mice exhibit decreased antigen-specific CD8<sup>+</sup> T cell numbers during MCMV-Ova infection.

**Fig. 3.8.** Similar OT-I numbers detected in C57BL/6 and Batf3<sup>-/-</sup> livers at 1 dpi.

**Fig. 3.9.** Hepatic antigen-specific T cells are primed *in situ* during Ad-OVA infection.

**Fig. 3.10.** Hepatic resident CD103<sup>+</sup> DCs exhibit maturation and enhanced priming capability at 12 hpi.

**Fig. 4.1.** CD49a<sup>+</sup> ILC1 are the major liver-resident ILC subset in the steady-state.

**Fig. 4.2.** Group 1 ILCs activate liver-resident DCs during Ad-OVA infection.

**Fig. 4.3.** Hepatic-resident CD49a<sup>+</sup> ILC1 express elevated NKG2A.

**Fig. 4.4.** Enhanced hepatic-resident DC numbers with enhanced priming by CD103<sup>+</sup> DCs in NKG2A<sup>-/-</sup> mice during Ad-OVA infection.

**Fig. 4.5.** Liver-resident DCs lack NKG2A but express Qa1b.

**Fig. 4.6.** Similar viral-load in NKG2A<sup>-/-</sup> livers at 3 dpi with Ad-OVA.

**Fig. 4.7.** Enhanced CD49a<sup>+</sup> ILC1 number and IFN $\gamma$  production in NKG2A<sup>-/-</sup> livers during Ad-OVA infection.

**Fig. 4.8.** NKG2A<sup>-/-</sup> liver-resident group 1 ILC exhibit no differences in IFN $\gamma$  production after IL-12 and IL-18 restimulation.

**Fig. 4.9.** Enhanced antigen-specific CD8<sup>+</sup> T cells in NKG2A<sup>-/-</sup> livers during Ad-OVA infection.

**Fig. 4.10.** NKG2A<sup>-/-</sup> mice exhibit increased hepatic CD8<sup>+</sup> T cells during Ad-OVA infection.

**Fig. 4.11.** NKG2A<sup>-/-</sup> mice exhibit increased hepatic IFN $\gamma$ <sup>+</sup> and CD107a<sup>+</sup> CD8<sup>+</sup> T cells during Ad-OVA infection.

**Fig. 4.12.** Enhanced tissue damage and cellular infiltrate in NKG2A<sup>-/-</sup> livers during Ad-OVA infection.

## Abbreviations

Ab	antibody
Ad	adenovirus
Ad-OVA	adenovirus-ovalbumin
Ag	antigen
APC	antigen presenting cell
B6	C57BL/6
Bim	BCL-2-interacting mediator of cell death
BM	bone marrow
BSA	bovine serum albumin
CAR	coxsackie adenovirus receptor
CD	cluster of differentiation
CDP	common dendritic cell progenitors
CFSE	5- (and 6)-carboxyfluorescein diacetate succinimidyl ester
cLN	coeliac and hepatic lymph node
CLP	common lymphoid progenitor
DAP	DNAX activation protein
DC	dendritic cell
DLN	draining lymph node
DNA	deoxyribonucleic acid
EDTA	ethylenediaminetetraacetic acid
Eomes	eomesodermin
FACS	fluorescence-activated cell sorter
FBS	fetal bovine serum
FcR	Fc receptors
Flt	Fms-like tyrosine kinase 3
FX	coagulation factor 10
GM-CSF	granulocyte-macrophage colony-stimulating factor
GrB	granzyme B
HBV	hepatitis B virus
HCV	hepatitis C virus

H&E	hematoxylin and eosin
HEPES	N-2-hydroxyethylpiperazine-N'-2-ethanesulfonic acid
HIV	human immunodeficiency virus
HLA	human leukocyte antigen
HSC	hepatic stellate cell
IFN	interferon
IL	interleukin
ILC	innate lymphoid cell
ILC1	innate lymphoid cell 1
iLN	inguinal lymph node
IMDM	Iscoe's modified Dulbecco's medium
i.p.	intraperitoneal
ITIM	immunoreceptor tyrosine-based inhibition motif
IU	infectious unit
i.v.	intravenous
KLRG1	killer-cell lectin-like receptor subfamily G, member 1
LN	lymph node
LSEC	liver sinusoidal endothelial cells
LT	lymphotoxin
MACS	magnetic-activated cell sorting
MCMV	murine choriomeningitis virus
MDP	macrophage dendritic cell progenitor
2-ME	2-mercaptoethanol
MEL-14	anti-L-selectin
MFI	mean florescent intensity
MHC	major histocompatibility complex
NBCS	newborn calf serum
NK	natural killer cell
NKG2	killer cell lectin-like receptor
NKP	natural killer cell progenitors
OCT	optimal cutting medium

OVA	ovalbumin
p	probability
PBS	phosphate-buffered saline
PCR	polymerase chain reaction
PFU	plaque-forming unit
PLP	periodate-lysine-paraformaldehyde
rAD	recombinant adenovirus
RBC	red blood cell
RNA	ribonucleic acid
RT-PCR	reverse transcriptase polymerase chain reaction
T-bet	T-box transcription factor
TCR	T-cell receptor
TGF	tumor growth factor
TH	helper T-cell
TLR	Toll-like receptor
TNF	tumor necrosis factor
TRAIL	TNF-related apoptosis-inducing ligand

## **Chapter 1: Introduction**

### **HCV and CD8<sup>+</sup> T Cell Dysfunction**

Chronic infections with the hepatitis C virus (HCV) are a major global health issue, where approximately 170 million people are infected worldwide (1). Only a minority of HCV patients is able to clear the virus spontaneously, where 70% of infected individuals develop a chronic infection in the liver (2). Numerous studies have shown that the generation of a vigorous and sustained T cell response strongly correlates both with those patients capable of spontaneous viral clearance and sustained responders completing the traditional peg-IFN $\alpha$  and ribavirin therapy (3). Conversely, chronic infection correlates with late, transient, weak, or narrowly focused T cell responses (4). Indeed, experimentally infected chimpanzees elimination of HCV coincides with the appearance of virus specific CD8<sup>+</sup> T cells in the liver (5). Although the exact mechanisms by which HCV-specific CD8<sup>+</sup> T cells control viral replication are not completely understood, general anti-viral CD8<sup>+</sup> T cell dysfunction is mainly characterized by an impaired proliferative capacity and the loss of anti-viral effector functions, i.e. secretion of IL-2 and IFN $\gamma$  (6, 7). The bulk of research investigating how HCV is able to evade CD8<sup>+</sup> T cell mediated clearance has focused on T-cell exhaustion and deletion. The intrinsic features of HCV-CD8<sup>+</sup> T cell dysfunction, including high expression of inhibitory receptors, i.e. PD-1 and Tim-3, as well as extrinsic contributions, i.e. elevated levels of IL-10 and high rate of viral escape, greatly influence the outcome of HCV infections (8, 9). However, little is known about the initial induction of anti-viral CD8<sup>+</sup> T cells, including the exact site and process of anti-viral CD8<sup>+</sup> T cell encounter with its specific

Ag (4). It is therefore necessary to more fully understand the initiation of CD8<sup>+</sup> T cell responses to viral infections in the liver.

### **CD8<sup>+</sup> T Cell Priming in the Liver**

Immunologically, the liver is an interesting tissue as it receives blood highly concentrated in foreign antigen arriving from the gastrointestinal tract (from the esophagus to the colon). Due to this constant influx of immunogenic material, i.e. degraded bacterial products and oral antigens, the liver has evolved to avoid unwarranted immune activation that would lead to hyper-inflammation and tissue damage (10-12). The most compelling evidence for hepatic immune tolerance is that in many mammalian species, the transplantation of the liver across a MHC difference does not result in rejection, which is not the case for other whole organ transplants, such as kidney, lungs and heart (13, 14). It is thought that many hepatotropic pathogens, i.e. HCV and malaria, are able to establish persistence by taking advantage of the liver's intrinsic suppression of its local immune repertoire, including cytotoxic CD8<sup>+</sup> T cells (1). Additionally, the anatomy of the liver is unique in that the liver sinusoidal endothelial cells (LSEC) are fenestrated, leading to a dramatic loss in blood pressure (5-fold) when compared to other tissues (15). Moreover, approximately 30% of the body's volume of blood flows through the liver every minute, with less than a third coming from the arterial supply (16). Although the liver is a major site of metabolic activity, where the products of digestion are processed, plasma proteins synthesized, and dangerous foreign chemicals detoxified, the considerably low concentration of oxygenated arterial blood keeps the liver in a hypoxic state (16).

There is a considerable range of literature detailing how the liver is able to suppress the local immune activation. In general, the cytokine milieu in the liver is anti-inflammatory in nature, including high levels of IL-10, TGF $\beta$ , retinoic acid, and prostaglandins, many of which are critical for suppressing innate immune cell activation (17-19). The liver is also considered an important site for peripheral and oral tolerance to the adaptive arm of the immune system, most notably CD8<sup>+</sup> T cells (20-23). It is debated as to whether the liver promotes traditional peripheral CD8<sup>+</sup> T cell tolerance, i.e. clonal deletion of auto-reactive T cells evading thymic selection, or simply that naïve CD8<sup>+</sup> T cells in the liver are poorly activated, leading to decreased proliferation and/or hastened cell death (24-26). Nonetheless, over the past two decades there have been great strides in understanding the many different cellular players controlling CD8<sup>+</sup> T cell dysfunction in the liver.

David Rubinstein and Peter Lipsky first demonstrated in 1986 that non-hematopoietic LSECs can present Ag to naïve T cells *in vitro* (27). Although it was not until 14 years later when Percy Knolle convincingly established that LSECs can cross-present acquired antigen to naïve CD8<sup>+</sup> T cells, albeit leading to poor effector functions, as measured by decreased IL-2 and IFN $\gamma$  production (28). Since then, a number of reports have firmly established that LSECs are efficient scavenger cells that express low levels of MHC-II in the steady-state and are considered the primary liver-resident APC to prime naïve CD8<sup>+</sup> T cells under non-inflammatory conditions (29-32). LSECs express high levels of PD-L1, but have not been shown to upregulate CD80/CD86 or express IL-12 (32, 33). Using a

transgenic mouse model in which the Ag is presented in the liver, and adoptively transferring naïve CD8<sup>+</sup> T cells specific for that Ag, demonstrated that liver primed CD8<sup>+</sup> T cells display a unique CD25<sup>low</sup>CD54<sup>low</sup> phenotype that was associated with increased expression of the pro apoptotic protein BCL-2-interacting mediator of cell death (Bim) and caspase-3 (34). An intriguing report has recently suggested that during the first 18 hours of viral infection LSECs, mediated by trans-signaling of IL-6, prime naïve anti-viral CD8<sup>+</sup> T cells to initially express high levels of GrB, yet die by 48 hpi (35). These data for the first time demonstrate LSECs priming anti-viral CD8<sup>+</sup> T cells to exhibit a robust effector function, as measured by their ability to express cytolytic proteins and kill cellular targets, albeit still exhibiting low levels of IFN $\gamma$  expression. Taken together, it is possible that LSECs mediate induction of naïve CD8<sup>+</sup> T cells exhibiting unique effector function, notably enhanced GrB expression, that ultimately leads to T cell tolerance, where Bim is the critical initiator of T cell death in the liver.

In addition to the contribution of LSECs in mediating CD8<sup>+</sup> T cell tolerance, other non-hematopoietic liver parenchymal cells have been reported to present Ag in the steady-state. Although they express low levels of MHC-I, hepatocytes can contact circulating lymphocytes directly through endothelial fenestrations (36). Naïve CD8<sup>+</sup> T cells primed by hepatocytes *in vitro* undergo initial clonal expansion, but are eventually eliminated owing to a lack of sufficient co-stimulation followed by Bim and caspase-dependent apoptosis (34). It is also possible that hepatocytes kill activated CD8<sup>+</sup> T cells by the process of suicidal emperipolesis, or cell-into-cell invasion (37). In this study the authors demonstrated that naïve auto-reactive CD8<sup>+</sup> T cells are rapidly eliminated in the liver

after intra-hepatic activation, whereby the activated T cells actively invade hepatocytes, entering the endosomal/lysosomal compartment to be degraded. In addition to hepatocytes and LSECs, the liver-resident pericytes (stellate cells) account for 8% of total liver cells, and store 80% of total body retinoic acid as cytoplasmic lipid droplets (38). Stellate cells have been demonstrated to prevent T cell IL-2R upregulation, and subsequent activation, via high expression of CD54 (30). Another report has suggested that stellate cells are able to initiate NKT priming using CD1d presentation of lipid motifs (38). This same investigation found that stellate cells are able to process and present antigen on MHC-I to induce CD8<sup>+</sup> T cell proliferation, although there was no data presented on the function or survival of these cells, and no follow up work has yet to validate these results.

The ability for non-hematopoietic cells acting as APCs to mediate peripheral CD8<sup>+</sup> T cell tolerance *in situ* has been firmly established. However, it is known that the liver is capable of switching from a hyporesponsive state to a pro-inflammatory environment during hepatotropic infections (39-41). The liver-resident cellular players controlling this immunological switch are still not well investigated. Moreover, the site of naïve CD8<sup>+</sup> T cell priming leading to efficient pathogen clearance, such as HCV, is an important point of interest for investigators attempting to more fully understand the requirements for potent anti-viral CD8<sup>+</sup> T cell responses. Dendritic cells (DC) are well characterized professional APCs, and have been shown to be essential for naïve CD8<sup>+</sup> T cell priming in many infection models. For this reason, liver-resident DCs may be important in

mediating anti-viral immunity in the liver. As such, hepatic DCs are discussed in later sections.

### **DC Development**

Dendritic cells (DC) were first discovered by Ralph Steinman and Zanvil Cohn in the late 1970s, for which Steinman was awarded the 2011 Nobel Prize in Physiology or Medicine (42, 43). DCs' towering role in immunology was not fully appreciated at first, however their proficient ability to present Ags and potently initiate the adaptive immune response is now indisputable. Today, the contribution of DCs in both robust immunogenicity and induction to tolerance has led to their intense investigation as potential targets in vaccine development and suppressive therapies.

DCs are short-lived hematopoietic cells that are constantly being replaced by blood-derived precursors produced in the bone marrow (40). Adoptive transfer studies of DC precursors into irradiated animals have helped establish the diversity of murine DC subsets in the steady-state. DCs are broadly classified into two major subsets; conventional DCs (cDC) and plasmacytoid DCs (pDC). Both pDCs and cDCs can be derived from clonal common lymphoid progenitors (CLP) and clonal common myeloid progenitors (CMP), although on a per cell basis CLPs are more efficient at generating thymic DCs, whereas CMPs preferentially give rise to splenic and LN resident DCs (44-48). The commitment of myeloid precursors to the mononuclear phagocyte lineage is thought to occur at the macrophage dendritic cell progenitor (MDP) stage, the immediate precursors to spleen macrophages, lymphoid-resident and nonlymphoid tissue-resident

cDCs, and pDCs (49). For MDPs to generate DCs, they first differentiate into common dendritic cell progenitors (CDP), which notably have no developmental potential for macrophage differentiation and are considered the first dedicated DC progenitor in the bone marrow (BM) (50).

CDPs are thought to give rise to both pDCs and the pre-classical dendritic cell (pre-cDC) (51, 52). pDCs accumulate mainly in the blood and lymphoid tissues and enter the lymph nodes (LN) through the blood circulation (53, 54). pDCs express low levels of the alpha X integrin CD11c and MHC-II in the steady-state. The most prominent attribute of pDCs is that they produce high levels of type-I IFN upon recognition of foreign nucleic acids by either TLR7 or TLR9. pDCs are able to acquire the capacity to present foreign antigen, although are thought to be less efficient APCs than their cDCs counterpart (53, 54). Pre-cDCs lack MHC-II, express CD11c and are able to differentiate into MHC-II<sup>+</sup> tissue-resident cDC subsets.

Currently the DC field discriminates cDCs by their tissue location, i.e. lymphoid versus nonlymphoid residency (henceforth annotated simply as DCs). Lymphoid resident DCs both differentiate and spend their entire existence within lymphoid tissues, i.e. spleen and LNs, and consist mainly of two subsets; CD8 $\alpha$ <sup>+</sup> and CD11b<sup>+</sup> DCs (55). Nonlymphoid resident DCs represent approximately 1-5% of tissue cells, depending on the organ, and also consist of two major subsets; CD103<sup>+</sup> and CD11b<sup>+</sup> DCs. CD103<sup>+</sup> DCs share their origin and function with lymphoid resident CD8 $\alpha$ <sup>+</sup> DCs, where both subsets preferentially reside at the tissue-environment interface (56, 57). Indeed, splenic CD8 $\alpha$ <sup>+</sup>

DCs are located in the marginal zone, an ideal location to filter blood antigens, whereas LN resident CD8 $\alpha$ <sup>+</sup> DCs are located in the subscapular sinus, the site of entry of afferent lymphatic vessels that drain nonlymphoid tissues (58, 59). CD8 $\alpha$ <sup>+</sup> and CD103<sup>+</sup> DCs require the Id2, IRF8 and Batf3 transcription factors (60), whereas CD11b<sup>+</sup> DCs require IRF2 and IRF4 for proper differentiation and survival (61, 62). CD8 $\alpha$ <sup>+</sup> and CD103<sup>+</sup> DCs express higher Flt3 levels when compared with CD11b<sup>+</sup> DCs, proliferate in response to Flt3 ligand, and are greatly reduced in Flt3L<sup>-/-</sup> mice (60). In addition to Flt3 signaling, nonlymphoid, but not lymphoid DCs require GM-CSF for survival (63-65). The expression of the alpha  $\epsilon$  integrin CD103 is dependent on the local production of GM-CSF and TGF $\beta$  (63, 66). However, CD103<sup>-/-</sup> mice appear to have no major defects in DC development. CD11b<sup>+</sup> DCs in both lymphoid and nonlymphoid tissues also depend on Flt3, albeit exhibit a less significant defect than CD8 $\alpha$ <sup>+</sup>/CD103<sup>+</sup> DCs in the Flt3<sup>-/-</sup> mice (67, 68). Unlike CD11b<sup>+</sup> DCs in nonlymphoid tissues and LNs, splenic CD11b<sup>+</sup> DCs can be discriminated into two populations; CD4<sup>+</sup> and CD4<sup>-</sup> DCs. CD4<sup>+</sup>CD11b<sup>+</sup> splenic DCs are derived from CDPs, whereas it is thought that CD4<sup>-</sup>CD11b<sup>+</sup> splenic DCs rise from circulating monocytes (69). Mice deficient in LT $\beta$ R have reduced numbers of splenic DCs, and transgenic overexpression of LT $\beta$ 1B2 leads to an enhanced splenic CD11b<sup>+</sup> DC population (70-72). However, the requirement of LT $\beta$ R signaling on LN resident CD11b<sup>+</sup> DCs has yet to be explored.

### **DC Migration and Activation**

Tissue-migratory DCs are located in the peripheral LNs, and refer to those DCs that have entered the DLN via the afferent lymphatics. Although constantly migrating to the LNs,

the majority of nonlymphoid resident DCs die once they arrive in the node. In the LNs, migratory DCs can be distinguished from resident DCs based on their CD11c<sup>int</sup>MHC-II<sup>hi</sup> expression, where the process of migration leads to upregulation of MHC-II and costimulatory receptors on the cell surface (73, 74). What controls DC trafficking is still not well understood, however DC migration to the DLNs requires expression of chemokine receptor CCR7 used to follow the CCL19/CCL21 gradient. Wild-type and CCR7 deficient mice have similar numbers of DCs in their peripheral organs, however the CD11c<sup>int</sup>MHC-II<sup>hi</sup> DC population is lacking in the CCR7<sup>-/-</sup> LNs, suggesting CCR7<sup>-/-</sup> DCs fail to migrate (75-77). It is important to note that recent evidence suggests that CCL19 and CCL21 might not only drive the migration of DCs but also more directly affect their ability to prime T cells. The exogenous addition of CCL19 to BMDCs induces their maturation as well as their ability to uptake antigen (78, 79). Although CCR7 is required for continuous migration of DCs in the steady-state, TLR stimulated DCs undergoing maturation significantly upregulate CCR7 expression (80, 81). During inflammatory conditions DCs also express the CXCR4 chemokine receptor, indicating a role for CXCL12 in driving DC egress from stressed tissues (81).

Upon activation via pathogen-associated molecules from damaged cells or by inflammation, CD8 $\alpha$ <sup>+</sup>/CD103<sup>+</sup> and CD11b<sup>+</sup> DCs upregulate maturation markers, including the costimulatory receptors CD40, CD70, CD80 and CD86, and exhibit enhanced expression of MHC-II. CD8 $\alpha$ <sup>+</sup>/CD103<sup>+</sup> DCs express similar TLR profiles, where they are the only DC subsets to express the double-stranded viral RNA sensor TLR3, and the *Toxoplasma gondii* protein sensor TLR11 (82-84). Upon acquiring Ag,

mature  $CD8\alpha^+/CD103^+$  DCs migrate to T cell zones in the LNs and spleen where they are poised to activate naïve T cells.  $CD8\alpha^+/CD103^+$  DCs have been shown to proficiently cross-present cell-associated Ags to naïve  $CD8^+$  T cells (85). Cross-presentation is defined by two critical factors that include, an endocytic pathway with low degradative potential, and a phagosome-to-cytosol transport step that allows both the transfer of Ags from the phagosome to the cytosol and their loading onto MHC-I molecules (86-88).  $CD8\alpha^+/CD103^+$  DCs also express more genes related to MHC-I presentation than do  $CD11b^+$  DCs, and they are the main source of IL-12 and IL-15, two cytokines involved in the differentiation of  $CD8^+$  T cells (89-91).  $Batf3^{-/-}$  mice, which lack  $CD8\alpha^+/CD103^+$  DCs have been shown to exhibit poor  $CD8^+$  T cell responses to viral infection (92).  $CD11b^+$  DCs also express unique TLR receptors, including the LPS sensor TLR4, the single-stranded viral RNA sensor TLR7, and the CpG DNA sensor TLR9, although further analysis as to whether these are truly specific for  $CD11b^+$  DCs is required.  $CD11b^+$  DCs are thought to have a predominant role in MHC-II presentation, and splenic  $CD4^+CD11b^+$  DCs express higher levels of genes coding for proteins involved in the MHC-II antigenic pathway than do  $CD8^+$  DCs (90). However, the lack of a genetic mouse model specific for the depletion of  $CD11b^+$  DCs has made it difficult to determine the exact contribution of these cells to  $CD4^+$  T cell priming *in vivo*. Lastly, although there are clear preferences, neither cross-presentation to  $CD8^+$  T cells nor direct-presentation to  $CD4^+$  T cells is exclusive to any one DC subset.

### **Hepatic DCs**

The liver maintains both pDC and cDC populations (16, 93). Although liver pDCs are found dispersed throughout the parenchyma, liver cDCs reside in the marginal zones of the portal triads where they are poised to sample Ags arriving from the intestinal blood (93). B220<sup>+</sup> pDCs are more abundant in the liver than they are in lymphoid tissues. Liver pDCs are a major source of IFN $\alpha$  in response to CpG treatment or viral infection with MCMV, however they exhibit 4-fold less IFN $\alpha$  production when compared to splenic pDCs experiencing the same treatment (93). Similarly, hepatic cDCs are considerably less immunogenic than splenic cDCs in the steady-state (94). Traditionally hepatic cDCs were characterized into three subsets; CD11b<sup>-</sup>CD8 $\alpha$ <sup>-</sup>, CD11b<sup>+</sup>CD8 $\alpha$ <sup>-</sup>, and CD11b<sup>-</sup>CD8 $\alpha$ <sup>+</sup> (93, 94). However, recent literature has described the presence of the nonlymphoid CD103<sup>+</sup> subset (95). CD8 $\alpha$ <sup>+</sup> hepatic DCs exhibit the capacity to promote the development of a Th1-type response through the production of large quantities of IL-12, whereas CD11b<sup>+</sup> DCs may promote Th2-type responses and Tregs through the production of IL-10 (94, 96). It is thought that the reduced ability for liver-resident DCs to drive T cell activation is due to their inherent immature state, most likely controlled by the constitutively high levels of IL-10, yet low levels of IL-12 present in the local cytokine milieu (94, 97, 98). Additional studies have shown that blocking IL-10, or treating mice with TLR9 agonists in vivo mediate enhanced liver-resident DC maturation, notably by their upregulation of costimulatory receptor expression, leading to an enhanced ability to present antigen and initiate naïve T cell activation (99).

Upon capturing Ags from the portal blood, liver-resident DCs transcytose into the space of disse and migrate toward the regional LNs (100). The coeliac and hepatic LNs are the

initial and primary sites draining hepatic DCs, although a small number of labeled hepatic cells can be found in the mesenteric LNs as well, suggesting that the liver lymphatics additionally drain to the intestinal nodes (101, 102). Hepatic DCs isolated from naïve livers express moderate levels of transcript for the chemokine receptors CCR1, CCR5, and CCR7, but high levels of CCR2. CCR1, CCR2, and CCR5 are all chemokine receptors responsible for migration of immature DCs to areas of inflammation (103, 104). Furthermore, hepatic DCs simulated overnight with GM-CSF significantly upregulate mRNA expression for CCR7 (103). Reports in the rat liver-transplant model have described a radio-resistant CD11b<sup>+</sup> DC population that drains the liver via the lymphatics to the regional DLNs (105). These investigations also suggest that the CD103<sup>+</sup> DCs are able to exit the liver tissue via the blood, however the work has yet to be validated. To date, the ability for hepatic DCs to prime T cells *in situ* has not been explored. Recent literature demonstrates that a chondronate liposome-sensitive population, that is neither a macrophage nor of non-hematopoietic origin, is responsible for priming anti-viral CD4<sup>+</sup> T cells *in situ* (106). It is highly feasible that a liver-resident DC is controlling CD4<sup>+</sup>, and possibly CD8<sup>+</sup> T cell induction directly in the liver tissue during hepatotropic viral infections.

### **DCs and HCV**

There are a number of reports investigating DCs isolated from the peripheral blood of infected HCV patients. In general DCs isolated from HCV patients exhibit an immature phenotype with functional defects when compared to DCs isolated from healthy individuals (107-109). More specifically, peripheral DCs from HCV patients generated

using GM-CSF and IL-4 expressed lower levels of CD86, and when cultured with allogeneic T cells, led to decreased levels of IFN $\gamma$  when compared to healthy donor cocultures (110). DCs derived from HCV patients also exhibit decreased expression of IL-12 p35 and p40 transcripts and failed to respond to TNF $\alpha$  stimulation (107). Human liver DCs have been shown to secrete more IL-10, as compared to skin DCs, and were also found to be less capable in stimulating T cell proliferation, leading to IL-10-producing T cells. In contrast, skin DC activation of T cells resulted in greater proliferation and more IFN $\gamma$  production (107). Interestingly, DC isolated from human hepatic LNs have also been characterized by high IL-10 production and low allogeneic stimulatory capacity, compared to human inguinal lymph node DC (111). Furthermore, DCs isolated from the livers of a murine model for chronic HBV carriers exhibited an immature phenotype and failed to stimulate allogeneic T cells (112). In summary, hepatic DCs are naturally held in a hyporesponsive state when compared to similar subsets isolated from lymphoid tissues, and DCs derived from the peripheral blood of patients infected with HCV appear to be suppressed when compared to DCs from healthy donors. These data suggests that therapeutics targeting the activation status of hepatic DCs may be required to induce robust anti-HCV CD8<sup>+</sup> T cell responses and efficient viral clearance in chronically infected patients.

### **ILC Subsets**

Innate lymphoid cells (ILCs) are a heterogeneous population of immune cells that can be divided into three populations, group 1 ILCs, group 2 ILCs, and group 3 ILCs, based on similarities in effector cytokine secretion and developmental requirements (113-115). All

ILCs differentiate from the common lymphoid progenitor (CLP), and are present throughout the body, albeit particularly enriched at mucosal surfaces (113). The earliest progenitor with restricted lineage potential for ILCs has been recently identified as the IL-7R $\alpha$ <sup>+</sup>CXCR6<sup>+</sup> common innate lymphoid progenitor (CLIP), which requires the basic leucine zipper transcription factor NFIL3 (116, 117). In recent years there has been an explosion of literature describing the diverse contributions of ILCs, where they are demonstrated to play important roles in early infection control, adaptive immune regulation, lymphoid tissue development, and tissue homeostasis and repair (113-115).

Although all three ILC groups are readily found in mucosal tissues, i.e. skin, lungs, and intestine, to date only group 1 ILCs has been described in the liver (118). Group 1 ILCs uniformly express the NKp46 and NK1.1 receptors in the mouse, and are specialized in their ability to produce IFN $\gamma$  (115, 118). The liver maintains two transcriptionally distinct group 1 ILC resident subsets, Tbet<sup>+</sup>Eomes<sup>+</sup> natural killer (NK) cells and Tbet<sup>+</sup>Eomes<sup>-</sup> ILC1 (118-123). It was previously thought that Tbet<sup>+</sup>Eomes<sup>-</sup> cells were immature NK cells that acquire Eomes upon maturation, however recent adoptive transfer studies have demonstrated that these two subsets are terminally differentiated with restricted progenitors in the BM (124). Indeed, Eomes<sup>-/-</sup> mice maintain ILC1 populations but lack mature NK cells, where Tbx21<sup>-/-</sup> mice lack ILC1 but maintain mature NK cells (119, 124). Importantly, although ILC1 express the IL-7R $\alpha$ , they do not require IL-7 for their development, which is in contrast to NK cells (119). However, ILC1 and NK cells both require IL-15 signaling, as they are equally absent in IL15<sup>-/-</sup> mice (119, 120).

## **NK Cell Development**

NK cells were initially defined as lymphocytes that could respond non-specifically to transformed or virally infected target cells without prior sensitization. The majority of NK cells develop in the BM from NK cell precursors (NKPs) while the development of NK cells also appears to occur at other lymphoid sites, such as the thymus and lymph nodes (125).

The earliest committed NKP population in the mouse BM is defined as CD49b<sup>-</sup>CD161<sup>-</sup>CD122<sup>+</sup> pre-pro NK cells, and is dependent on the Id2 transcription factor (126). NK cell development follows a stepwise acquisition of phenotypic markers, including the expression of CD161 (NK1.1), followed by CD94/NKG2 receptors, Ly49 receptors, and CD49b (DX5). The surface expression of CD11b and CD27 have been used to define the maturation status of mouse NK cells (127). Adoptive transfer experiments indicated a linear progression of maturation from CD11b<sup>-</sup>CD27<sup>+</sup> to CD11b<sup>+</sup>CD27<sup>+</sup> to CD11b<sup>+</sup>CD27<sup>-</sup>. With regards to function, CD11b<sup>-</sup>CD27<sup>+</sup> NK cells produce higher amounts of cytokines and show decreased cytotoxicity compared to CD11b<sup>+</sup>CD27<sup>-</sup> NK cells. In contrast, CD11b<sup>+</sup>CD27<sup>-</sup> NK cells express higher levels of killer-cell lectin-like receptor subfamily G, member 1 (KLRG1) and DNAX accessory molecule-1 (DNAM-1), which are induced following NK cell activation and proliferation (128). In addition, CD11b<sup>+</sup>CD27<sup>-</sup> NK cells are predominant in the spleen, while CD11b<sup>-</sup>CD27<sup>+</sup> NK cells are found at a greater proportion in the liver (129).

## **ILC1 Development**

In contrast with NK cells, which recirculate in the blood, ILC1 appear to be exclusively tissue-resident populations (118). ILC1 have been reported in the spleen, intestine, skin, uterus and liver; however, the majority of literature detailing ILC1 is limited to the liver

(118, 119, 123). Indeed, it was only in 2013 that Zhigang Tian's group first described the two subsets as distinct cell types (130). ILC1 appear phenotypically similar to immature NK cells in that they are predominantly CD27<sup>+</sup>CD11b<sup>low</sup>, and express high levels of TRAIL (118). As stated earlier, NK cells and ILC1 are transcriptionally distinct based on the unique expression of the transcription factors Tbet and Eomes; however further developmental cues driving ILC1 differentiation have yet to be thoroughly investigated. Moreover, it is not clear whether ILC1 derive from a circulating precursor that then differentiates upon arrival to a particular tissue, or if ILC1 are terminally differentiated before leaving the BM. There are important phenotypic differences between NK cells and ILC1 in the liver, where their full profiles are detailed more extensively in the ILC receptor section below. In general, the consensus in the field currently defines NK cells as CD122<sup>+</sup> CD49a<sup>-</sup> CD49b<sup>+</sup> TRAIL<sup>-</sup> CD127<sup>-</sup> CD69<sup>-</sup> CXCR3<sup>-</sup> CXCR6<sup>-</sup>, where CD122<sup>+</sup> CD49a<sup>+</sup> CD49b<sup>-</sup> TRAIL<sup>+</sup> CD127<sup>+</sup> CD69<sup>+</sup> CXCR3<sup>+</sup> CXCR6<sup>+</sup> best defines ILC1 (119-123).

### **NK Cell Licensing**

Immature NK cells that develop into mature NK cells have been characterized as either educated (also termed "licensed") or uneducated (131). An educated NK cell is defined as possessing full functional capacity; that is, NK cells responding to stimulation of activation receptor triggering. NK cell education appears to be regulated by signaling through MHC class I receptors, as NK cells lacking the expression of self-specific MHC class I receptors are functionally hyporesponsive (132, 133). Indeed, NK cells isolated from MHC class I deficient mice display a lower functional capacity compared to NK cells from wild-type mice. Furthermore, the ITIM (located on the cytoplasmic tail of MHC class I inhibitory

receptors) has been demonstrated to be critical for full functional capacity of NK cells (133). It has been recently reported that the ITIM binding phosphatase SHP-1 is required for efficient NK cell licensing. The engagement of self-specific MHC class I receptors is critical in maintaining NK cell tolerance in the face of activating receptor signaling. Taken together, host MHC class I molecules are crucial for regulating NK cell responsiveness and receptor repertoire formation. Although ILC1 express low levels of MHC-I specific receptors, the requirement or contribution of licensing on controlling the functional capacity of ILC1 has yet to be explored. Indeed, ILC1 may not employ MHC-I dependent signaling, using instead unique and uncharacterized mechanisms to establish tolerance to self.

At present, multiple models have been postulated for the functional maturation of NK cells (134, 135). Two of these models, arming and disarming, are based on the idea that NK cell licensing is aimed at ensuring that a functional NK cell is equipped with an appropriate inhibitory receptor whose signaling acts as a balance to regulate signaling via activating receptors. The arming model suggests that direct signaling through a MHC class I receptor supplies a signal that conveys functional capacity on the NK cell. The disarming model, similar to the concept of T cell exhaustion, suggests that, in the absence of inhibitory signaling via the MHC class I receptors, continual signaling through activating receptors renders the NK cell hyporesponsive. A more recently proposed third model, rheostat, satisfies both arming and disarming by suggesting that NK cells are educated through the strength of inhibitory receptor signaling, where tuning the NK cell with a higher inhibitory input can lead to better IFN $\gamma$  production, whereas potential granzyme release can be triggered

at lower input (136). To date, the data is insufficient to determine the precise role of each model in acquiring NK cell effector function.

### **Inhibitory and Activating Receptors on Liver Group 1 ILCs**

Besides the critical role for NK cell education through MHC class I receptors, NK cell activation is regulated by the balance of anti- and pro-activation signals mediated through the expression of inhibitory and activating receptors (Ly49 and NKG2). In mice, several NK cell receptors have been identified in the Ly49 receptor family (137). Ly49 receptors are type II transmembrane glycoproteins that are expressed on NK cells and form disulfide linked homodimers, with the majority of NK cells expressing one to four individual Ly49 receptors (138). Most of the 19 Ly49 receptors identified are inhibitory receptors (incorporating one ITIM) and recognize MHC class I and MHC class I-like molecules (139). In contrast, many of the ligands for the activating Ly49 receptors remain unknown. While structurally different from Ly49 receptors, a family of functional homologues of the Ly49 receptor molecules is expressed on human NK cells, referred to as the killer cell immunoglobulin-like receptor (KIR) family, and include both activating and inhibitory receptors. Importantly, there is a high genetic diversity in the KIR and Ly49 receptor families, where the genes vary in number, genomic organization, and allelic polymorphism among individual haplotypes (140). The expression of KIRs on human liver-resident ILC1 is currently unknown.

The NKG2 group of receptors are C-type lectin-like receptors that are present in both humans and mice (141). The NKG2 receptors include NKG2A, C, and E, (with NKG2F also expressed in humans) and are expressed at the surface as heterodimers with CD94. NKG2A

is a highly conserved inhibitory receptor, with two ITIMs present in the cytoplasmic tail, while NKG2C and E receptor engagement results in an activating signal via the adaptor protein DAP12 (142). In mice, NKG2A is expressed on most NK cells, while NKG2C and E are expressed at significantly lower frequencies. The ligand for NKG2A is the nonclassical MHC class I molecule Qa-1b (human HLA-E), whose expression is dependent on peptides derived from classical MHC class I molecules and thus acts as an overall measurement of MHC class I expression (143-145). Importantly, the KIR, Ly49, and NKG2 receptors on NK cells are stochastically expressed, resulting in heterogeneous expression of NK cell receptors on NK cells (146-148). While the level of Ly49 and KIR receptors appear to be stably maintained, NKG2 receptor expression is regulated by the inflammatory stimuli. In particular, IL-10 and TGF- $\beta$  are able to induce the expression of NKG2A (149). Thereby, the local microenvironment may influence group 1 ILCs receptor profiles, and unique responses to infection.

In general liver NK cells exhibit low expression of Ly49 receptors when compared to splenic NK cells, however, liver ILC1 express Ly49A, C/I, F, and G2 at even lower frequencies than liver NK cells (118). ILC1, unlike liver NK cells, lack the activating receptors Ly49D and Ly49H (118). Interestingly, ILC1 express high levels of Ly49E in comparison to both liver and splenic NK cells (118). Ly49E is unusual in that it is the only allelically identical Ly49 receptor in all mouse strains analyzed to date, and is highly expressed on fetal liver ILCs (150). The NKG2A transcript is the highest expressed NK cell receptor in liver-resident ILC1, as measured by gene arrays, where NKG2A expression is similar between liver and splenic NK cells (117). Importantly, NKG2A<sup>+</sup>Ly49<sup>-</sup> ILCs are hyporesponsive to IL-12/IL-18

stimulation in the liver compartment (129). In addition, adoptively transferred splenic NK cells exhibit phenotype and function more closely resembled to that of liver NK cells after migration into the liver (129). These results support a view that the liver environment can modify NK cell receptor expression and responsiveness to cytokine stimulation, and possibly is also driving the highly skewed ILC1 repertoire of NK cell receptors.

Although initially described as being part of the NKG2 group of receptors, NKG2D has very little homology to the other NKG2 receptors. NKG2D does not bind CD94, but is expressed as a homodimer on both mouse and human NK cells (151). NKG2D is an activating receptor, and recognizes ligands induced by cellular stress on virally infected or transformed cells (152). In mice, two isoforms of NKG2D are present, characterized by either a long or short cytoplasmic tail (142). The long-tailed isoform associates with the adaptor protein DAP10, while the short-tailed isoform can associate with DAP10 or DAP12. However, the expression of only the long-tailed isoform of NKG2D has been reported in humans. Notably, NKG2D is expressed by most NK cells and the cytokine environment can modulate the level of expression: IL-15 and TNF- $\alpha$  increase the expression of NKG2D whereas TGF $\beta$  downregulates NKG2D expression. Similar to the Ly49 receptors, NKG2D has limited expression on both liver NK cells and ILC1 (118).

The natural cytotoxicity receptors (NCR) are activating Ig-like transmembrane glycoproteins. While the NCR's consist of NKp30, NKp44, and NKp46 in humans, mice only express NKp46 and have a *NKp30/Ncr3* pseudogene. Unlike the previously defined NK cell receptors, NKp46 is equally expressed on all splenic and liver group 1 ILC subsets. NKp46

has two extracellular C2-type Ig-like domains, and a positively charged transmembrane region that associates with the ITAM containing CD3 $\zeta$ , FcR $\gamma$ , and DAP12 (153-155). It appears that the majority of normal resting target cells either express low level or no NCR-ligands (154). Although no cellular NCR ligands have been formally identified, the extracellular form of the intermediate filament protein vimentin may be associated with NKp46 cross-linking (156-158). NKp46 may also bind membrane-associated heparan sulfate proteoglycans and has been demonstrated to bind hemagglutinin-neuraminidase from influenza and sendai viruses, although these studies have not been validated (154, 159).

In addition to the canonical NK cell receptor profiles, liver-resident ILCs exhibit unique frequencies of activation makers, where it has been suggested ILC1 are constitutively held in an activated state. When compared to liver NK cells, ILC1 express high levels of TRAIL, CD69, CD44, CD160, and CD11c, but do not express CD62L (118).

### **Group 1 ILC Effector Function(s)**

The main group 1 ILC effector functions include direct cell killing of infected or transformed cells by perforin, granzymes, and TRAIL as well as the secretion of a variety of pro- and anti-inflammatory cytokines (160, 161). Notably, cytokine production by ILCs can be regulated through both activating and inhibitory receptors: activating receptor engagement leads to high production of IFN $\gamma$ , which plays a critical role in shaping the subsequent adaptive immune response. In addition to the cross-linking of activating receptor, ILC activation can also be induced by various cytokines, including type I IFNs, IL-2, IL-12, IL-15, and IL-18. Distinct ILC functions have been attributed to stimulation with different cytokines having

some synergistic effects. Type I IFNs lead to ILC cytotoxic activity, while IL-12 and IL-18 are potent inducers of IFN $\gamma$  production (142, 162). Although recent reports have described the requirement of type I IFN signaling on CD8<sup>+</sup> to avoid NKp46<sup>+</sup> NK cell mediated killing (219, 220). Liver ILC1, but not liver NK cells, express high levels of TRAIL and granzymes in the steady-state. Additionally, ILC1 functionally exhibit increased cytotoxic ability toward MHC-I deficient targets, although considerably decreased IFN $\gamma$  production after IL-12 and IL-18 stimulation.

### **Group 1 ILC Regulation of Hepatic Fibrosis**

Hepatic fibrosis is a wound-healing response to injury, commonly seen in chronic liver disease, and most often attributed to cell death within the liver. Fibrosis can be characterized by the formation of new blood vessels (angiogenesis), sinusoidal remodeling, and (stellate cell) expansion (163). Hepatic stellate cells (HSCs) are activated through the phagocytosis of apoptotic bodies and cell debris, leading to their differentiation, proliferation and pro-fibrotic progression. Therefore HSC death is believed to deliver anti-inflammatory and anti-fibrotic responses. Primarily, ILCs appear to be involved in HSC death and thereby depletion of ILCs leads to greater observed fibrosis in the murine fibrosis model. Quiescent HSCs are relatively resistant to apoptotic signals whereas activated HSCs are more prone to cell death. Of the many pro-apoptotic molecules investigated in activated HSCs, the expression of TRAIL may be an essential ILC1 mediated cytolytic ligand (164). Interestingly, activated HSCs also upregulate a variety of intermediate filaments, including desmin and vimentin, whose levels increase strongly between day 2 and 6 in primary cultures, but only vimentin levels remain consistently high (165). If extracellular vimentin is indeed an activating ligand

for the NCR NKp46, it would be an intriguing mechanism behind ILC mediated killing of HSCs.

### **Immunoregulatory Function of Group 1 ILCs**

Recently, our understanding of the role of group 1 ILCs in regulating the overall host immunity has increased dramatically. Through the production of a wide range of cytokines, ILCs contribute to enhance the immune response by triggering the activation of other innate immune cells and inducing the pro-inflammatory responses. ILCs also play a critical role in shaping the adaptive immune response through optimal T cell activation via direct cell-to-cell interaction with DC. As a result of ILC-DC crosstalk, DC mature and secrete cytokine/chemokines, resulting in productive T cell responses (162, 166). In contrast, ILCs have been shown to dampen the adaptive immune responses by selective killing of macrophages, DC, and/or T cells (167, 168). Thus, ILCs exhibit numerous functions to regulate host immunity. However, it is yet to be determined whether these multiple immunoregulatory functions of group 1 ILCs are differentially exerted by the two independent subsets.

Given a large proportion of ILCs in the liver lymphocyte populations, NK cells and ILC1 may help maintain liver tolerance through their interactions with various cell types.

Interestingly, NK cells cocultured with hepatocytes appear to alter the ability of DC to prime CD4<sup>+</sup> T cells, resulting in a regulatory T cell phenotype and function (149). In addition, DC induction of a T cell regulatory phenotype is dependent on NKG2A engagement on NK cells during coculture with hepatocytes (169). NKG2A expression is reportedly increased on NK cells from chronic HCV patients, suggesting a role for NKG2A in persistent viral infection

(170, 171). Indeed, NK cells from chronic HCV patients have been demonstrated to poorly activate DCs, compared to NK cells from healthy donors (172). Moreover, maturation and activation of monocyte-derived DCs were negatively modulated in the presence of HVC-NK and hepatoma cells, which were restored with the addition anti-NKG2A. It has also been reported that freshly isolated NK cells from HCV patients shows significant production of IL-10 (173). Although, recent evidence has suggested that NKp30 expressing NK cells may contribute to innate resistance and help reduce HCV infection (174).

In sum, these results indicate that liver ILCs contribute to limited antiviral T cell responses that facilitate pathogen persistence. Given the central role that DC play in driving a strong and competent antiviral immune response, and the ability of ILCs to influence DC maturation, dysregulation of the ILC-DC interaction in favor of a weakened T cell response would be an effective means of establishing a persistent infection. It is plausible that HCV and other persistent liver pathogens may take advantage of tolerance mechanisms already in place within the naïve liver, thus emphasizing the importance of investigating such mechanisms that contribute to a tolerogenic liver environment. The understanding of the mechanism(s) involved in the regulation of host immunity by ILCs is crucial for designing immunotherapeutic agents to boost host immunity to viral infection and tumor.

### **Recombinant Adenoviruses Vaccines For Chronic Viral Infections**

Human adenovirus (Ad), from the family *Adenoviridae*, was first isolated from adenoid tissue in the 1950s as novel viral agents associated with respiratory infections (175, 176). Since its discovery, over 100 Ad family members have been identified and characterized in a wide range of host organisms (177). The Ad virion is a non-enveloped icosahedral

capsid with a diameter of approximately 80-90nm, containing a linear double stranded DNA genome of 35kb (177). Of the Ad viruses, human Ad serotype 5 of subclass C (Ad5) has been most extensively characterized. Ad5 encodes 39 genes, which are classified as either early or late depending on whether they are expressed before or after DNA replication (178). Four early transcription units (E1a, E1b, E3, and E4) encode proteins required for transactivating other viral regions, modifying the host cellular environment, or altering the immune response. E2 encodes proteins directly involved in viral DNA replication. The late transcriptional units (L1-5) give rise to multiple mRNA and proteins via differential processing (179). The Ad capsid is comprised of several minor and three major capsid proteins: hexon is the most abundant structural component and constitutes the bulk of the protein shell; five subunits of penton form the penton base platform at each of the 12 capsid vertices to which the 12 fiber homotrimers attach (179). Entry of Ad into cells involves two distinct steps: attachment to a primary receptor molecule at the cell surface, followed by interaction with molecules responsible for virion internalization. In cell culture the coxsackie and adenovirus receptor (CAR) is the primary receptor for most Ad stereotypes, including Ad5, by which the fiber serves as the major viral attachment site (180). When i.v. administered to mice, Ad5 exhibit extreme propensity for hepatocyte infection, where greater than 99% of the virus is sequestered in the liver (181). The virus is primarily cleared by Kupffer cells, the liver-resident macrophages. However, elimination of Kupffer cells using clodronate liposomes results in higher hepatocyte infection with Ad5, suggesting additional mechanisms for liver sequestration (182). Recently it was demonstrated that vitamin K dependent coagulation factor X (FX) directly binds the Ad5 hexon protein, not fiber, via interaction between the

FX Gla domain and hypervariable regions of the hexon surface. Moreover, hepatocyte infection by FX-Ad5 complex is mediated through a heparin-binding exosite in the FX serine protease domain, and that FX-Ad5 affinity is 40-fold stronger than the reported affinity of Ad5 fiber for the CAR (183, 184).

Recombinant Ad viruses have been extensively investigated for their use as potential vaccine vectors delivering an antigen of choice in chronic viral infections, i.e. HCV and HIV (185, 186). Recent studies using the rAd in human HCV vaccine trials have demonstrated promising results, where patients' receiving rAd expressing HCV antigens have been shown to induce sustained T cell responses with robust effector function over extended periods of time (185). Recombinant Ad can be constructed either by insertion in, or replacement of, viral sequences, and can be replication-competent or defective. The principal sites of insertion or replacement of viral sequences with exogenous DNA are the early regions E1, E3, and E4. Replication defective Ad has lost the E1 region, and viral replication (via restored packaging) is rescued in E1-producing 293A cells. The studies in this report use a replication-defective recombinant Ad5 lacking the E1 and E3 regions, where the chicken ovalbumin protein under the hCMV promoter has been inserted into the E1 region (187).

## **Chapter 2: Statement of rational and purpose**

Unlike traditional mucosal tissues, e.g. skin, lungs, and intestine, the liver is neither in direct contact with the external environment, nor does it harbor a detectable population of commensal organisms. However, the liver does experience continuous exposure to foreign material arriving in the intestinal blood via the portal vein. Many of these degraded bacterial constituents and other alimentary products exhibit immunogenic features that normally induce pro-inflammatory responses. For this reason it is generally accepted that the liver actively maintains a tolerogenic environment. Indeed, due to its self-induced state of immunosuppression, yet lack of protective commensal populations found in mucosal tissues, the liver is unusually susceptible to invading pathogens. It has long been theorized that chronic and reoccurring infections, e.g. HCV and malaria, take advantage of the liver's vulnerable state by monopolizing the employed mechanisms that have evolved to limit perpetual pro-inflammatory stimuli and tissue damage.

The hepatitis C virus is notoriously successful at evading host immune responses required to efficiently clear the infection, so much so that there is still no effective vaccine available. Since its discovery in 1989, there has been incredible discoveries detailing the numerous biological features of HCV, and how it effectively shuts down anti-viral immune response in the liver. Although the advances over the past 25 years have been extraordinary, those of us investigating anti-viral immune responses in the liver appreciate how little is actually known about the contributing factors controlling liver tolerance. The signature of HCV persistence is its correlation with impaired anti-viral CD8<sup>+</sup> T cell responses. As such, the field of HCV immunology has primarily focused on

understanding intrinsic mediators of CD8<sup>+</sup> T cell suppression *in vitro*, i.e. upregulation of inhibitory receptors PD-1 and Tim-3. Due to lack of a small animal model for HCV, there is little information on the early events controlling anti-HCV CD8<sup>+</sup> T cell dysfunction *in vivo*. Hepatotropic viral mouse models have proven invaluable for studying CD8<sup>+</sup> T cell priming in the liver; however, the data thus far has focused on how non-hematopoietic cells induce anti-viral CD8<sup>+</sup> T cell deletion. Surprisingly, little is known about how the liver is capable of switching from a hyporesponsive state to an immunogenic environment capable of priming potent and sustainable anti-viral CD8<sup>+</sup> T cells. As such, it is the overarching goal of this thesis to more fully understand what liver-resident APCs are crucial for promoting robust anti-viral CD8<sup>+</sup> T cell priming, and how these APCs are naturally suppressed in the tolerogenic liver environment.

The recent development of new tools in DC biology has made it possible to dissect the diverse subsets of DCs, where previous studies have demonstrated that CD103<sup>+</sup> DCs preferentially cross-present acquired antigen to naïve anti-viral CD8<sup>+</sup> T cells in the influenza virus model. There have also been significant gains in understanding how DC activation/suppression is controlled by local cellular mediators, including NK cells.

Therefore, it is of interest to use modern immunological techniques to fully explore the diverse contribution of liver-resident CD103<sup>+</sup> DCs as APCs for anti-viral CD8<sup>+</sup> T cells, and to further analyze the control of liver-resident DC activation by local NK cells.

We hypothesize that CD103<sup>+</sup> DCs are potent inducers of effective CD8<sup>+</sup> T cell responses during hepatotropic viral infection. To determine the capacity of hepatic CD103<sup>+</sup> DCs to

prime naïve CD8<sup>+</sup> T cells during viral infection, we propose to utilize the Ad-OVA infection model in mice genetically deficient in CD103<sup>+</sup> DCs. We additionally propose to investigate the location(s) of DC mediated CD8<sup>+</sup> T cells priming by using mice genetically modified to limit DC migration from their resident tissues. Upon establishing that CD103<sup>+</sup> DCs contribute to the induction of anti-viral CD8<sup>+</sup> T cell responses, and their primary tissue of action, we propose to assess the functional regulation liver NK cells on DC activation during Ad-OVA infection. Recently, hepatic NK cells have been reclassified as group 1 innate lymphoid cells (ILCs), where the liver maintains two independent ILC resident subsets, CD49b<sup>+</sup> natural killer (NK) cells and CD49a<sup>+</sup> ILC1. Our lab previously demonstrated that liver-resident group 1 ILCs express elevated levels of the inhibitory receptor NKG2A in the steady-state. Previous reports have established that NKG2A signaling suppresses NK cell pro-inflammatory cytokine production; as such, we hypothesize that NKG2A signaling on CD49a<sup>+</sup> ILC1 is inhibiting robust DC activation via similar mechanisms. To determine the contribution of NKG2A<sup>+</sup>CD49a<sup>+</sup> ILC1 on controlling liver-resident DC fates during hepatotropic viral infection, we propose to utilize the Ad-OVA infection model in mice genetically deficient in NKG2A, where we will assess differences of CD103<sup>+</sup> DCs to promote anti-viral CD8<sup>+</sup> T cells.

Taken together, these results will help elucidate what hepatic APCs are required to promote potent anti-viral CD8<sup>+</sup> T cell induction, and how the liver has evolved to suppress the anti-viral immune response. This proposal raises the possibility for an exciting therapeutic approach for developing next generation vaccines, i.e. targeting

antigen to hepatic CD103<sup>+</sup> DCs while inhibiting ILC1 NKG2A signaling in order to induce a more robust and sustainable anti-viral CD8<sup>+</sup> T cell response in HCV patients.

## **Chapter 3: Liver-resident CD103<sup>+</sup> dendritic cells prime anti-viral CD8<sup>+</sup> T cells *in situ***

### **Abstract**

The liver maintains a tolerogenic environment to avoid unwarranted activation of its resident immune cells upon continuous exposure to food and bacterially derived antigens. However, in response to hepatotropic viral infection, the liver's ability to switch from a hyporesponsive to a pro-inflammatory environment is mediated by select sentinels within the parenchyma. To determine the contribution of hepatic DCs to activate naïve CD8<sup>+</sup> T cells, we first characterized resident DC subsets in the murine liver. Liver DCs exhibit unique properties, including the expression of CD8 $\alpha$  (traditionally lymphoid tissue specific), CD11b and CD103 markers. In both steady-state and following viral infection, liver CD103<sup>+</sup> DCs express high levels of MHC-II, CD80 and CD86, and contribute to the high number of activated CD8<sup>+</sup> T cells. Importantly, viral infection in the Batf3<sup>-/-</sup> mouse, which lacks CD8 $\alpha$ <sup>+</sup> and CD103<sup>+</sup> DCs in the liver, exhibits a three-fold reduction in the proliferative response of antigen-specific CD8<sup>+</sup> T cells. Limiting DC migration out of the liver does not significantly alter CD8<sup>+</sup> T cell responsiveness, indicating that CD103<sup>+</sup> DCs initiate the induction of CD8<sup>+</sup> T cell responses *in situ*. Collectively, these data suggest that liver resident CD103<sup>+</sup> DCs are highly immunogenic in response to hepatotropic viral infection and serve as a major APC to support the local CD8<sup>+</sup> T cell response. It also implies that CD103<sup>+</sup> DCs present a promising cellular target for vaccination strategies to resolve chronic liver infections.

### **Introduction**

The liver maintains a tolerogenic environment due to continuous exposure to bacterial constituents and food-derived antigens (188). As a result, hepatic microbial pathogens such as HCV and malaria often establish persistent infection in the liver (189). Impaired T cell responses have been reported to be associated with persistence of hepatotropic pathogens; however, little is known about the cellular and molecular basis for the immunoregulatory mechanisms linked to this persistence (4). Moreover, next generation vaccine design must focus on inducing robust and durable T cell responses to clear pathogens from the liver. Currently, adenovirus (Ad) has been considered for use as a vector for vaccines, since the recombinant Ad system is useful for delivery of antigen *in vivo* to generate vigorous antigen-specific immune responses (190). Thus, detailed analysis of the T cell responses to adenovirus infection in the liver may prove helpful toward better vaccine design and efficacy.

To generate CD8<sup>+</sup> T cells capable of clearing virus, naïve CD8<sup>+</sup> T cells must first come in contact with specialized antigen presenting cells (APCs) that have both processed viral antigen for MHC-I presentation and upregulated expression of costimulatory molecules (191, 192). Activation of naïve CD8<sup>+</sup> T cells by APCs of hematopoietic origin (e.g., DCs) in response to local infections typically occurs in secondary lymphoid organs draining the sites of pathogen entry and its replication (193). In contrast to mucosal tissues (i.e., skin, lung and gut), however, the contributing APCs and the location for CD8<sup>+</sup> T cell activation during hepatic viral infections are poorly understood. Antiviral CD8<sup>+</sup> T cells with competent effector activities (e.g., IFN $\gamma$ , granzyme) are generated in response to hepatic viral challenges (194, 195). Antigen presentation by non-

hematopoietic parenchymal cells (e.g., LSEC) has been demonstrated to prime naïve CD8<sup>+</sup> T cells, albeit resulting in activated T cells with poor effector functions (27-29, 38). Thus, the cell type(s) responsible for initiating the functional hepatic CD8<sup>+</sup> T cell response to viral infections remains unknown.

Conventional dendritic cells (DCs) are highly immunogenic APCs with the full capacity of capturing, processing and presenting antigens to naïve CD8<sup>+</sup> T cells (196, 197). Immature DCs use broadly conserved pattern recognition receptors (such as TLRs) to become activated (198-200). Upon activation/maturation, they upregulate antigen presenting molecules (i.e., MHC class I and II) and costimulatory molecules (i.e., CD80 and CD86) (201). Lymph node-resident DCs, which are commonly divided into CD11b<sup>+</sup> or CD8α<sup>+</sup> subsets, express high levels of MHC-II and costimulatory molecules upon activation and serve as potent APCs (193, 202). Conversely, CD11b and CD103 expression demarcate nonlymphoid tissue DCs subsets, with both populations primarily utilizing CCR7 for migration out of the parenchyma via the lymphatic conduit system to enter the regional LNs (60, 203). Lymphoid tissue-resident CD8α<sup>+</sup> and nonlymphoid tissue-resident CD103<sup>+</sup> DCs play crucial roles in priming CD8<sup>+</sup> T cells as they are functionally specialized in MHC class I-restricted cross-presenting antigen (204, 205). These DC subsets also share a developmental pathway requiring the transcriptional factor *Batf3* (206). Although the liver is believed to have DCs that patrol the tissue, the characterization of liver-resident DC subsets in a steady-state and their contribution to antiviral CD8<sup>+</sup> T priming have yet to be investigated.

In this study, we sought to determine the primary APC regulating the anti-viral CD8<sup>+</sup> T cell activation and differentiation in response to liver infections. Employing the hepatotropic adenovirus engineered to express ovalbumin (Ad-OVA) and the OT-I (OVA-specific) TCR transgenic CD8<sup>+</sup> T cell adoptive transfer model, we demonstrate that liver-resident CD103<sup>+</sup> DCs undergo maturation following Ad-OVA infection and are the major APCs capable of driving extensive CD8<sup>+</sup> T cell proliferation and effector differentiation following infection. Thus, our study identifies the hepatic CD103<sup>+</sup> DC subset as the primary cell type that establishes productive anti-viral CD8<sup>+</sup> T responses *in situ* to pathogens invading the liver. Implications of these findings in designing vaccine strategies and therapeutic venues for chronic hepatic viral infections (e.g. HCV) are discussed (185, 186, 207).

## **Materials and Methods**

### *Mice.*

All experiments used gender/aged matched male and female mice, 8-12 wks old. Thy1.2<sup>+</sup> C57BL/6 (B6, H-2<sup>b</sup>) and Thy1.1<sup>+</sup> OT-I TCR Tg (OT-I, H-2<sup>b</sup>) mice were purchased from Taconic Farms (Hudson, NY). CCR7<sup>-/-</sup> (H-2<sup>b</sup>, 29) mice were purchased from The Jackson Laboratory (Bar Harbor, ME). Batf3<sup>-/-</sup> (H-2<sup>b</sup>, 25) mice were kindly provided by Dr. Thomas Braciale (University of Virginia, Charlottesville, VA). All mice were housed in a pathogen-free facility and were tested routinely for mouse hepatitis virus and other pathogens. All mice were handled according to protocols approved by the University of Virginia Institutional Animal Care and Use Committee.

*Viruses.*

Replication-deficient recombinant adenovirus type 5 expressing ovalbumin (rAd5-OVA) under the human CMV promoter and lacking E1 and E3 genes were purchased from the Iowa Gene Transfer Vector Core (Iowa City, IA). Recombinant murine cytomegalovirus expressing ovalbumin (rMCMV-OVA) was gifted from Dr. Ann B. Hill (Oregon Health and Science University, Portland, OR). Mice were injected intravenously (i.v.) with  $2.5 \times 10^7$  IU Ad-OVA, or  $1 \times 10^4$  PFU MCMV-OVA.

*Liver, Spleen, and LN leukocyte isolation.*

Livers were perfused with PBS via the portal vein until fully blanched, then put on ice in Iscove's Modified Dulbecco's Medium (IMDM) supplemented with 10% newborn calf serum (NBCS). Whole livers were passed through a metal spleen screen and digested with 0.05% collagenase IV (Sigma-Aldrich, St. Louis, MO) for 30 min at 37°C.

Intrahepatic mononuclear cells were purified on a 21% Histodenz (Sigma-Aldrich, St. Louis, MO) gradient after centrifugation at 1250 x g for 20 min without braking. Spleens and lymph nodes were passed through a mesh spleen screen, followed by RBC lysis. All samples were washed and re-suspended in IMDM plus serum and leukocytes were counted via a hemocytometer.

*Flow cytometry and intracellular staining.*

Cells were labeled with Abs against CD45, B220, I-A/I-E, CD11c, CD11b, CD8 $\alpha$ , CD103, CD80, CD86, PD-L1, H2-D<sup>k</sup>, MHC-I<sup>SIINFEKL</sup>, Thy1.1, CD25, CD69, IFN $\gamma$ , and GranzymeB (all obtained from eBioscience, San Diego, CA). For cell surface labeling, 1

$1 \times 10^6$  cells were blocked with anti-CD16/CD32 (2.4G2; University of Virginia, Charlottesville, VA) and incubated with the corresponding Abs for 30 min at 4°C in staining buffer (PBS with 2% FBS and 0.1% NaN<sub>3</sub>). For cytokine staining,  $1 \times 10^6$  cells were incubated for 5 hours in IMDM supplemented with 10% FBS, 10 U/mL penicillin G, 2 mM L-glutamine, 5 mM β-mercaptoethanol, and 1 μL/mL of GolgiPlug/GolgiStop (BD Biosciences). OT-I cells were restimulated with 2 μg/mL SIINFEKL peptide (AnaSpec). After incubation, the cells were surface labeled as described above, fixed using Cytofix/Cytoperm (BD Biosciences) according to the manufacturer's instructions prior to intracellular IFN $\gamma$  staining. All samples were run on a BD FACS Canto II (BD Immunocytometry Systems, San Jose, CA) and analyzed using FlowJo software 8.8.6 (Tree Star Inc., Ashland, OR).

#### *Microscopic studies.*

For fluorescence microscopy, mouse liver tissues were perfused with 1 x PBS and periodate-lysine-paraformaldehyde (PLP) fixative, excised, incubated in PLP for 3 hours at 4°C, and passed over a sucrose gradient. Tissues were frozen in optimal cutting temperature (OCT) medium, sectioned at 5 μm thickness, blocked with 2.4G2 solution (2.4G2 supernatant containing anti-CD16/32, 10% each of chicken, donkey and horse serum, and 0.1% NaN<sub>3</sub>), and stained with Abs from Biolegend, eBioscience, Santa Cruz Biotechnology, and Sino Biological (Beijing, China). Confocal microscopy was performed on a Zeiss LSM-700, and data were analyzed using Zen 2009 Light Edition software (Carl Zeiss MicroImaging GmbH, Jena, Germany). For histology, mouse liver tissues were perfused with 1 x PBS, excised, incubated in 10% buffered formalin acetate

(Fisher Scientific) overnight at 4°C, washed with 70% ethanol and embedded in paraffin wax. Tissues were sectioned at 5 µm thickness and stained with hematoxylin and eosin. Light microscopy was performed on an Olympus BX51 microscope.

*Adoptive transfer of TCR transgenic T cells.*

CD8<sup>+</sup> T cells were isolated from the spleens and mesenteric lymph nodes of Thy1.1<sup>+</sup>OT- $\Gamma$ <sup>+</sup> mice using anti-CD8 $\alpha$  Ab-conjugated magnetic bead separation kits (Miltenyi Biotec). Cells were labeled with 1.8 µM CFSE for 8 min at room temperature, and transferred by i.v. injection into naïve Thy1.2<sup>+</sup> recipients. In the experiments that used splenectomized mice, recipients were i.v. treated with either 150 µg IgG or MEL-14 (anti-CD62L) one day prior to i.v. transfer of CFSE labeled OT-I T cells. One day post OT-I T cell transfer the mice were i.v. infected with 2.5 x 10<sup>7</sup> IU Ad-OVA or 1 x 10<sup>4</sup> pfu MCMV-Ova.

*DC isolation.*

Liver DCs were isolated from animals (C57BL/6/ 7-10 mice) either uninfected or infected with 2.5 x 10<sup>7</sup> IU Ad-OVA for 12 hr prior to analyses. CD11c<sup>+</sup> cells were first enriched by a positive selection using magnetic bead-based purification kits (Miltenyi Biotec). DCs were stained using antibodies for CD45, MHC-II, CD11c, B220, CD11b and CD103, and sorted by flow cytometry using a BD FACSVantage SE sorter at the Flow Cytometry Core Facility (University of Virginia, Charlottesville, VA). DCs were identified by staining with a cocktail of antibodies against CD45, MHC-II, CD11c, CD11b and CD103; plasmacytoid (pDCs) were determined by staining with antibodies against CD45, MHC-II CD11c and B220.

*In vitro priming of naïve OT-I T cells.*

FACS-sorted liver DCs were pulsed with either OVA (SIINFEKL) or  $\beta$ -gal (ICPMYARV) peptides at 0, 25, or 500 ng/mL for 20 min at 37°C and washed. DCs ( $4 \times 10^3$ ) and CFSE labeled OT-I T cells ( $4 \times 10^4$ ) were cultured together for 4 days at 37°C *in vitro*. FACS sorted liver DCs isolated 12 hpi from livers of infected C57Bl/6 mice were cultured with CFSE labeled OT-I T cells at a ratio of 1 to 10 for 4 days at 37°C *in vitro*. All DC:T cell coculture media included IMDM supplemented with 10% heat-inactivated HyClone FBS, 10 U/mL penicillin G, 2mM L-glutamine, 5 mM  $\beta$ -mercaptoethanol, 20 mM HEPES, and 100ug/mL Gentamycin (all from Invitrogen).

*Statistical analysis*

Student's *t* tests (two-tailed) were used to evaluate the significance of the differences. A value of  $p < 0.05$  was regarded as statistically significant. \* $p < 0.05$ , \*\* $p < 0.01$ , \*\*\* $p < 0.001$ .

**Results***Characterization of DC subtypes resident in the liver at steady-state.*

DCs are represented widely both in lymphoid (i.e. spleen, LNs) and nonlymphoid (i.e. lung, skin) tissues. Lymphoid DCs, such as CD11c<sup>hi</sup>MHC-II<sup>hi</sup>B220<sup>-</sup> splenic DCs, are conventionally defined by the surface expression of CD8 $\alpha$  or CD11b molecules. In contrast, a distinct DC subset in nonlymphoid tissues such as the lung, express CD103

( $\alpha$ E integrin, a ligand for E-Cadherin) rather than CD8 $\alpha$ , while another subset retains the CD11b<sup>+</sup> expression. To determine whether the liver displays characteristics of DC subsets from nonlymphoid tissue, we probed the diversity of DC populations in the liver by analyzing the expression of CD11b, CD103 and CD8 $\alpha$ . Gating strategies for analyzing liver resident DCs are shown in the Fig. 3.1. CD11c<sup>hi</sup>MHC-II<sup>hi</sup>B220<sup>-</sup> DCs resident in the livers of naïve mice could be first discriminated into CD11b<sup>+</sup>CD103<sup>-</sup>, CD11b<sup>-</sup>CD103<sup>+</sup> and CD11b<sup>-</sup>CD103<sup>-</sup> subsets (Fig. 3.2.A.; top panel), which were further distinguished based on CD8 $\alpha$  expression (Fig. 3.2.A.; lower panel). This analysis revealed that liver CD11b<sup>-</sup> DCs consist of four distinct subsets: CD103<sup>-</sup>CD8 $\alpha$ <sup>-</sup>, CD103<sup>+</sup>CD8 $\alpha$ <sup>-</sup>, CD103<sup>+</sup>CD8 $\alpha$ <sup>+</sup> and CD103<sup>-</sup>CD8 $\alpha$ <sup>+</sup> cells, suggesting that liver resident DCs segregate into subsets displaying unique cell surface markers with phenotypic characteristics of both lymphoid and nonlymphoid DCs. These findings suggest that the liver has the physiological properties of both lymphoid and nonlymphoid tissues, which are consistent with the view that the liver serves as a tertiary-lymphoid organ.

As most of the current emphasis in DC biology focuses on the unique differences between CD11b<sup>+</sup>CD103<sup>-</sup> and CD11b<sup>-</sup>CD103<sup>+</sup> subsets (henceforth designated as CD11b<sup>+</sup> and CD103<sup>+</sup> DCs, respectively), we limited our analysis to these two dominant liver DC populations. Accordingly, the CD103<sup>+</sup> DCs are the primary subset of naïve liver resident DCs by both percentage and total cell number (Fig. 3.2.B.).

*CD103<sup>+</sup> DCs localize to the portal tract and constitutively express costimulatory molecules.*

Early reports describing liver DCs often note their localization to the portal tracts of the liver parenchyma (208, 209). Consistent with these earlier observations, we found that CD103<sup>+</sup> DCs were most frequently localized around the portal tracts (Fig. 3.2.C.). The liver anatomy is unique in that the highest volume of blood flow comes directly from the gastrointestinal tract, entering from the portal veins. As this blood is highly concentrated in microbial products and other food antigen it is likely that liver-resident DCs may congregate closely to these gateways in order to sample newly arriving potential antigens, including pathogenic microorganisms.

Although murine liver DCs have been reported to exhibit a less mature phenotype than splenic DCs, the expression of MHC-II and costimulatory molecules (i.e., CD80 and CD86) are readily detectable on DCs in the liver (Fig. 3.2.D.) (94). Interestingly, PD-L1 expression is lower on CD103<sup>+</sup> liver resident DCs, when compared to the CD11b<sup>+</sup> subset, suggesting that CD103<sup>+</sup> cells may be less inhibitory as APCs, and thereby display increased capacity to support naïve lymphocyte activation (210).

*Liver resident CD103<sup>+</sup> DCs prime OT-I T cells in vitro with higher efficiency than CD11b<sup>+</sup> DCs.*

In view of the display of costimulatory ligands by hepatic DCs, it was of interest to assess their capacity to support the activation of antigen specific CD8<sup>+</sup> T cells. To this end we sorted hepatic DCs from the livers of uninfected donors into CD103<sup>+</sup> and CD11b<sup>+</sup> subsets and analyzed the capacity of these DCs to support proliferative expansion of naïve TCR Tg OT-I CD8<sup>+</sup> T cells *in vitro* following pulsing of the DC with varying concentrations

of the OT-I T cell ligand SIINFEKL peptide. As assessed by CFSE dilution, CD103<sup>+</sup> DCs stimulated more potent peptide dose-dependent proliferative responses than their peptide pulsed CD11b<sup>+</sup> DC counterparts (Fig. 3.3.A.). Compared to DC subsets, pDCs were least efficient in triggering CD8<sup>+</sup> T proliferation. This enhanced stimulatory capacity of CD103<sup>+</sup> DCs was also evident from the elevated numbers of total OT-I CD8<sup>+</sup> T cells recovered at the end of the *in vitro* culture (Fig. 3.3.B.). Taken together, these findings suggest that the hepatic CD103<sup>+</sup> DC subset in a steady-state displays an intrinsically enhanced capacity to present the processed antigenic peptides to naïve CD8<sup>+</sup> T cells when compared to CD11b<sup>+</sup> DCs.

*CD103<sup>+</sup> DCs are the major APCs for OT-I induction in the liver following adenovirus infection.*

The above findings suggested that liver resident CD103<sup>+</sup> DCs were potent APCs and potentially could serve as the primary APC to support CD8<sup>+</sup> T cell differentiation following exposure to a hepatotropic virus infection (e.g. high-dose of intravenous adenovirus). To examine the impact of CD103<sup>+</sup> liver resident DCs in response to infection we utilized mice deficient in the transcription factor *Batf3*, which is reported to be necessary for the development of the CD103<sup>+</sup> (and corresponding CD8 $\alpha$ <sup>+</sup>) DC lineage (206). As expected, *Batf3*<sup>-/-</sup> mice lacked both CD103<sup>+</sup> and CD8 $\alpha$ <sup>+</sup> liver resident DCs (Fig. 3.4.A.). Moreover, following adenovirus infection the expression of CD103<sup>+</sup> liver DCs was not increased (Fig. 3.4.), suggesting that this subset was not induced in response to Ad-mediated liver inflammation.

To explore the impact of CD103<sup>+</sup> DC deficiency on naïve CD8<sup>+</sup> T cells responding in the liver to virus infection, we adoptively transferred naïve CFSE labeled OT-I T cells into wild-type and Batf3<sup>-/-</sup> mice one day prior to i.v. infection with the replication-deficient recombinant adenovirus expressing the OVA gene. This administration route primarily results in virus infection of the liver, including hepatocyte and non-hepatocyte cell populations. Livers, spleens, and liver-draining and -non-draining lymph nodes were then analyzed at various time points after infection for accumulation of OT-I T cells and for CFSE dilution. OT-I T cells were not detectable in any site at 2 dpi (data not shown). Responding OT-I T cells to adenovirus were readily detectable at 3 dpi with the highest accumulation of T cells evident in the liver (Fig. 3.5.A.). By contrast, infected Batf3<sup>-/-</sup> T cell recipients displayed decreased frequency and total numbers of responding OT-I T cells in all tissues examined (Fig. 3.5.B-C.). Due to the defect in adenovirus replication, the virus clearance and titers cannot be directly assessed. Using quantitative real-time PCR to measure the message of adenovirus hexon protein showed no differences between the wild-type and Batf3<sup>-/-</sup> livers at 2 or 3 dpi (data not shown). Furthermore, we performed histological studies to assess liver damage. Notably, there was increased mononuclear cell infiltrates detectable in the wild-type compared to Batf3<sup>-/-</sup> livers at 3 dpi (Fig. 3.5.D.).

When the CFSE dilution profile of OT-I T cells responding in the wild-type and Batf3<sup>-/-</sup> T cell recipients was evaluated, we noted that the tempo of OT-I cell division was more rapid in the livers of wild-type mice. However, this accelerated CFSE dilution profile and OT-I T cell accumulation was not evident in the liver-draining lymph nodes of the

wild-type and *Batf3*<sup>-/-</sup> recipients (Fig. 3.5.E.) (101, 102). Activated (responding) OT-I T cells isolated from the livers of wild-type and *Batf3*<sup>-/-</sup> mice at 3 dpi display comparable levels and frequencies of the activation markers CD69 and CD25 (Fig. 3. 6.). Similarly, responding OT-I T cells isolated from the two liver sources demonstrated comparable capacity to secrete IFN $\gamma$  in terms of both cell frequency and MFI upon *in vitro* stimulation with cognate synthetic peptide epitope (Fig. 3.6.). Lastly, i.v. infection with MCMV-OVA, another hepatotropic virus, exhibits similar loss of OT-I T cell accumulation in the *Batf3*<sup>-/-</sup> livers with no significant differences in IFN $\gamma$  expression (Fig. 3.7.).

The pattern of responsiveness of transferred OT-I T cells in the livers of wild-type and *Batf3*<sup>-/-</sup> mice following adenovirus infection was not influenced by the cell inoculum dose of OT-I T cells transferred. Adoptive transfer of  $2 \times 10^6$  naïve OT-I T cells into wild-type and *Batf3*<sup>-/-</sup> mice (i.e. 10 fold higher cell inoculum dose than employed above) allows us to identify the transferred T cells as early as 1 dpi. At this early time point of infection, the frequency of transferred OT-I T cells in wild-type and *Batf3*<sup>-/-</sup> livers were comparable (Fig. 3.8.A-B.). Thus, the enhanced expansion of the adoptively transferred T cells observed in infected wild-type recipients was not due to a difference in homing efficiency to the livers of *Batf3*<sup>-/-</sup> mice.

*Liver resident DCs prime naïve OT-I T cells in situ.*

Upon activation, tissue-resident DCs upregulate CCR7 and follow the CCL19/21 chemokine gradient into the lymphatics to ultimately reside in secondary lymphoid

organs, particularly lymph nodes draining the site of antigen deposition in the target organ. Previous work from our laboratory implicated liver parenchymal cells (e.g. hepatocytes, LSECs) as APCs for antiviral CD8<sup>+</sup> T cells responding to virus infection of the liver (211). It was of interest to determine the contribution of liver resident DCs to the induction of CD8<sup>+</sup> T cell responses following adenovirus infection. In particular we wanted to ascertain whether liver DCs upon encountering viral antigen must migrate to secondary lymphoid organs in order to stimulate responses from naïve CD8<sup>+</sup> T cells trafficking through the sites. To explore this possibility we carried out adoptive transfer of naïve CCR7<sup>+</sup> OT-I T cells into CCR7<sup>-/-</sup> mice, which limit DC migration, and examined the proliferative expansion and tissue localization of the transferred T cells following IV adenovirus infection (212).

The frequency and absolute number of responding OT-I T cells were dramatically reduced in secondary lymphoid organs (e.g. spleen, liver draining LN etc.) of the CCR7<sup>-/-</sup> mice at 3 dpi, exhibiting ~10 fold decrease (Fig. 3.9.A.). The frequency and absolute number of OT-I T cells present in the liver was unaffected by CCR7 deficiency in the liver DCs (Fig. 3.9.B.).

In order to more directly assess *in situ* priming of CD8<sup>+</sup> T cells by hepatic CD103<sup>+</sup> DCs, we adoptively transferred naïve OT-I T cells into B6 and Batf3<sup>-/-</sup> mice that were first splenectomized and treated with anti-CD62L (MEL-14) antibody to eliminate naïve OT-I T cells from entering secondary lymphoid tissues. Splenectomized and MEL-14-treated wild-type mice exhibit increased hepatic OT-I accumulation at 3 dpi when compared to

either sham and isotype-treated or splenectomized and isotype-treated controls. The level of OT-I accumulation in the livers of splenectomized and MEL-14-treated  $Batf3^{-/-}$  mice increases to the level of sham and isotype-treated B6 livers, and is consistent with the differences seen in Fig. 3.5.C., where there are fewer numbers compared to the equally treated splenectomized and MEL-14 B6 livers (Fig. 3.9.C). Taken together, these data suggest that  $CD103^{+}$  DCs significantly contribute to the accumulation of liver OT-I T cells *in situ*.

*Liver  $CD103^{+}$  DCs are able to induce  $CD8^{+}$  T cell responses at the early time point of infection.*

As hepatic-resident DCs are capable of priming naïve OT-I's *in situ*, we next characterized the maturation status of DCs in the liver directly following infection. Although there is a difference in the frequency and numbers of  $CD11b^{+}$  and  $CD103^{+}$  DCs by 12 hpi, (Fig. 3.10.A-B.), hepatic  $CD103^{+}$  DCs exhibit the highest expression of MHC-II and the costimulation markers CD80 and CD86, common indicators of DC activation (Fig. 3.10.C.). Additionally, hepatic  $CD103^{+}$  DCs stained highest for MHC-I and MHC-I<sup>SIINFEKL</sup> by 12 hpi (Fig. 3.10.D.), suggesting they are the primary DCs presenting antigen during the early phase of viral infection. As a positive control for MHC-I<sup>SIINFEKL</sup> staining, total splenocytes were pulsed with SIINFEKL peptide for 20 min. at 37°C. LN DCs were below the limit of detection for MHC-I<sup>SIINFEKL</sup> at 12 h.p.i (data not shown).

To test if hepatic  $CD103^{+}$  DCs present endogenous viral antigen to naïve  $CD8^{+}$  T cells *in vitro*, we isolated liver DCs 12 hpi and cocultured the DCs with naïve OT-I T cells. After

4-day incubation, there were more CFSE diluted OT-I CD8<sup>+</sup> T cells in the CD103<sup>+</sup> DCs coculture when compared to the CD11b<sup>+</sup> DC stimulation (Fig. 3.10.E.). These results reinforce a critical role of CD103 DCs in antigen presentation at the early viral infection and contributing to prime CD8<sup>+</sup> T cells.

## Discussion

In the present study, we examined the role of liver resident CD103<sup>+</sup> DCs in the activation of naïve CD8<sup>+</sup> T cells and the site of their accumulation after activation in response to hepatic viral infection using a hepatotropic adenovirus infection model. The liver is believed to differ from other organs such as lung and skin, in that naïve CD8<sup>+</sup> T cells can be activated within the hepatic parenchymal site (213). Studies have demonstrated that non-hematopoietic antigen-presenting cells in the liver contribute to the induction of naïve CD8<sup>+</sup> T cell proliferation and differentiation. However, the role of hematopoietic cells, such as DCs, in processing and presenting local antigens to initiate the CD8<sup>+</sup> T cell response *in situ* has not been well established. *Batf3* is a transcription factor that controls the CD103<sup>+</sup>/CD8 $\alpha$ <sup>+</sup> DC development, and thereby *Batf3*-deficient (*Batf3*<sup>-/-</sup>) mice result in a selective loss of these subsets. *Batf3*<sup>-/-</sup> mice have been widely employed in studying DC biology and provide a unique and valuable experimental tool to investigate the contribution of CD103<sup>+</sup> DCs to anti-viral immunity *in vivo*. While there are potential caveats from using any global gene deficient transgenic, thus far we are not aware in the literature of any defect beyond the selective deficiency of this DC subset in the *Batf3*<sup>-/-</sup> mice. By employing *Batf3*-deficient mice, we demonstrated that liver-resident CD103<sup>+</sup> DCs play a critical role in the establishment of optimal CD8<sup>+</sup> T cell response to hepatic

adenovirus infection. In support of the dominant role as APCs in inducing anti-viral CD8<sup>+</sup> T cell responses, CD103<sup>+</sup> hepatic DCs displayed a superior capacity capable of processing and presenting virus-derived antigenic peptide to naïve CD8<sup>+</sup> T cells at a steady state and following infection. Lastly, we demonstrated that liver DC priming of naïve CD8<sup>+</sup> T cells occurs independently of CCR7-mediated DC egress, supporting the view that DCs can activate naïve CD8<sup>+</sup> T cells *in situ*. Our findings demonstrate for the first time that hematopoietic-driven hepatic DCs, in particular the CD103<sup>+</sup> DC subset, serve as the prominent APC in the liver in response to viral infections and induce antigen-specific CD8<sup>+</sup> T cell responses within the liver tissue early in infection.

Based on our finding that there is a decrease (3 fold) of accumulating OT-I CD8<sup>+</sup> T cells in the livers of Batf3<sup>-/-</sup> mice that received OT-I cells mice at 3 dpi of Ad-OVA infection compared to control B6 mice (Fig. 3.5.A.), it is likely that liver-resident CD103<sup>+</sup> DCs play a major role in induction and accumulation of antigen-specific CD8<sup>+</sup> T cells at the site of hepatic viral infection. Notably, there is a similar decrease of OT-I CD8<sup>+</sup> T cells accumulating in the non-draining iLNs and draining cLNs, but a far less significant loss of OT-I cells in the spleens of Batf3<sup>-/-</sup> mice. These results are likely due to the contribution of CD11b<sup>+</sup> DCs on OT-I accumulation in the secondary lymphoid tissues. It is also possible that splenic CD11b<sup>+</sup> DCs and/or additional APCs are better at priming than their lymph node counterparts but that they contribute to a lesser degree than those OT-I cells induced by CD8 $\alpha$ /CD103<sup>+</sup> DCs. Moreover, the proliferation index (P.I.) formula to measure OT-I divisions (Fig. 3.5.E,) indicates a significant decrease in the Batf3<sup>-/-</sup> livers, having less accumulation of CFSE<sup>low</sup> OT-I cells, which is only trending in

the lymphoid tissues. The proliferation index differences in the livers of control B6 and *Batf3*<sup>-/-</sup> mice suggest that resident CD103<sup>+</sup> DCs lead to sustained OT-I accumulation, and that non-CD103<sup>+</sup> APCs, such as CD11b<sup>+</sup> DCs and non-hematopoietic presenting cells, are either less efficient at priming, or more-likely induce unsustainable antigen-specific CD8<sup>+</sup> T cells. At 1 dpi there is no difference in the number of liver accumulating OT-I cells between the B6 and *Batf3*<sup>-/-</sup> mice, leading us to speculate that initial CD8<sup>+</sup> T cell priming is independent of CD103<sup>+</sup> DCs, but that at 3 dpi any remaining OT- T cells are greatly outnumbered by OT-I cells primed by resident CD103<sup>+</sup> DCs.

Infection of peripheral tissues (e.g., lung and skin) triggers the mobilization of tissue-resident DCs to egress out of the sites of pathogen entry and replication. These Ag-bearing migratory tissue-resident DCs arrive to the tissue-draining regional LNs where they participate in instructing naïve antigen-specific CD8<sup>+</sup> T cell activation and differentiation. In contrast, blood-borne pathogens are captured by phagocytic cells (e.g., DCs and macrophages) in the spleen, and antigen-specific CD8<sup>+</sup> T responses are initiated primarily by lymphoid tissue-resident DCs (i.e., CD8 $\alpha$ <sup>+</sup> DC). However, there is limited understanding as to how the inductive phase of CD8<sup>+</sup> T cell immune response is orchestrated in response to hepatotropic infections. Previously published reports have described hepatic-resident DCs, suggesting that the CD11b<sup>+</sup> subset is dominant in the liver (21, 25). However, our data shows that CD103<sup>+</sup> DCs represents the largest population of liver-resident DCs. Having optimized the isolation techniques and gating strategies, we believe our results most accurately represent liver-resident DC populations to date. We further demonstrated that the liver displays a distinct DC compartment in

which they harbor both CD103<sup>+</sup> and CD8 $\alpha$ <sup>+</sup> DCs along with the CD11b<sup>+</sup> subset and pDCs. This finding is in agreement with the view that the liver may inherently possess lymphoid-like features and serves as a tertiary lymphoid organ (106). This unique composition of DC network within the liver could support the T cell activation locally while permitting migratory DC-dependent T cell activation in the regional DLN after migration. As we see a decrease in hepatic DCs at 12 hpi, it is possible that these cells are either eliminated or migrate out of the parenchyma. Indeed, it is well established that initial contact between DC and T cells is sufficient to trigger the full activation and differentiation pathways. Thus we believe that the decrease in CD103<sup>+</sup> DC numbers after infection have a minimal impact on the onset of CD8<sup>+</sup> T cell priming in the liver. Migratory DCs employ *CCR7* to migrate out of infected tissues and trigger T cell proliferation in the DLN. By limiting DC egress and subsequent homing of the CD8<sup>+</sup> T cells primed by hepatic migratory DC in the DLN in *CCR7*<sup>-/-</sup> mice, our findings suggest that intrahepatic DCs are capable of activating CD8<sup>+</sup> T cell response to hepatotropic virus infection. Furthermore, limiting naïve OT-I T cells from entering secondary lymphoid organs by administering anti-CD62L antibody to splenectomized B6 and *Batf3*<sup>-/-</sup> mice demonstrate that hepatic CD103<sup>+</sup> DCs are a primary resident APC for induction of naïve CD8<sup>+</sup> T cell responses. It is possible that blocking naïve OT-I cell accumulation in the peripheral lymphoid organs prior to infection will increase their availability to hepatic APCs, accounting for the considerable increase of OT-I cells in splenectomized and anti-CD62L treated livers when compared to the sham and anti-IgG controls at 3 dpi. After i.v. administration of the replication-deficient Ad5 virus, the virus is primarily cleared by liver Kupffer cells with the majority of residual virus entering hepatocytes via factor

X/Ad5 complexes (182, 184). CD103<sup>+</sup> DCs (and possibly CD8 $\alpha$ <sup>+</sup> DCs) are predominantly localized within the marginal areas of the portal veins, where they are ideally poised to take up antigen from circulation and/or neighboring infected cells and present processed antigen to CD8<sup>+</sup> T cells *in situ*. At present, the extent by which intrahepatic priming of CD8<sup>+</sup> T cells is controlled by either CD8 $\alpha$ <sup>+</sup> DCs or CD103<sup>+</sup> DCs has yet to be determined. Of note, it is an intriguing possibility that intrahepatic CD8<sup>+</sup> T cell priming is carried out by CD8 $\alpha$ <sup>+</sup> DCs, whereas CD103<sup>+</sup> DCs initiate T cell response in the DLN after migration.

In contrast, OT-I CD8<sup>+</sup> T cells in the B6 wild-type mice appear to be activated in the spleen and iLNs with similar kinetics to those T cells activated in the liver and cLNs, but no activated OT-I T cells are observed in the spleen and iLNs of CCR7<sup>-/-</sup> mice. These results suggest that non-draining peripheral secondary lymphoid tissues depend on a CCR7<sup>+</sup> APC entering those sites (possibly coming from the liver via the blood). Moreover, fewer activated OT-I T cells in the CCR7<sup>-/-</sup> liver DLNs compared to those in wild-type mice suggest that either activated liver DCs utilize additional chemokine receptors when trafficking through their draining lymphatics, possibly CXCR4, or that antigen is brought to the draining nodes via alternative mechanisms.

The immunologically hyporesponsive (tolerogenic) microenvironment of the liver is necessitated by its continuous exposure to food and bacterially derived antigen. Liver-resident DCs localized in the vicinity of the portal veins are likely exposed to actively encounter material draining from the gut and circulation. However, unwarranted

activation to non-pathogenic antigens requires DCs to be under tight immune control to continuously maintain the 'normal' state. Our studies reported here demonstrate that resident DCs express significant amounts of PD-L1. Of note, the CD11b<sup>+</sup> subset preferentially expresses the greatest amount of this coinhibitory molecule. Our data argues that immediately following Ad-OVA infection, hepatic CD103<sup>+</sup> DCs significantly upregulate CD80, CD86 and MHC-II and are capable of inducing anti-viral CD8<sup>+</sup> T cell immune responses, whereas CD11b<sup>+</sup> DCs may provide counter-regulatory signals to CD103<sup>+</sup> DC-mediated T cell activation. This potential cross-talk between CD103<sup>+</sup> DCs and CD11b<sup>+</sup> DCs may control the threshold in the liver either to induce anti-viral immunity or to induce tolerogenic immune responses. Consistent with our previously published studies, intrahepatic CD8<sup>+</sup> T cells primed in Batf3<sup>-/-</sup> exhibit equally poor effector function as compared to those primed in B6 mice. This impaired CD8<sup>+</sup> T cell effector function might be reflected by additional factors controlling hepatic CD8<sup>+</sup> T cell responses in the liver compartment. Interventions utilizing anti-PD-L1 blockade agents could thus lead to an increase of T cell activation by these hepatic DCs (214). Collectively, these data suggest that liver-resident CD103<sup>+</sup> DCs may serve as critical regulators of immunity to intrahepatic antigenic challenges.

Although there have been substantial therapeutic agents toward curing chronic infection such as HCV, the current medical cost for treating chronic HCV patients is unsustainable. Therefore, vaccine development is necessary to protect the host from microbial infection. In particular, hepatotropic pathogens (i.e., HCV, malaria) exploit the immunosuppressive liver microenvironment and often establish persistent infection, resulting in severe liver

diseases including cirrhosis and hepatocellular carcinoma. Thus, it is crucial for understanding liver immunology and studying ways to generate effective immune responses. Given the ability of CD103<sup>+</sup> DCs to mount sustainable CD8<sup>+</sup> T cell responses specific to antigen *in situ* as described in this report, targeting of antigen to liver resident DCs (i.e. CD103<sup>+</sup> DCs) would be helpful in designing vaccine against hepatotropic pathogens and boost host immune responses to combat infection. In summary, our study highlights the prominent contribution of liver-resident CD103<sup>+</sup> DCs in initiating anti-viral CD8<sup>+</sup> T cell immune responses to hepatotropic infections. Further, this work opens up the possibility of targeting liver-resident CD103<sup>+</sup> DCs for potential vaccination strategies.

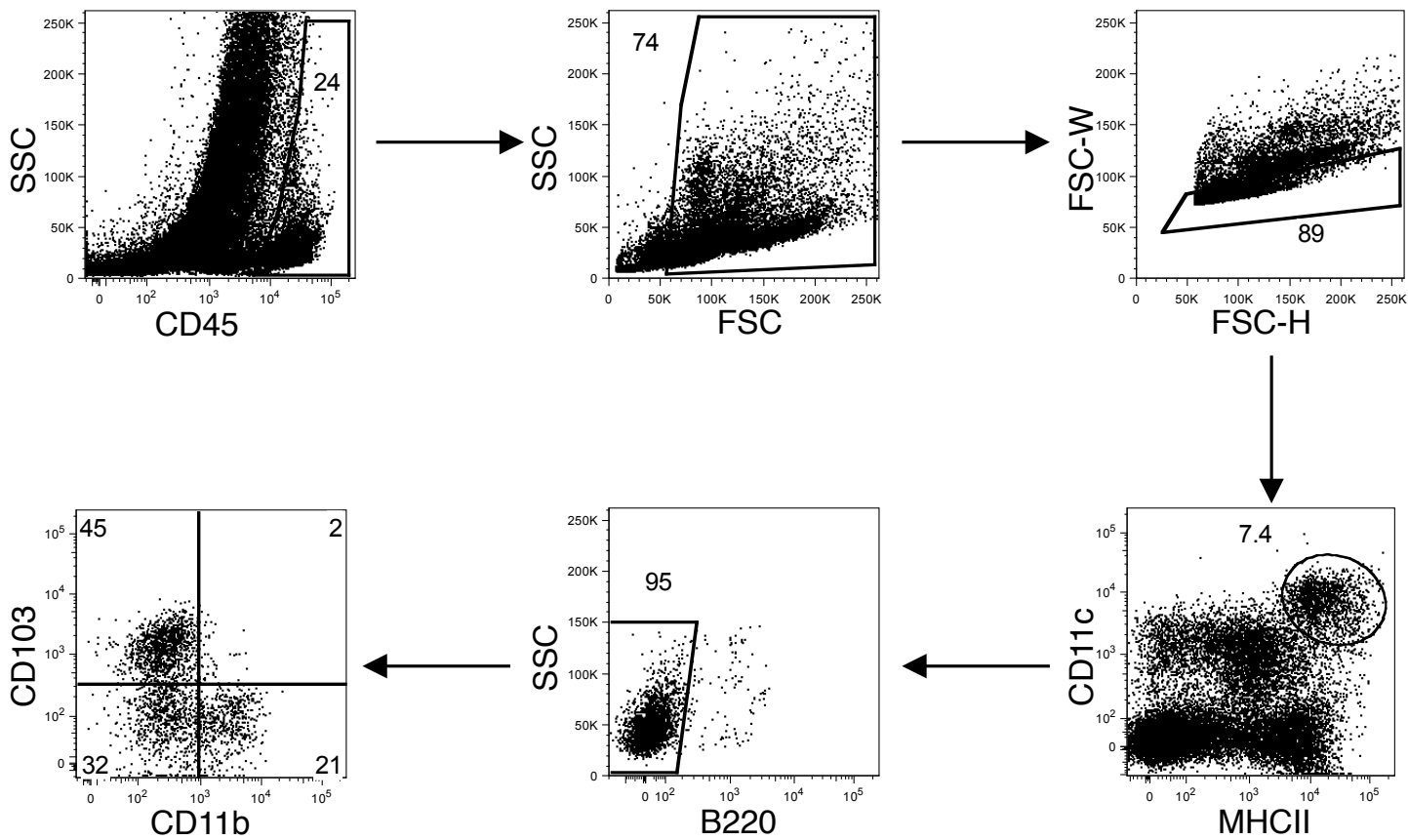
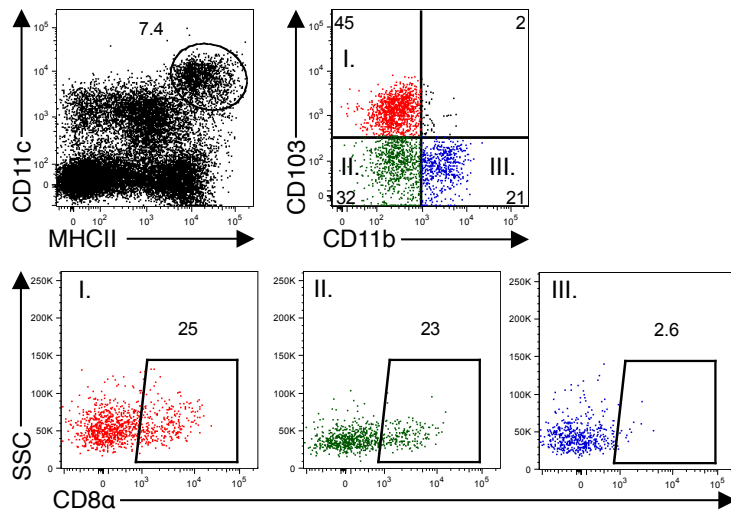
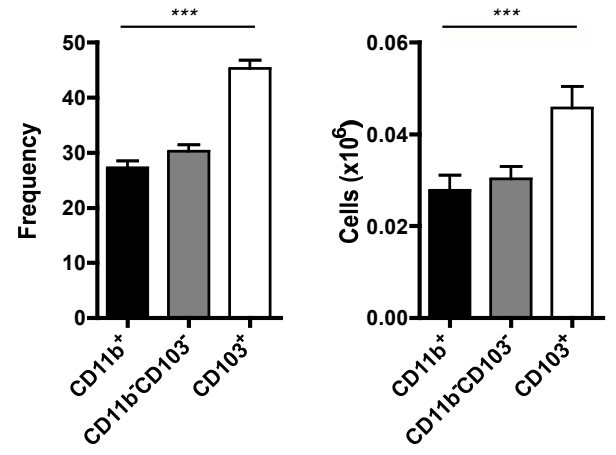


**Figure 3.1. Liver resident conventional dendritic cell (DC) subsets.** Representative dot plots for liver resident DCs gating strategy. 8-12 week old C57Bl/6 livers were collagenase digested and spun on a sedimentation gradient. CD11c<sup>hi</sup>MHCII<sup>hi</sup> DCs are gated from CD45<sup>+</sup> events, followed by debris and doublet exclusion. B220<sup>+</sup> cells are dumped to eliminate contaminating plasmacytoid DCs. Three DC subtypes are separated into CD11b<sup>-</sup>CD103<sup>+</sup>, CD11b<sup>-</sup>CD103<sup>-</sup> and CD11b<sup>+</sup>CD103<sup>-</sup> gates. Representative of 3 independent experiments.

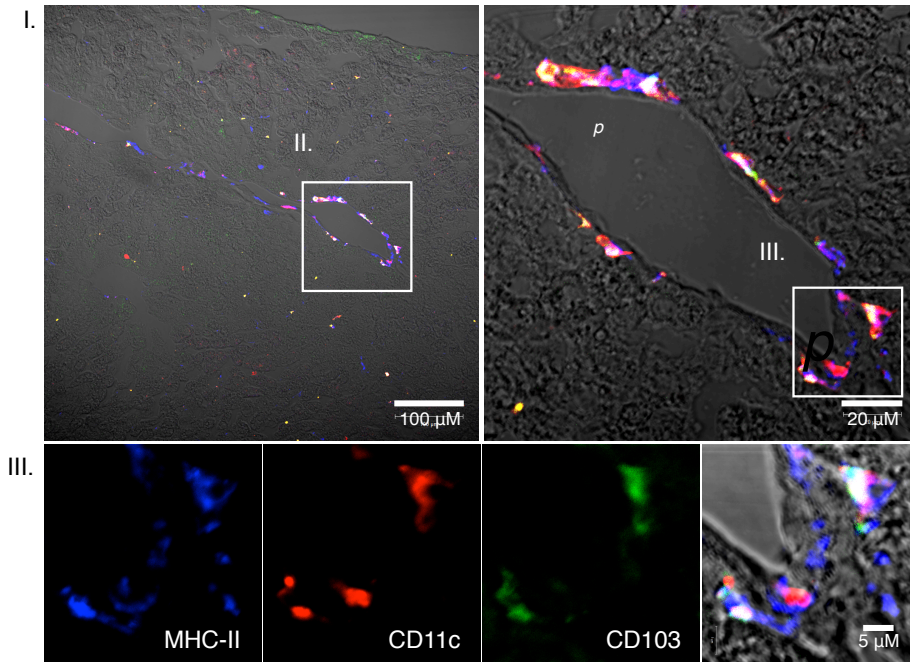
A



B



C



D

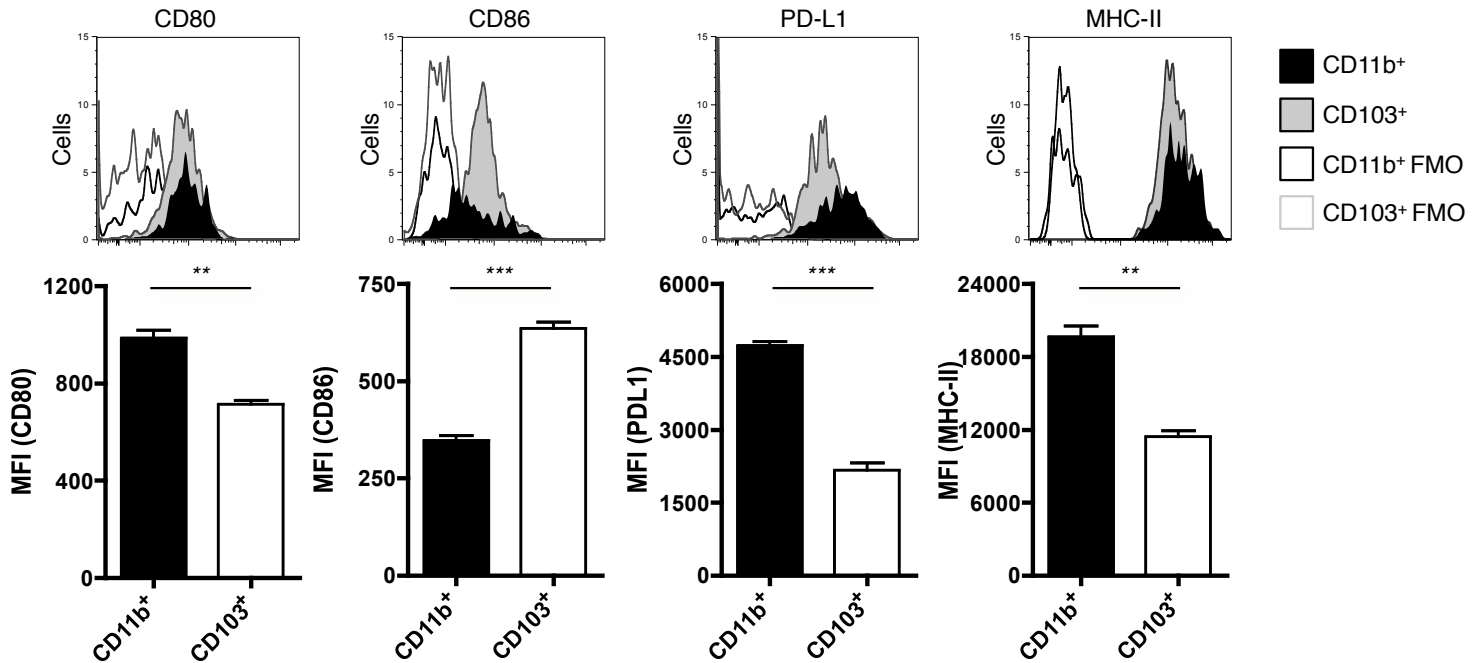
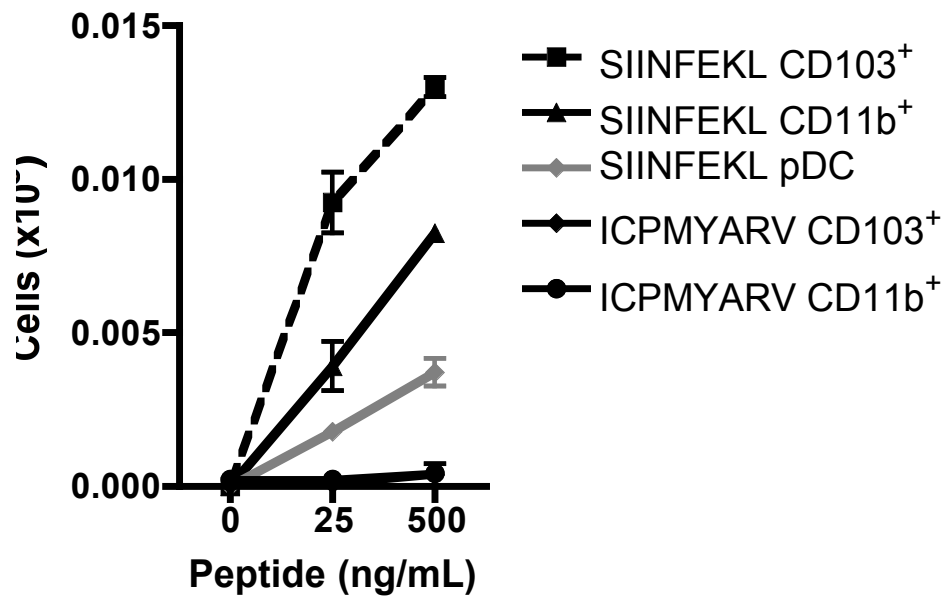
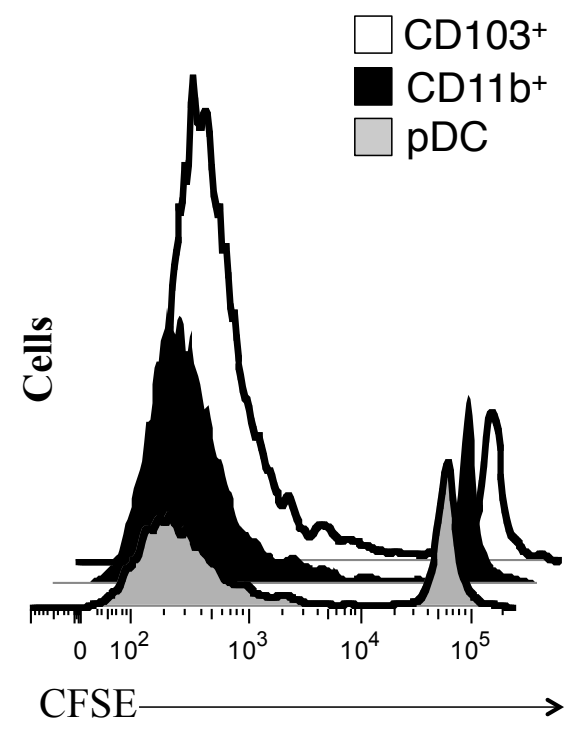


**Figure 3.2. Phenotype of naïve liver resident conventional dendritic cells (DC).** 8 – 12 week old C57BL/6 livers were perfused, enzymatically digested and the mononuclear cells isolated by density gradient centrifugation. (A – B) Using flow cytometry, resident CD11c<sup>hi</sup>MHC-II<sup>hi</sup>B220<sup>-</sup> DC populations, gated from debris and doublet excluded CD45<sup>+</sup> cells, are discriminated by CD11b, CD103 and CD8 $\alpha$  surface expression. (B) Graphical representation of CD11b<sup>+</sup> (black) and CD103<sup>+</sup> (white) DC frequencies and cellularity (n = 9). (C) Fluorescence microscopy on a naïve liver section stained for CD103<sup>+</sup> DCs using antibodies for MHC-II (blue), CD11c (red) and CD103 (green). (D) Histograms show the expression levels and (E) quantified MFI of CD80, CD86, PD-L1 and MHC-II on CD11b<sup>+</sup> (black) and CD103<sup>+</sup> (gray) DCs (n = 9). 3 independent experiments, mean  $\pm$  SEM. Student's t test (two-tailed): \*\* $p < 0.01$ , \*\*\* $p < 0.001$ .

A

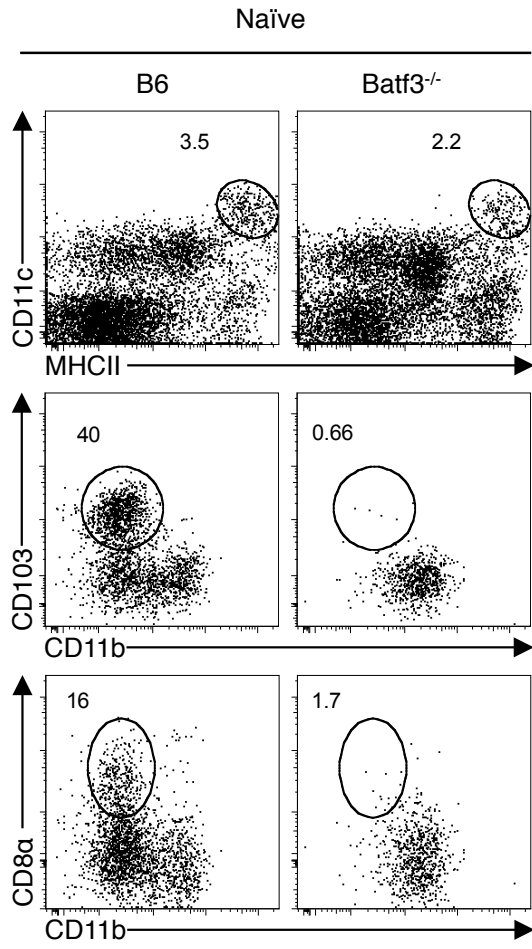
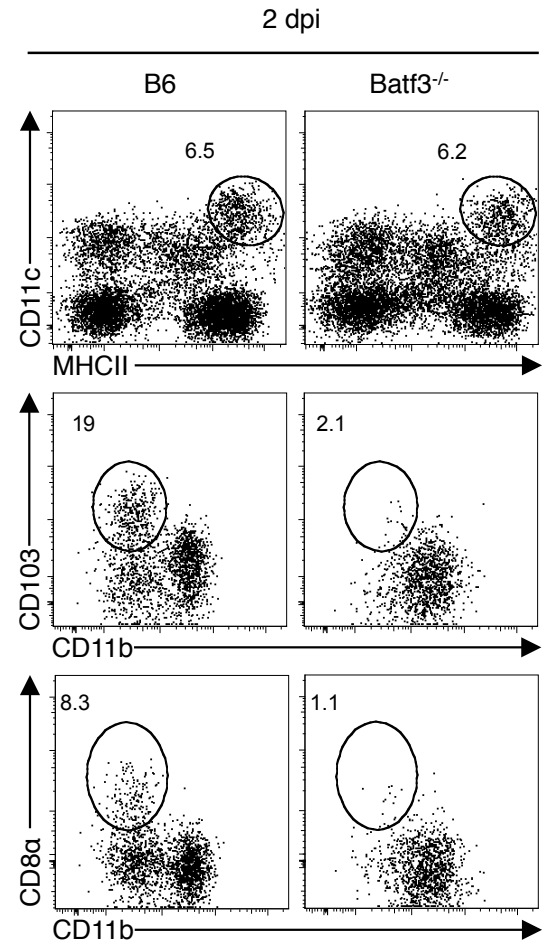


B



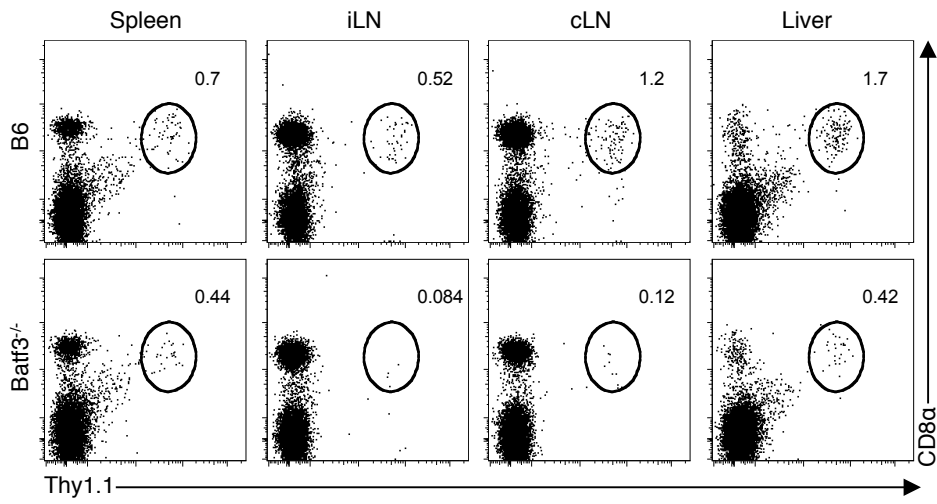
**Figure 3.3. Hepatic resident CD103<sup>+</sup> exhibit enhanced priming capability *in vitro*:**

FACS sorted naïve hepatic CD11b<sup>+</sup>, CD103<sup>+</sup> and plasmacytoid DCs were pulsed with either SIINFEKL or nonspecific peptide at 0, 25 or 500 ng/mL for 20 min at 37°C, washed and cocultured with CFSE labeled naïve OT-I cells at a ratio of  $4 \times 10^3 : 4 \times 10^4$  for 4 days at 37°C. (A) Representative histogram of OT-I CFSE dilution in the 25ng/mL pulsed DC cocultures. (B) Number of total OT-I cells (via counting beads, Spherotech<sup>inc</sup>) from the cocultures of 0, 25 and 500 ng/mL pulsed DC cell subsets. Representative of 4 independent experiments done in triplicate.

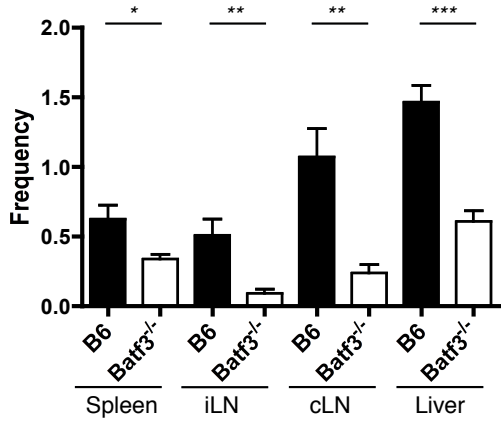
**A****B**

**Figure 3.4. Batf3<sup>-/-</sup> livers lack CD103<sup>+</sup> and CD8 $\alpha$ <sup>+</sup> DCs.** (A) Naïve or (B) 2 day i.v. infected ( $2.5 \times 10^7$  IU Ad-OVA) C57Bl/6 and Batf3<sup>-/-</sup> liver mononuclear cells were analyzed by flow cytometry for DCs using the previously described gating strategy. Representative dot plots of DC subsets stained for CD11b, CD103 and CD8 $\alpha$  surface marker expression (n = 13). Representative of 5 independent experiments.

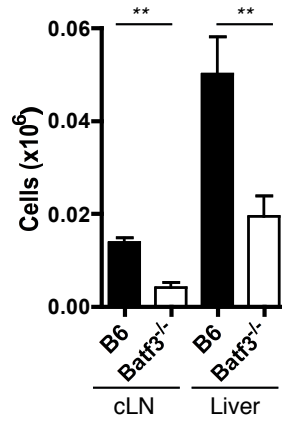
**A**



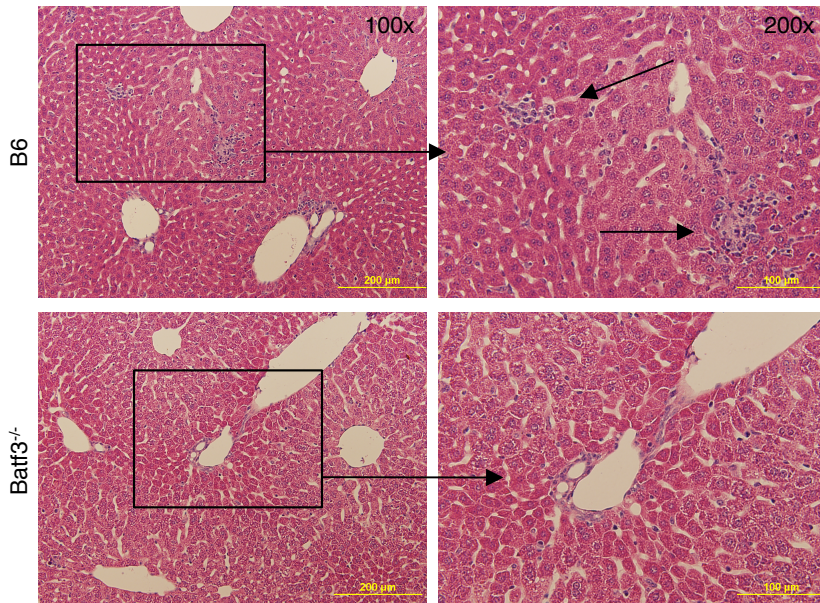
**B**



**C**



**D**



**E**

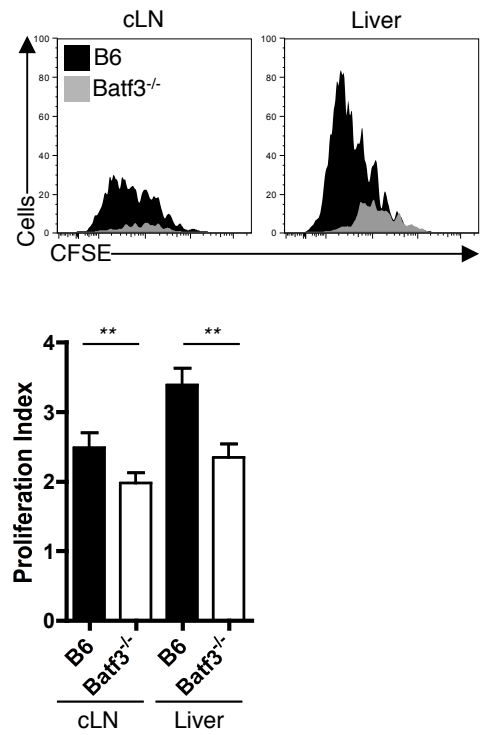
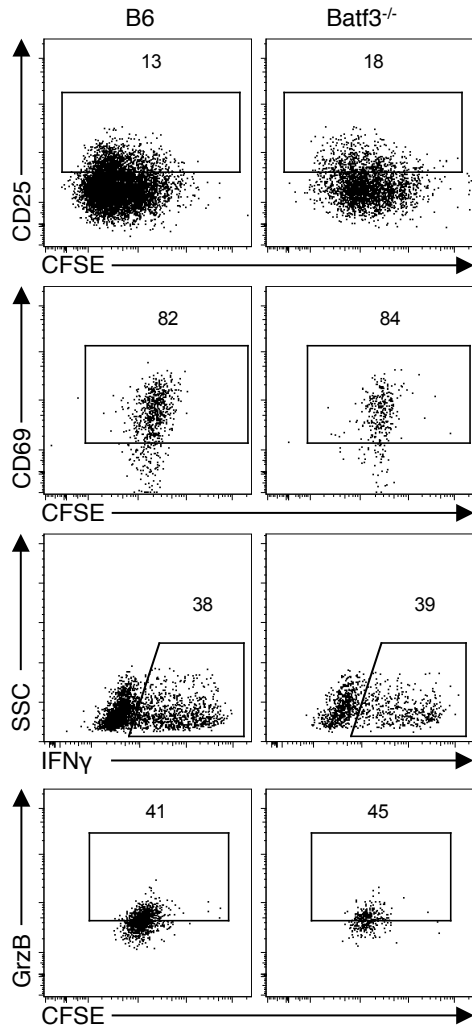


**Figure 3.5. *Batf3*<sup>-/-</sup> mice exhibit decreased antigen-specific CD8<sup>+</sup> T cell numbers during Ad-OVA infection.** (A – D)  $2 \times 10^5$  naïve CFSE<sup>+</sup> OT-I cells were transferred via the tail vein into C57Bl/6 and *Batf3*<sup>-/-</sup> mice 1 day prior to  $2.5 \times 10^7$  IU Adenovirus-OVA infection (i.v.). The spleens, inguinal lymph nodes (iLN), coeliac/hepatic lymph nodes (cLN) and livers were harvested 3 dpi. OT-I cell frequency, cellularity and proliferation were quantified using flow cytometry. (A) Representative CD45<sup>+</sup>CD8 $\alpha$ <sup>+</sup>Thy1.1<sup>+</sup> OT-I flow plots and (B) quantified frequencies from C57Bl/6 and *Batf3*<sup>-/-</sup> spleens (n = 11, 12), iLNs (n = 8, 8), cLNs (n = 12, 12) and livers (n = 15, 15). (C) OT-I cellularity quantified from C57Bl/6 and *Batf3*<sup>-/-</sup> cLNs and livers (n = 13, 13). (D) Representative H&E staining on C57Bl/6 and *Batf3*<sup>-/-</sup> livers (n = 6, 6). (E) Histograms show representative OT-I CFSE dilution and the proliferation index (calculated using FlowJo analysis) from C57Bl/6 and *Batf3*<sup>-/-</sup> cLNs and livers (n = 12, 12). 2 - 5 independent experiments, mean  $\pm$  SEM. Student's t test (two-tailed): \* $p < 0.05$ , \*\* $p < 0.01$ , \*\*\* $p < 0.001$ .

A



B

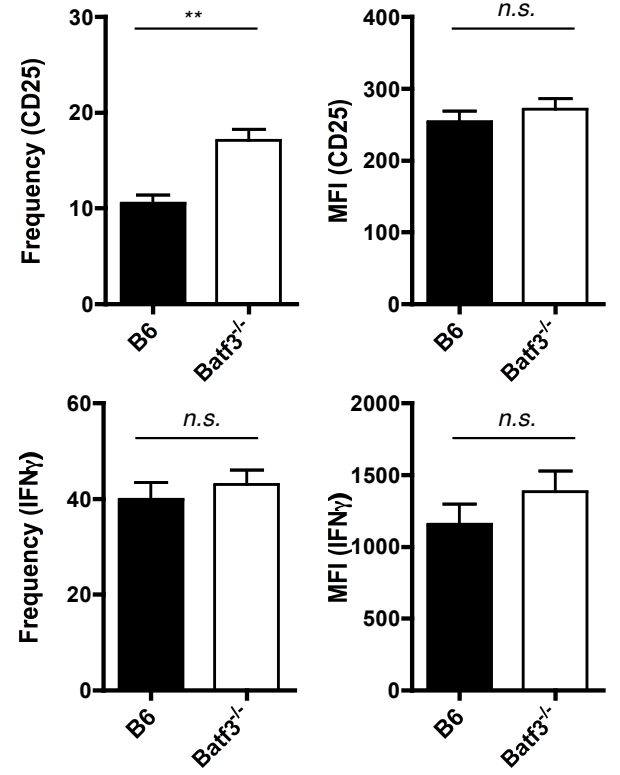
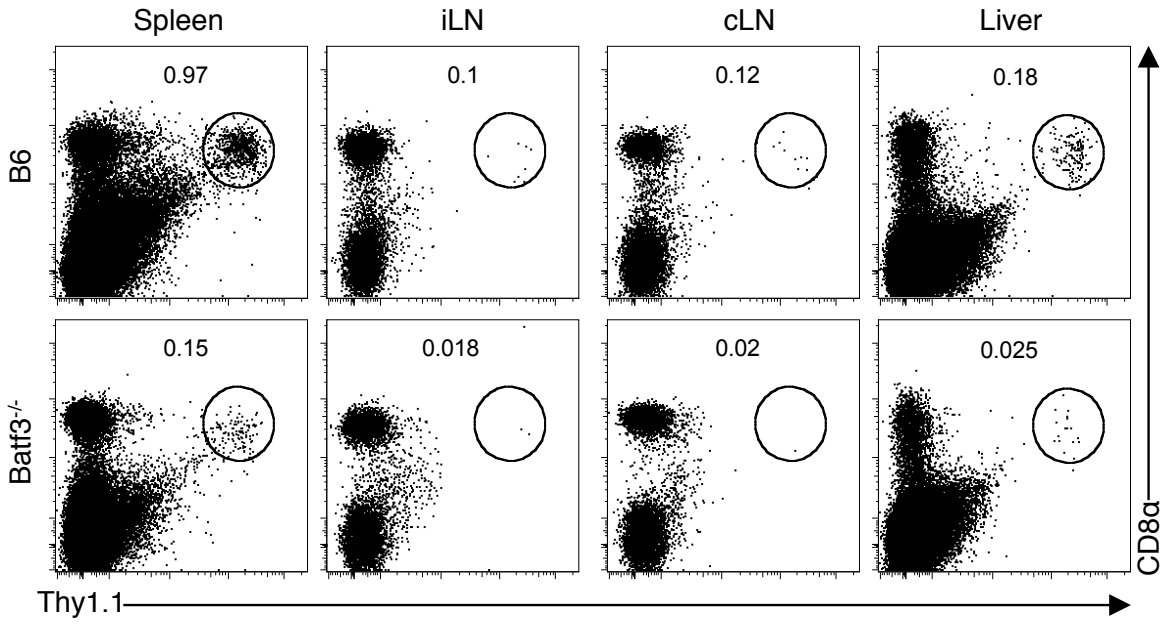
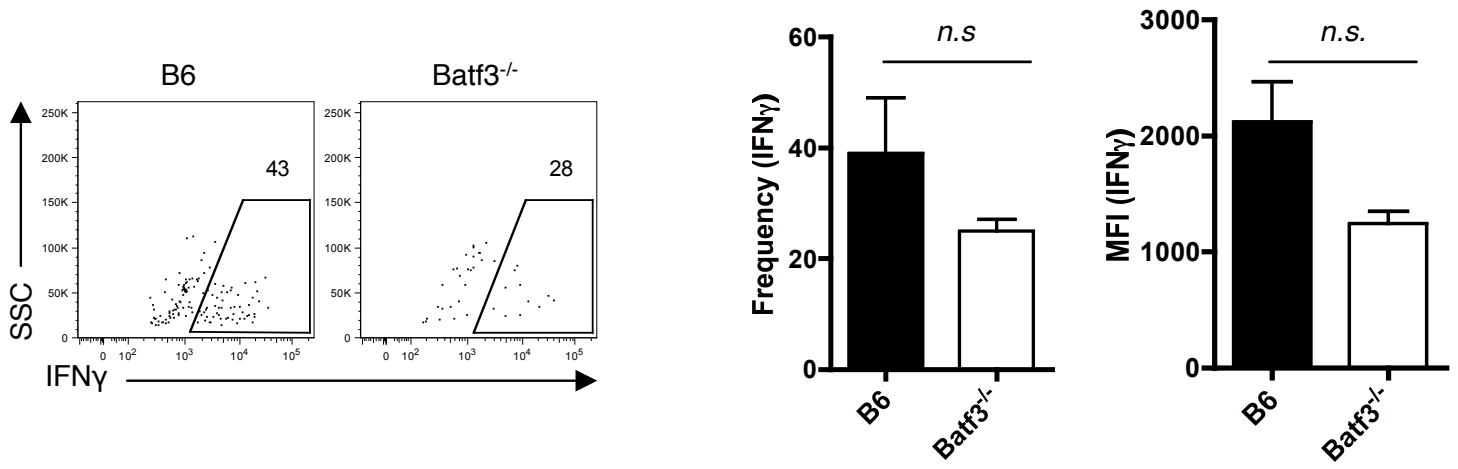


**Figure 3.6. Antigen-specific T cells in the liver have similar CD25 and IFN $\gamma$  expression in the absence of CD103<sup>+</sup>/CD8 $\alpha$ <sup>+</sup> DCs.** (A – B)  $2 \times 10^5$  naïve CFSE<sup>+</sup> OT-I cells were transferred via the tail vein into C57Bl/6 and Batf3<sup>-/-</sup> mice 1 day prior to  $2.5 \times 10^7$  IU Ad-OVA infection (i.v.). (A) Representative CD45<sup>+</sup>CD8 $\alpha$ <sup>+</sup>Thy1.1<sup>+</sup> OT-I expression flow plots for CD25, CD69, IFN $\gamma$  and GrzB from 3 dpi C57Bl/6 and Batf3<sup>-/-</sup> livers (n = 6-13). (B) Quantified frequency and MFI for CD25 and IFN $\gamma$  expression from 3 dpi C57Bl/6 and Batf3<sup>-/-</sup> livers (n = 13). Representative of 2-5 independent experiments. Student's t test (two-tailed): \*\* $p < 0.01$ , mean  $\pm$  SEM.

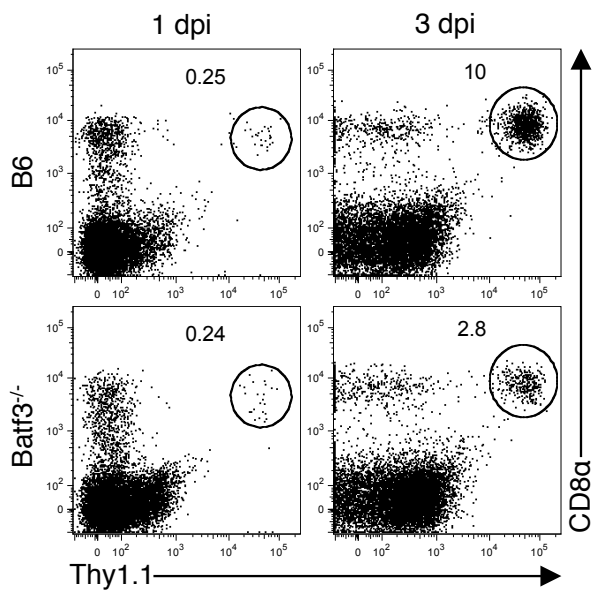
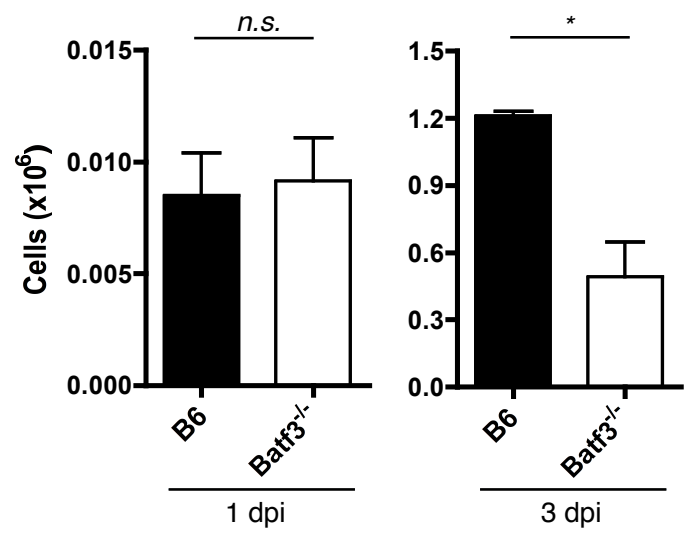
A



B

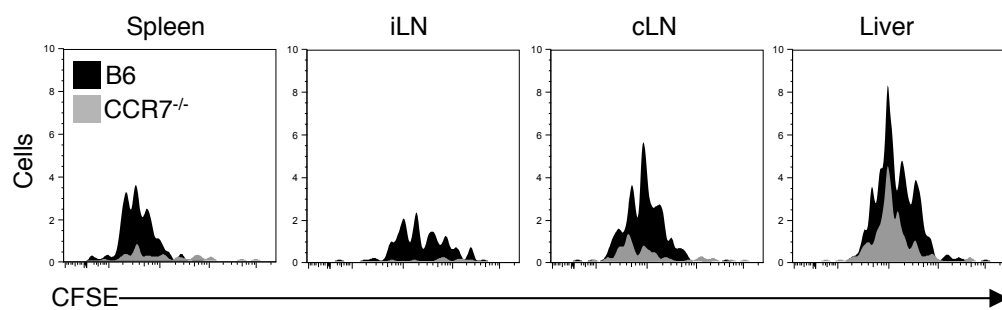


**Figure 3.7. Batf3<sup>-/-</sup> mice exhibit decreased antigen-specific CD8<sup>+</sup> T cell numbers during MCMV-Ova infection.** (A – B)  $2 \times 10^5$  naïve CFSE<sup>+</sup> OT-I cells were transferred via the tail vein into C57Bl/6 and Batf3<sup>-/-</sup> mice 1 day prior to  $4 \times 10^5$  PFU MCMV-OVA infection (i.v.). (A) Representative CD45<sup>+</sup>CD8 $\alpha$ <sup>+</sup>Thy1.1<sup>+</sup> OT-I flow plots from spleens, inguinal lymph nodes (iLN), coeliac/hepatic lymph nodes (cLN) and livers harvested from C57Bl/6 and Batf3<sup>-/-</sup> mice 3 dpi (B) Representative CD45<sup>+</sup>CD8 $\alpha$ <sup>+</sup>Thy1.1<sup>+</sup> IFN $\gamma$ <sup>+</sup> OT-I flow plots and quantified IFN $\gamma$  frequency and MFI (n = 3). Student's t test (two-tailed): \* $p < 0.05$ , mean  $\pm$  SEM.

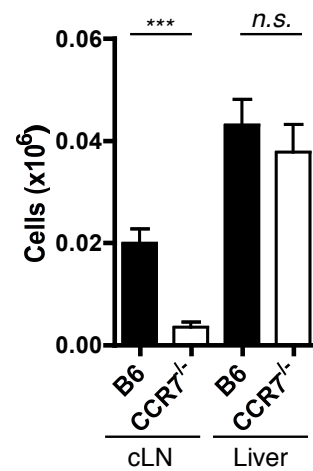
**A****B**

**Figure 3.8. Similar OT-I numbers detected in C57Bl/6 and Batf3<sup>-/-</sup> livers 1 day post infection.**  $2 \times 10^6$  CFSE<sup>+</sup> OT-I T cells were i.v. transferred into C57Bl/6 and Batf3<sup>-/-</sup> mice 1 day prior to infection with  $2.5 \times 10^7$  IU Ad-OVA (i.v.). (A) The dot plots of OT-I T cells from livers at 1 and 3 dpi were (B) quantified by hemocytometer counts prior to staining (n = 6, 6). 2 independent experiments, mean  $\pm$  SEM. Student's t test (two-tailed): \* $p < 0.05$

A



B



C

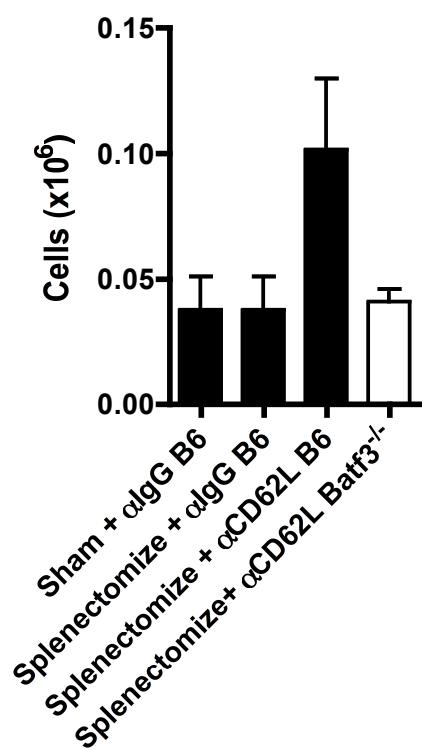
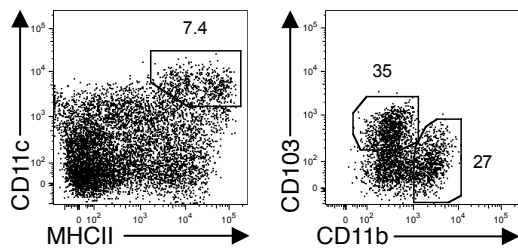


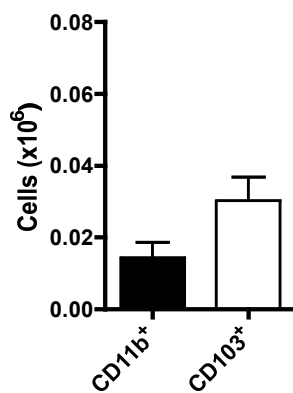
**Figure 3.9. Hepatic antigen-specific T cells are primed *in situ* during Ad-OVA**

**infection.** (A – B)  $2 \times 10^5$  naïve CFSE<sup>+</sup> OT-I cells were transferred via the tail vein into C57Bl/6 and CCR7<sup>-/-</sup> mice 1 day prior to  $2.5 \times 10^7$  IU Adenovirus-OVA infection (i.v.). The spleens, inguinal lymph nodes (iLN), coeliac/hepatic lymph nodes (cLN) and livers were harvested 3 days post infection. OT-I cell frequency, cellularity and proliferation were quantified using flow cytometry. (A) Representative CD45<sup>+</sup>CD8 $\alpha$ <sup>+</sup>Thy1.1<sup>+</sup> OT-I CFSE dilution histograms from C57Bl/6 and CCR7<sup>-/-</sup> spleens, iLN, cLN and livers (B) OT-I cellularity quantified from C57Bl/6 and CCR7<sup>-/-</sup> cLNs (n = 6, 6) and livers (n = 12, 12). (C) Representative graph of OT-I cell numbers in splenectomized and anti-CD62L treated C57Bl/6 and Batf3<sup>-/-</sup> mice that received  $2 \times 10^5$  naïve CFSE<sup>+</sup> 1 day prior to  $2.5 \times 10^7$  IU Adenovirus-OVA infection (i.v.). 2-3 independent experiments, mean  $\pm$  SEM. Student's t test (two-tailed): \*\*\* $p < 0.001$ .

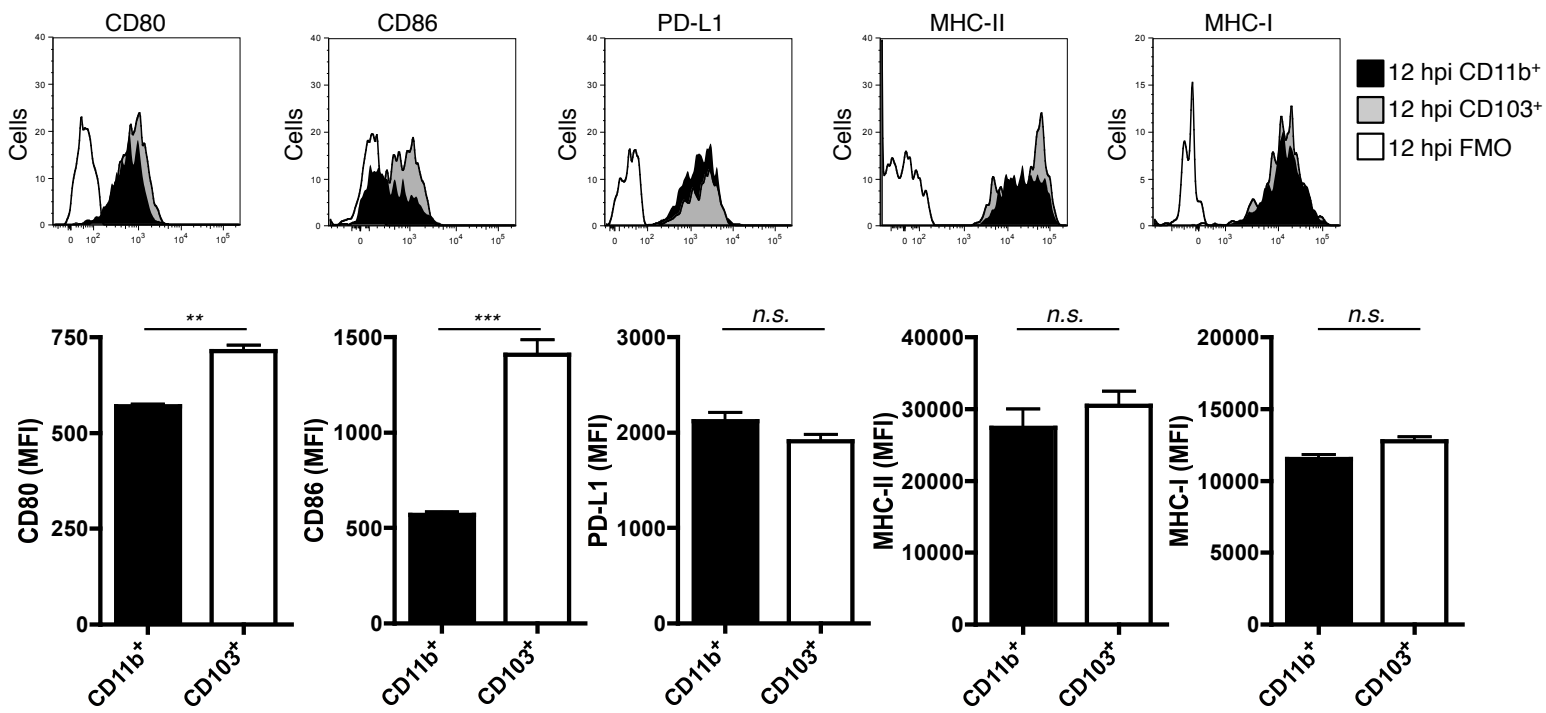
A



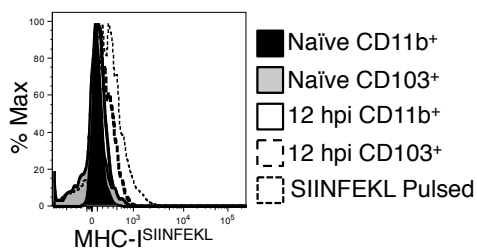
B



C



D



E

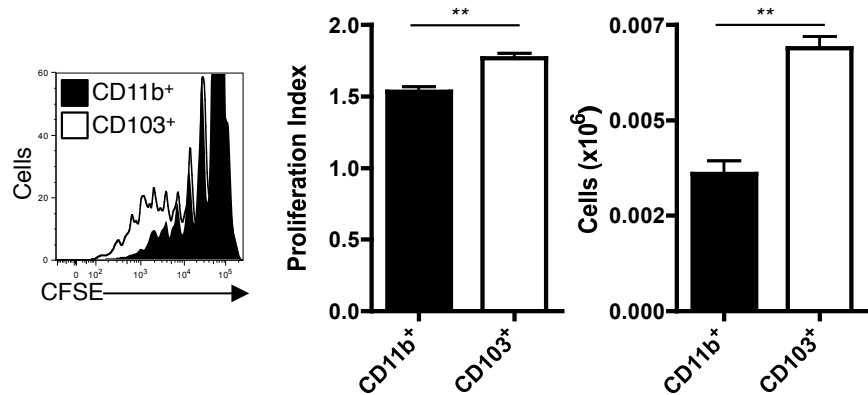


**Figure 3.10. Hepatic resident CD103<sup>+</sup> DCs exhibit maturation and enhanced priming capability at 12 hpi:** (A – C) 12 hours i.v. infected ( $2.5 \times 10^7$  IU Ad-OVA) C57BL/6 liver mononuclear cells were analyzed by flow cytometry for DCs using the previously described gating strategy. (A) Representative DC histograms were stained for CD11b and CD103 and (B) cellularity quantified by hemocytometer counts prior to staining surface markers. (C) MFI was quantified for CD80, CD86, PD-L1, MHC-II and MHC-I. (D) Representative histogram for naïve and 12 hpi liver DCs and peptide pulsed splenic DCs ( $1\mu\text{g/mL}$  for 20 min at  $37^\circ\text{C}$ ) surface stained for MHC-I<sup>SIINFEKL</sup>. (A – D) 2 independent experiments,  $n = 6$ , mean  $\pm$  SEM. (E) Representative divided OT-I CFSE dilution histograms, quantified proliferation index (calculated using FlowJo analysis) and cell numbers (via counting beads, Spherotech<sup>inc</sup>) from cocultures of FACs sorted hepatic CD11b<sup>+</sup> and CD103<sup>+</sup> DCs, from 12 hours i.v. infected ( $2.5 \times 10^7$  IU Ad-OVA) C57Bl/6 mice, to OT-Is at a ratio of  $2 \times 10^4 : 2 \times 10^5$  for 4 days at  $37^\circ\text{C}$ . Representative of 3 independent experiments done in triplicate. Student's t test (two-tailed):  $**p < 0.01$ ,  $***p < 0.001$ .

## **Chapter 4: NKG2A<sup>+</sup>CD49a<sup>+</sup> ILC1 Mediate Anti-viral CD103<sup>+</sup> DC Activation**

### **Abstract**

The liver maintains a tolerogenic environment in response to continuous exposure to highly immunogenic material arriving in the intestinal blood, leaving it vulnerable to chronic infections, such as HCV. Impaired T cell responses correlate strongly to HCV persistence; however, little is known about the cellular and molecular mechanisms contributing to T cell dysfunction. In response to hepatotropic viral infection, liver DCs are able to upregulate maturation markers and present viral antigen to induce robust CD8<sup>+</sup> T cell responses. To determine the contribution of hepatic group 1 ILCs on DC activation, we first characterized the anatomical location of ILC subsets in murine livers. Liver ILC1 localize near DCs in the perivascular spaces surrounding portal triads. Depletion of group 1 ILCs leads to a loss of hepatic DC accumulation following viral infection, suggesting they are required for efficient DC activation. Importantly, viral infection in the NKG2A<sup>-/-</sup> mouse exhibits sustained increase in the proliferative response of both adoptively transferred antigen-specific CD8<sup>+</sup> T cells and endogenous anti-viral CD8<sup>+</sup> T cells. CD103<sup>+</sup> DCs, but not CD11b<sup>+</sup> DCs isolated from the NKG2A<sup>-/-</sup> livers are capable of priming naïve CD8<sup>+</sup> T cells *in vitro* to a greater degree than their wild-type counterparts. NKG2A<sup>-/-</sup> ILC1 express comparatively elevated levels of IFN $\gamma$ , a cytokine that enhances DC activity. In summary, we demonstrate that NKG2A<sup>+</sup>CD49a<sup>+</sup> ILC1 limit DC activation by suppressing IFN $\gamma$  production via NKG2A signaling. Collectively, these data help elucidate how the liver suppresses anti-viral immune responses and raises the possibility for an exciting therapeutic approach for developing next generation

vaccines for persistence liver pathogens, i.e. inhibiting ILC1 NKG2A signaling in order to induce a more robust and sustainable anti-viral CD8<sup>+</sup> T cell response.

## **Introduction**

The liver possesses distinct tolerogenic properties to avoid unwanted immune activation to bacterial derived constituents and food-derived Ag. Its immunosuppressive environment leaves the liver susceptible to persistent infection by hepatic microbial pathogens, such as HCV and malaria. The lack of robust and sustainable CD8<sup>+</sup> T cells correlates with the persistence of hepatic pathogens. Liver-resident DCs have been reported to be potent APCs for anti-viral CD8<sup>+</sup> T cell induction, however, little is known about the immunoregulatory mechanisms controlling DC activation during hepatotropic infections. Future therapeutics designed to enhance hepatic DCs ability to induce effective and durable CD8<sup>+</sup> T cell responses may prove beneficial in elimination of life-threatening pathogens in the liver.

Immature DCs use broadly conserved pattern recognition receptors (such as TLRs) to become activated. However, DC maturation can also be induced or amplified by pro-inflammatory cytokines, such as IFN $\gamma$ . Upon activation/maturation, DCs upregulate antigen presenting molecules (i.e., MHC class I and II) and costimulatory molecules (i.e., CD80 and CD86). The liver exhibits diverse DC populations, including the conventional tissue-resident CD11b<sup>+</sup> and CD103<sup>+</sup> subsets. During viral insult, hepatic CD103<sup>+</sup> DCs upregulate expression of costimulatory molecules and preferentially present viral Ag for MHC-I presentation to naïve anti-viral CD8<sup>+</sup> T cells. However, chronic viral infection in

the liver leads to dysfunctional T cells, suggesting CD103<sup>+</sup> DCs may exhibit inefficient activation/maturation leading to limited capacity to generate robust CD8<sup>+</sup> T cell responses capable of clearing virus. Group 1 innate lymphoid cells (ILC) are able to kill immature DCs via their expression of cytolytic molecules (i.e. granzymes, perforin), and in contrast, are also able to enhance DC activation via production of immunoregulatory cytokines (i.e. IFN $\gamma$ , TNF $\alpha$ ).

The liver maintains two transcriptionally diverse group 1 ILC populations; CD49b<sup>+</sup> conventional NK cells, and CD49a<sup>+</sup> ILC1. When compared to the spleen, hepatic group 1 ILCs exhibit unique profiles including limited Ly49 receptor(s) expression and reduced capacity to produce IFN $\gamma$  with IL-12/IL-18 stimulation. Moreover, CD49a<sup>+</sup> ILC1 express high levels of NKG2A and GrB, as well as traditional activation markers CD69 and CD44, in the steady-state. Although it has been proposed that liver-resident ILC1 contribute the liver's tolerogenic environment, their ability to regulate DC activation during hepatotropic viral infection has yet to be explored.

In this study, we sought to determine the regulatory capacity of CD49a<sup>+</sup> ILC1 on suppressing hepatic-resident DC activation, leading to subsequent inhibition of anti-viral CD8<sup>+</sup> T cell activation and differentiation in response to liver infections. Employing the hepatotropic adenovirus engineered to express ovalbumin (Ad-OVA), we demonstrate that CD49a<sup>+</sup> ILC1 signal through NKG2A to limit IFN $\gamma$  production required for potent CD103<sup>+</sup> DCs maturation. Thus, our study identifies the hepatic NKG2A<sup>+</sup>CD49a<sup>+</sup> ILC1 subset as the primary cell type regulating the activation of liver-resident APCs, namely

CD103<sup>+</sup> DCs, which in turn ultimately dictate anti-viral CD8<sup>+</sup> T responses to pathogens invading the liver. Implications of these findings in designing vaccine strategies and therapeutic venues for chronic hepatic viral infections (e.g. HCV) are discussed.

## **Materials and Methods**

### *Mice.*

All experiments used gender/aged matched male and female mice, 8-12 wks old. Thy1.2<sup>+</sup> C57BL/6 (B6, H-2<sup>b</sup>) and Thy1.1<sup>+</sup> OT-I TCR Tg (OT-I, H-2<sup>b</sup>) mice were purchased from Taconic Farms (Hudson, NY). Batf3<sup>-/-</sup> (H-2<sup>b</sup>) mice were kindly provided by Dr. Thomas Braciale (University of Virginia, Charlottesville, VA). NKG2A<sup>-/-</sup> (H-2<sup>b</sup>) mice were kindly provided by Dr. Richard Enelow (Dartmouth, Hanover, VT). All mice were housed in a pathogen-free facility and were tested routinely for mouse hepatitis virus and other pathogens. All mice were handled according to protocols approved by the University of Virginia Institutional Animal Care and Use Committee.

### *Viruses.*

Replication-deficient recombinant adenovirus type 5 expressing ovalbumin (rAd5-OVA) under the human CMV promoter and lacking E1 and E3 genes were purchased from the Iowa Gene Transfer Vector Core (Iowa City, IA). Mice were injected intravenously (i.v.) with  $2.5 \times 10^7$  IU Ad-OVA.

### *Liver and Spleen leukocyte isolation.*

Livers were perfused with PBS via the portal vein until fully blanched, then put on ice in Iscove's Modified Dulbecco's Medium (IMDM) supplemented with 10% newborn calf serum (NBCS). Whole livers were passed through a metal spleen screen and digested with 0.05% collagenase IV (Sigma-Aldrich, St. Louis, MO) for 30 min at 37°C.

Intrahepatic mononuclear cells were purified on a 21% Histodenz (Sigma-Aldrich, St. Louis, MO) gradient after centrifugation at 1250 x g for 20 min without braking. Spleens and lymph nodes were passed through a mesh spleen screen, followed by RBC lysis. All samples were washed and re-suspended in IMDM plus serum and leukocytes were counted via a hemocytometer.

*Flow cytometry and intracellular staining.*

Cells were labeled with Abs against CD45, CD3 $\epsilon$ , NKp46, NK1.1, CD49a, CD49b, NKG2A-B6, NKG2A/C/E/, CD94, CD69, Qa-1b, CD4, B220, I-A/I-E, CD11c, CD11b, CD8 $\alpha$ , CD103, CD80, CD86, Thy1.1, Thy1.2, IFN $\gamma$ , CD107a, and GranzymeB (all obtained from eBioscience, San Diego, CA). For cell surface labeling, 1 x 10<sup>6</sup> cells were blocked with anti-CD16/CD32 (2.4G2; University of Virginia, Charlottesville, VA) and incubated with the corresponding Abs for 30 min at 4°C in staining buffer (PBS with 2% FBS and 0.1% NaN<sub>3</sub>). For cytokine staining, 1 x 10<sup>6</sup> cells were incubated for 5 hours in IMDM supplemented with 10% FBS, 10 U/mL penicillin G, 2 mM L-glutamine, 5 mM  $\beta$ -mercaptoethanol, and 1 $\mu$ L/mL of GolgiPlug/GolgiStop (BD Biosciences). OT-I cells and CD8<sup>+</sup> T cells were restimulated with 2  $\mu$ g/mL SIINFEKL peptide (AnaSpec) in the presence of CD107a when stated. Group 1 ILCs were restimulated with either 100ng IL-12/IL-18 or YAC-1 targets at a 1:1 ratio. After incubation, the cells were surface labeled

as described above, fixed using Cytofix/Cytoperm (BD Biosciences) according to the manufacturer's instructions prior to intracellular IFN $\gamma$  staining. All samples were run on a BD FACS Canto II (BD Immunocytometry Systems, San Jose, CA) and analyzed using FlowJo software 8.8.6 (Tree Star Inc., Ashland, OR).

#### *Microscopic studies.*

For fluorescence microscopy, mouse liver tissues were perfused with 1 x PBS and periodate-lysine-paraformaldehyde (PLP) fixative, excised, incubated in PLP for 3 hours at 4°C, and passed over a sucrose gradient. Tissues were frozen in optimal cutting temperature (OCT) medium, sectioned at 5  $\mu$ m thickness, blocked with 2.4G2 solution (2.4G2 supernatant containing anti-CD16/32, 10% each of chicken, donkey and horse serum, and 0.1% NaN<sub>3</sub>), and stained with Abs from Biolegend, eBioscience, Santa Cruz Biotechnology, and Sino Biological (Beijing, China). Confocal microscopy was performed on a Zeiss LSM-700, and data were analyzed using Zen 2009 Light Edition software (Carl Zeiss MicroImaging GmbH, Jena, Germany). For histology, mouse liver tissues were perfused with 1 x PBS, excised, incubated in 10% buffered formalin acetate (Fisher Scientific) overnight at 4°C, washed with 70% ethanol and embedded in paraffin wax. Tissues were sectioned at 5  $\mu$ m thickness and stained with hematoxylin and eosin. Light microscopy was performed on an Olympus BX51 microscope.

#### *Adoptive transfer of TCR transgenic T cells.*

CD8<sup>+</sup> T cells were isolated from the spleens and mesenteric lymph nodes of Thy1.1<sup>+</sup>OT-I<sup>+</sup> mice using anti-CD8 $\alpha$  Ab-conjugated magnetic bead separation kits (Miltenyi Biotec).

Cells were labeled with 1.8  $\mu$ M CFSE for 8 min at room temperature, and transferred by i.v. injection into naïve Thy1.2<sup>+</sup> recipients.

*DC and ILC1 isolation.*

Liver DCs and ILC1 were isolated from animals (C57BL/6 or NKG2A<sup>-/-</sup> 7-10 mice) infected with 2.5 x 10<sup>7</sup> IU Ad-OVA for 12 hr prior to analyses. CD11c<sup>+</sup> cells were first enriched by a positive selection using magnetic bead-based purification kits (Miltenyi Biotec). DCs were stained using antibodies for CD45, MHC-II, CD11c, B220, CD11b and CD103. ILC1 were stained using antibodies for CD45, CD3 $\epsilon$ , NKp46 and CD49a. Cells were sorted by flow cytometry using a BD FACSVantage SE sorter at the Flow Cytometry Core Facility (University of Virginia, Charlottesville, VA). DCs were identified by staining with a cocktail of antibodies against CD45, MHC-II, CD11c, CD11b and CD103; plasmacytoid (pDCs) were determined by staining with antibodies against CD45, MHC-II CD11c and B220.

*In vitro priming of naïve OT-I T cells.*

FACS sorted liver DCs isolated 12 hpi from livers of infected C57Bl/6 or NKG2A<sup>-/-</sup> mice were cultured with CFSE labeled OT-I T cells at a ratio of 1 to 10 for 4 days at 37°C *in vitro*. All DC:T cell coculture media included IMDM supplemented with 10% heat-inactivated HyClone FBS, 10 U/mL penicillin G, 2mM L-glutamine, 5 mM  $\beta$ -mercaptoethanol, 20 mM HEPES, and 100ug/mL Gentamycin (all from Invitrogen).

*Statistical analysis*

Student's *t* tests (two-tailed) were used to evaluate the significance of the differences. A value of  $p < 0.05$  was regarded as statistically significant. \* $p < 0.05$ , \*\* $p < 0.01$ , \*\*\* $p < 0.001$ .

## Results

*CD49a<sup>+</sup> ILC1 are the major liver-resident ILC subset in the steady-state.*

The liver maintains two transcriptionally distinct innate lymphoid cell (ILC) compartments: NK cells, which are traditionally characterized by the expression of the alpha2 integrin CD49b (DX5); and ILC1, which express the alpha1 integrin CD49a. Although recent studies describing transcriptional differences among liver-resident ILC subsets have helped establish their key defining features, there is contrasting data as to the accurate representation of ILC1 in the liver in the steady-state. Moreover, the anatomical location of hepatic-resident ILCs has not been well explored. To resolve a more physiologically relevant representation of liver ILC1, we isolated mononuclear cells from murine livers using histodenz gradient centrifugation following tissue digestion with the *Clostridium histolyticum* enzyme, collagenase IV. We confirmed the presence of CD49a<sup>+</sup> ILC1 in the liver and found that they represent the dominate hepatic-resident ILC subset after digestion for 30 min. at 37°C (Fig. 4.1.A.). Along with CD49a expression, we probed for additional NK cell markers. Notably, we found that CD49a<sup>+</sup> ILC1 preferentially express CD11c, CD69 and NKG2A in the steady-state (Fig. 4.1.A.). Moreover, it is interesting that when we subjected naïve livers to various digestion times, the number of isolated CD49a<sup>+</sup> ILCs increased proportionally to the digestion time (data not shown).

*Liver-resident CD49a<sup>+</sup> ILC1 preferentially localize to the portal areas.*

The enhanced recovery of liver-resident CD49a<sup>+</sup> ILC1 with longer digestion times intimates that these cells may be held in tight association with the liver parenchyma. Therefore, to more carefully assess the anatomical location of liver-resident ILC1, we performed fluorescence microscopy to visualize where CD49a<sup>+</sup> ILC1 localize in reference to endothelial cells within the liver parenchyma. Using CD31 to demarcate liver sinusoidal endothelial cells, we found that CD49a<sup>+</sup> ILC1 primarily reside in the perivascular spaces surrounding the portal areas, whereas CD49b<sup>+</sup> NK cells are markedly more dispersed throughout the tissue (Fig. 4.1.B.). In addition to the visualization of liver ILCs using conventional fluorescence microscopy, we also assessed the anatomical location of liver-resident ILCs with regard to the vascular architecture. We therefore tested the ability of CD49a<sup>+</sup> ILC1 to bind antibody *in situ* by injecting anti-CD45, after initial perfusion with PBS, directly into the liver via the portal vein. Total liver mononuclear cells were then isolated and stained again with anti-CD45 conjugated to a different fluorochrome. When compared to total CD45<sup>+</sup> cells, both CD49b<sup>+</sup> NK cells and CD49a<sup>+</sup> ILC1 exhibit less intra-tissue CD45<sup>+</sup> staining (Fig. 4.1.C.; right panel). As a positive control, traditionally perivascular-resident CD103<sup>+</sup> DCs exhibited similarly less *in situ* CD45<sup>+</sup> staining (Fig. 4.1.C.; left panel). Collectively, this data suggests that liver-resident ILCs predominantly reside outside of the blood vessels within the liver, but that CD49a<sup>+</sup> ILC1 preferentially localize to areas surrounding the portal veins.

*Group 1 ILCs associate with liver-resident DCs during Adenovirus infection.*

The finding that liver-resident CD49a<sup>+</sup> ILC1 predominantly reside in the perivascular spaces of the portal areas of the liver posits that these cells may be in close association with other portal-resident leukocytes (i.e. liver-resident DCs). It is well established that NK cells are important in controlling DC fates during viral insult, leading us to speculate whether liver-resident CD49a<sup>+</sup> ILC1 cross-talk with local DCs during hepatotropic viral infection. In order to assess the ability of CD49a<sup>+</sup> ILC1 to associate with tissue-resident DCs following hepatotropic Ad infection, we used Batf3<sup>-/-</sup> mice, which lack CD103<sup>+</sup> DCs in the liver. Previous reports show that NK cells are capable of acquiring MHC-II from DCs through trogocytosis, or the ability of cells to purloin surface markers off neighboring cells for expression on their own surface. Consequently, we assessed the capacity of ILCs to trogocytose surface markers from local cells, most likely CD103<sup>+</sup> DCs, by analyzing the expression of MHC-II on liver ILCs at 12 hpi with Ad-OVA in both the C57BL/6 (B6) and Batf3<sup>-/-</sup> mice. When compared to the B6 wild-type controls, liver-resident ILCs from the Batf3<sup>-/-</sup> mice exhibit a loss of MHC-II accumulation at 12 hpi (Fig. 4.2.A.).

*Liver-resident ILCs initially activate and later suppress DCs during Adenovirus infection.*

The data given above suggests that liver-resident ILCs are in direct communication with DCs. To further assess the functional consequences of this interaction between group 1 ILCs and liver DCs early in hepatotropic viral infection, we eliminated ILCs prior to Ad-OVA infection by i.v. administration of the anti- $\alpha$ GM1 antibody and evaluated the number of DCs present in the liver at 2 dpi. Depleting ILCs 48 hours prior to infection

led to a significant decrease in both CD11b<sup>+</sup> and CD103<sup>+</sup> DCs by 2 dpi (Fig. 4.2.B.), suggesting that ILCs are necessary for DC accumulation in the liver during infection. If ILCs are indeed required for DC sustainability, proliferation and/or infiltration during the onset of Ad-OVA infection, we next investigated whether continual ILC support is required for DC maintenance in the liver. Therefore, we depleted ILCs with anti- $\alpha$ GM1 antibody at 12 hpi and assessed the DC populations at 2 dpi. To our surprise, depleting ILCs at 12 hpi led to an increase in DC accumulation in the liver at 2 dpi (Fig 4.2.B.), suggesting that ILCs may exhibit a dual role in regulating DC activity. When comparing the differences in liver DC frequencies during the two ILC depletion time points, we find that the total DC percentages trend with cellularity (Fig. 4.2.C.). Interestingly, when compared to isotype treated animals, both the CD11b<sup>+</sup> and CD103<sup>+</sup> DC numbers are reduced at 2 dpi when ILCs are depleted prior to infection; however, CD11b<sup>+</sup> DC frequency and numbers increased to a greater extent when ILCs are depleted at 12 hpi (Fig. 4.2.B-C.). Lastly, it is important to note that depleting ILCs at both 48 hours prior to infection and 12 hpi led to an efficient reduction of NK1.1<sup>+</sup> ILCs at 2 dpi (data not shown).

*NKG2A is required for the suppression of liver-resident DCs during adenovirus infection.*

The ability of the ILCs to regulate DCs in the liver during infection led us to consider small-molecules that could potentially mediate liver-resident ILCs' control of local DC fates. Liver-resident CD49a<sup>+</sup> ILC1 express high levels of the inhibitory receptor NKG2A in the steady-state (Fig. 4.3.A.). Furthermore, previous reports have shown that NKG2A<sup>+</sup> NK cells are capable of suppressing DCs during viral infections. Therefore, we

investigated the role of NKG2A on CD49a<sup>+</sup> ILC1 in controlling liver-resident DCs during Ad-OVA infection. To examine the functional impact of NKG2A on ILCs, we utilized mice deficient in the NKG2A gene, *KLRC1*. Liver ILCs exhibit the loss of surface expression of both NKG2A and CD94 in the NKG2A<sup>-/-</sup> mice (Fig. 4.3.B.). Additionally, sorted NKG2A<sup>-/-</sup> ILCs lack NKG2A mRNA as assessed by qRT-PCR (Fig. 4.3.C.). When compared to B6 mice, the NKG2A<sup>-/-</sup> livers exhibit moderately higher frequencies, but significantly increased numbers of total DCs from mice at 0, 12, and 24 hpi (Fig. 4.4.A-B.). In contrast to total DCs, the CD11b<sup>+</sup> and CD103<sup>+</sup> subsets from the NKG2A<sup>-/-</sup> livers appear to have similar frequencies at all time points analyzed (Fig. 4.4.C.).

In order to rule out any intrinsic influence of NKG2A signaling on liver-resident DCs during Ad-OVA infection, we probed for NKG2A on total DCs at 12 hpi. As expected, hepatic DCs lack both NKG2A surface expression (Fig. 4.5.A.; right panel), and *KLRG1* transcript as assessed by qRT-PCR (data not shown). We then investigated the expression of Qa-1<sup>b</sup>, the ligand for NKG2A, on liver-resident DCs during Ad-OVA infection. Using sorted CD11b<sup>+</sup> and CD103<sup>+</sup> DCs from B6 and NKG2A<sup>-/-</sup> livers at 12 hpi, we quantified Qa-1<sup>b</sup> transcript using qRT-PCR. Although CD11b<sup>+</sup> and CD103<sup>+</sup> DCs transcribe similar amounts of Qa-1<sup>b</sup> mRNA in both the B6 and NKG2A<sup>-/-</sup> livers, there is markedly higher Qa-1<sup>b</sup> expression on total DCs at 12 hpi in the NKG2A<sup>-/-</sup> mice (Fig. 4.6.B.). These findings were corroborated at the protein level, as Qa-1<sup>b</sup> surface expression is increased in the DCs of NKG2A<sup>-/-</sup> mice when compared to those of B6 mice

(Fig. 4.6.C.). Notably, CD11b<sup>+</sup> DCs from both B6 and NKG2A<sup>-/-</sup> livers expressed higher levels of Qa-1<sup>b</sup> when compared to their CD103<sup>+</sup> counterparts (Fig. 4.6.C.).

In addition to investigating DC cellularity in NKG2A<sup>-/-</sup> livers during Ad-OVA infection, we evaluated the maturation status of CD11b<sup>+</sup> and CD103<sup>+</sup> DCs via expression of the costimulatory receptors CD80 and CD86. Although equal in the naïve livers, at 12 hpi both the CD11b<sup>+</sup> and CD103<sup>+</sup> DCs in the NKG2A<sup>-/-</sup> preferentially expressed higher levels of CD86 when compared to the corresponding DC subset from B6 mice (Fig. 4.4.D-E.). In contrast, although the CD103<sup>+</sup> DCs continue to express moderately enhanced CD86 expression in the NKG2A<sup>-/-</sup> livers at 24 hpi, as measured by the MFI, the CD11b<sup>+</sup> DC subset exhibit no differences in CD86 expression between the B6 and NKG2A<sup>-/-</sup> mice. Interestingly, whereas CD11b<sup>+</sup> DCs from the NKG2A<sup>-/-</sup> livers exhibit no differences in CD80 MFI at 12 hpi and 24 hpi, the CD103<sup>+</sup> subset exhibit significantly enhanced CD80 expression at 12 hpi, which returns to levels similar to the B6 mice by 24 hpi (Fig. 4.4.E).

*NKG2A<sup>-/-</sup> CD103<sup>+</sup> DCs prime OT-I T cells in vitro with higher efficiency than C56BL/6 CD103<sup>+</sup> DCs.*

Given that CD11b<sup>+</sup> and CD103<sup>+</sup> DCs from the NKG2A<sup>-/-</sup> livers at 12 hpi expressed high levels of costimulatory receptors, we next examined their capacity to activate antigen-specific CD8<sup>+</sup> T cells. To this end, we sorted liver DCs from B6 and NKG2A<sup>-/-</sup> mice infected with Ad-OVA for 12 hours and analyzed their ability to support proliferative expansion of OT-I CD8<sup>+</sup> T cells *in vitro*. As assessed by CFSE dilution, NKG2A<sup>-/-</sup> CD103<sup>+</sup> DCs stimulated more potent proliferative responses than their B6 CD103<sup>+</sup> DC

counterparts (Fig. 4.4.F.). This enhanced stimulatory capacity of NKG2A<sup>-/-</sup> CD103<sup>+</sup> DCs was also evident from the elevated numbers of total OT-I CD8<sup>+</sup> T cells recovered at the end of the *in vitro* coculture (Fig. 4.4.G.). In contrast to the differences in OT-I CD8<sup>+</sup> T cell expansion seen with the CD103<sup>+</sup> DC subsets, the CD11b<sup>+</sup> DCs from both the B6 and NKG2A<sup>-/-</sup> livers exhibited similar proliferative responses in OT-I CD8<sup>+</sup> T cells *in vitro* (Fig. 4.4.F-G.). Taken together, these findings suggest that CD103<sup>+</sup>, but not CD11b<sup>+</sup> DCs, from the NKG2A<sup>-/-</sup> livers at 12 hpi are intrinsically better at appropriating and/or presenting antigenic peptides to naïve CD8<sup>+</sup> T cells when compared to the CD103<sup>+</sup> and CD11b<sup>+</sup> DCs sorted from the B6 livers.

*CD49a<sup>+</sup> ILC1 are enhanced in number and IFN $\gamma$  production in NKG2A<sup>-/-</sup> livers during Adenovirus infection.*

To identify what mechanism is controlling the distinctive DC phenotypes in the NKG2A<sup>-/-</sup> livers during Ad-OVA infection, we considered possible differences in the availability of antigen, as it potentiates DC maturation and/or recruitment. When administered systemically, the replication-deficient recombinant Ad-OVA is primarily cleared by liver Kupffer cells, with the majority of residual virus entering hepatocytes via factor X/Ad5 complexes. In order to measure the viral burden in B6 and NKG2A<sup>-/-</sup> livers, we isolated RNA from whole liver homogenates and quantified OVA mRNA via qRT-PCR. There was no difference in OVA message at 3 dpi between the B6 and NKG2A<sup>-/-</sup> mice (Fig. 4.6.A.). The lack of differences in Ad-OVA burden early during infection suggests that antigen availability is not contributing to enhanced DC cellularity or maturation in NKG2A<sup>-/-</sup> mice. We therefore evaluated differences in cytokines that regulate the

maturation and function of DCs. The proinflammatory cytokine IFN $\gamma$  has been shown to strongly activate naïve DCs; quantification of IFN $\gamma$  mRNA in whole liver homogenates using qRT-PCR revealed that in comparison to B6 mice, IFN $\gamma$  mRNA is increased at 3 and 6 dpi in NKG2A<sup>-/-</sup> livers (Fig. 4.6.B.). These data suggest that IFN $\gamma$  production by a local cellular source is increased in the absence of NKG2A.

We then considered liver-resident ILCs as the cellular source of IFN $\gamma$  as they express high levels of NKG2A. We therefore characterized naïve liver-resident ILCs in NKG2A<sup>-/-</sup> mice. Although there are no differences in the percentages of total ILCs from naïve B6 and NKG2A<sup>-/-</sup> livers, only NKG2A<sup>-/-</sup> CD49a<sup>+</sup> ILC1 exhibit higher cellularity in the steady-state (Fig 4.7.A-B.). In contrast, during Ad-OVA infection, the NKG2A<sup>-/-</sup> livers display an approximate 2-fold increase in the frequencies of total ILCs at 12 hpi and 24 hpi, when compared to B6 livers. However, unlike naïve livers, both the CD49b<sup>+</sup> NK cell and CD49a<sup>+</sup> ILC1 subsets isolated from infected NKG2A<sup>-/-</sup> livers were significantly increased in cellularity (Fig 4.7.A-B.).

To address the capacity of liver-resident ILC subsets to produce IFN $\gamma$  post-infection, we first measured IFN $\gamma$  mRNA in sorted CD49b<sup>+</sup> NK cells and CD49a<sup>+</sup> ILC1 from B6 and NKG2A<sup>-/-</sup> livers at 12 hpi with Ad-OVA. Interestingly, CD49a<sup>+</sup> ILC1 from the NKG2A<sup>-/-</sup> livers exhibit enhanced IFN $\gamma$  expression when compared to the same subset isolated from the B6 mice (Fig. 4.7.C.). In order to verify that the increase in IFN $\gamma$  transcript in NKG2A<sup>-/-</sup> CD49a<sup>+</sup> ILC1 was recapitulated at the protein level, we isolated total mononuclear cells from B6 and NKG2A<sup>-/-</sup> livers at 12 hpi and restimulated the ILCs with

IL-12 and IL-18 *in vitro*. CD49b<sup>+</sup> NK cells express significantly higher IFN $\gamma$  when compared to CD49a<sup>+</sup> ILC1; however, there were no differences in IFN $\gamma$  production in either liver-resident ILC subset between B6 and NKG2A<sup>-/-</sup> mice (Fig. 4.7.D. and Fig 4.8.A-B.). Previous reports have demonstrated that signals driving IFN $\gamma$  production in NK cells via stimulation with IL-12 and IL-18 can override the input of surface receptor signals that induce IFN $\gamma$ . Therefore, we assessed the ability of hepatic ILCs to make IFN $\gamma$  in response to cellular targets, i.e. YAC-1 T cell lymphoma. Accordingly, we isolated mononuclear cells from B6 and NKG2A<sup>-/-</sup> livers at 12 hpi, cultured them with YAC-1 targets *in vitro*, and probed for IFN $\gamma$  production in the ILC subsets. Compared to B6 mice, CD49a<sup>+</sup> ILC1 from NKG2A<sup>-/-</sup> livers produced more IFN $\gamma$  when stimulated with YAC-1 targets. Interestingly, CD49b<sup>+</sup> NK cells from both B6 and NKG2A<sup>-/-</sup> mice exhibit moderately enhanced IFN $\gamma$  production following the YAC-1 restimulation (Fig. 4.7.E.). In sum, liver-resident NKG2A<sup>-/-</sup> ILCs exhibit increased cellularity during Ad-OVA infection, but display enhanced IFN $\gamma$  production only when restimulated with a cellular target. Furthermore, assessing IFN $\gamma$  production in ILC subsets after IL-12 and IL-18 restimulation overrides intrinsic differences in IFN $\gamma$  expression seen with surface receptor signaling.

*NKG2A<sup>-/-</sup> livers have increased OT-I T cell accumulation and IFN $\gamma$  production in vivo*

To explore the impact of NKG2A deficiency in CD49a<sup>+</sup> ILC1 on naïve CD8<sup>+</sup> T cells responding to Ad-OVA infection *in vivo*, we adoptively transferred naïve CFSE labeled OT-I T cells into B6 and NKG2A<sup>-/-</sup> mice one day prior to i.v. Ad-OVA infection and analyzed the livers at 3 dpi for both the accumulation of OT-I T cells and their CFSE

dilution profiles. Infected NKG2A<sup>-/-</sup> T cell recipients displayed increased frequency and total numbers of responding OT-I T cells in the livers at 3 dpi (Fig. 4.9.A-B.). Moreover, the CFSE dilution profile of OT-I T cells in B6 and NKG2A<sup>-/-</sup> recipients revealed a more rapid division in the NKG2A<sup>-/-</sup> livers (Fig. 4.9.A.). In addition to an accelerated rate of proliferation, activated (responding) OT-I T cells isolated from the livers of NKG2A<sup>-/-</sup> mice display increased capacity to secrete IFN $\gamma$  in terms of both cell frequency and MFI upon *in vitro* stimulation with cognate synthetic peptide epitope (Fig. 4.9.C-D.).

*Increased endogenous CD8<sup>+</sup> T cell accumulation in the NKG2A<sup>-/-</sup> livers during Adenovirus infection*

In view of the enhanced accumulation of OT-I T cells in the NKG2A<sup>-/-</sup> livers at 3 dpi, it was of interest to identify any potential differences in the endogenous CD8<sup>+</sup> T cell response during hepatotropic viral infection. We therefore i.v. administered Ad-OVA and assessed the kinetics of total and OVA-specific CD8<sup>+</sup> T cells from 3 dpi through 40 dpi. Although the frequencies of CD8<sup>+</sup> T cells in the spleens are not significantly different between the B6 and NKG2A<sup>-/-</sup> mice (Fig. 4.10.A.), the frequencies and numbers of total and OVA-specific CD8<sup>+</sup> T cells are significantly increased in the NKG2A<sup>-/-</sup> livers starting at 6 dpi through 40 dpi (Fig. 4.10.B-D.). To corroborate that the endogenous CD8<sup>+</sup> T cell response recapitulates the OT-I transfer model (Fig. 4.9.) not only in cellularity, but also in function, we restimulated the endogenous CD8<sup>+</sup> T cells with cognate synthetic peptide and measured production of IFN $\gamma$ . As expected, the endogenous CD8<sup>+</sup> T cells display an increased capacity to secrete IFN $\gamma$ , as measured by frequency and MFI, upon *in vitro* stimulation with peptide at 6 dpi through 40 dpi (Fig

4.11.A-B.). In addition to a heightened intrinsic ability to produce IFN $\gamma$ , the absolute number of IFN $\gamma$ <sup>+</sup>CD8<sup>+</sup> T cells is also increased in the NKG2A<sup>-/-</sup> livers (Fig. 4.11.C.). Moreover, when compared to B6 mice, the IFN $\gamma$  message quantified from whole-liver homogenate at 6 dpi is increased in NKG2A<sup>-/-</sup> livers (Fig. 4.6.B.). Interestingly, in contrast to IFN $\gamma$  production, there appears to be no intrinsic difference in the endogenous CD8<sup>+</sup> T cells' ability to degranulate in either the B6 or NKG2A<sup>-/-</sup> livers, as measured by the frequencies of CD107a expression after similar restimulation (Fig. 4.11.D.). However, it must be noted that the NKG2A<sup>-/-</sup> livers accumulate a greater number of CD107a<sup>+</sup>CD8<sup>+</sup> T cells from 9 dpi through 40 dpi (Fig. 4.11.E.).

*Increased liver damage in the NKG2A<sup>-/-</sup> livers.*

The influx of activated immune cells within the liver is typically accompanied by hepatic damage. Given that the number of endogenous CD8<sup>+</sup> T cells was increased from 6 dpi to 40 dpi in the NKG2A<sup>-/-</sup> liver, we expected to see increased hepatic damage in NKG2A<sup>-/-</sup> mice. Not surprisingly, serum concentrations of alanine aminotransferase were increased in NKG2A<sup>-/-</sup> mice, which corroborated the increase in cellular infiltrate and tissue damage with greater cellular infiltrate in livers seen by H&E staining (Fig. 4.12.A-B.). It was of interest to assess the antigen burden during the endogenous CD8<sup>+</sup> T cell response to Ad-OVA infection. We therefore measured the level of OVA message in the B6 and NKG2A<sup>-/-</sup> livers at 6 dpi by qRT-PCR, and found that the NKG2A<sup>-/-</sup> mice exhibit decreased OVA message at 6 dpi, suggesting that the enhanced CD8<sup>+</sup> T cell accumulation is driving faster viral clearance (Fig. 4.12.C.).

## Discussion

In the present study, we examined the role of NKG2A<sup>+</sup> liver-resident innate lymphoid cells 1 (ILC1) in governing CD103<sup>+</sup> DC activation, leading to the functional induction of anti-viral CD8<sup>+</sup> T cells during hepatotropic viral infection. We have recently demonstrated that liver-resident CD103<sup>+</sup> DCs act locally as potent APCs early in Ad infection. Moreover, NK cell-mediated control of DC activation is a well-established phenomenon. However, the influence of liver-resident ILC subsets, namely ILC1, on DC activation in the liver during viral infection is not known. We found that depleting ILCs using the anti-aGM1 antibody prior to Ad infection leads to a significant loss of DC accumulation in the liver at 2 dpi, indicating the requirement for ILC help to efficiently activate DCs *in vivo*. Interestingly, depleting ILCs shortly following Ad infection enhances DC accumulation in the liver at 2 dpi, suggesting that resident ILCs have dual functional roles during infection and may be instrumental in dampening the immune response after initial activation (Fig. 2). By employing *KLRC1*-deficient mice, which globally lack expression of NKG2A, we demonstrate that liver-resident NKG2A<sup>+</sup> ILC1 play a critical role in suppressing an optimal CD8<sup>+</sup> T cell response to hepatic Ad infection, as NKG2A<sup>-/-</sup> ILC1 confer CD103<sup>+</sup> DCs with an enhanced ability to induce anti-viral CD8<sup>+</sup> T cells (Fig 3F). We further demonstrate that NKG2A signaling in liver-resident ILC1 via crosslinking with Qa-1b on cellular targets contributes to a reduction in their IFN $\gamma$  production during Ad infection (Fig 4E). Lastly, we find an increased endogenous anti-viral CD8<sup>+</sup> T cell response specifically in the NKG2A<sup>-/-</sup> livers, with heightened IFN $\gamma$  production, starting at 6 dpi through 40 dpi (Fig 7). Indeed, using histological staining we find enhanced liver cellular infiltrate, increased tissue damage as

measured by serum ALT levels, and a decreased viral load by 6 dpi in NKG2A<sup>-/-</sup> livers (Fig. 8).

In a previous study, we reported that when compared to splenic NK cells, hepatic ILCs are unique in their enhanced expression of the inhibitory receptor NKG2A and exhibit poor IFN $\gamma$  production upon IL-12 and IL-18 restimulation. We further demonstrated that liver ILCs transferred intravenously preferentially home back to the liver, suggesting that resident ILC subsets possess unique receptors that target liver-parenchymal ligands. Indeed, recently published inquiries substantiate that liver-resident ILC1, formally annotated as traditional NK cells, express the alpha-2 integrin CD49a. Consistent with these investigations, we confirm the presence of a liver-resident CD49a<sup>+</sup> ILC1 population that, expectedly, exhibits high expression of NKG2A in the steady-state (Fig 1A). We additionally find that the majority of CD49a<sup>+</sup> ILC1 constitutively express the alpha X integrin CD11c in the steady-state, suggesting that ILC1 may use additional integrins to trap in the liver tissue. Examining the relationship between ILC1 and the liver parenchyma using collagenase IV to disrupt tissue architecture, we find that increased enzymatic exposure led to increased ILC1 extraction (Fig 1A, B). We also demonstrate by fluorescent microscopy and *in situ* antibody tagging for flow cytometric analysis that CD49a<sup>+</sup> ILC1 represent the major ILC subset and preferentially reside in the perivascular spaces in the portal triads of the liver (Fig 1 C, D). The finding that both CD103<sup>+</sup> DCs and CD49a<sup>+</sup> ILC1 localize to similar anatomical sites was compelling evidence that liver-resident ILC1 may readily potentiate the function of CD103<sup>+</sup> DCs during hepatotropic viral infection. Furthermore, the ability of NK cells to associate with DCs during

inflammation was verified by their trogocytosis of surface receptors, i.e. MHC-II, from activated DCs. *Batf3*-deficient (*Batf3*<sup>-/-</sup>) mice exhibit a selective loss of CD103<sup>+</sup> and CD8a<sup>+</sup> DC subsets. Further confirming the association of ILC1 with CD103<sup>+</sup> DCs during Ad infection, the *Batf3*<sup>-/-</sup> mice display a loss of MHC-II uptake by liver-resident ILCs (Fig. 2A). Liver-resident ILC1 also express high levels of CD69 in the steady-state (Fig. 1A). It is interesting to note that CD69 is structurally related to CD94 and NKG2A, and that these proteins can be found in close proximity to each other on chromosome 6 in the murine genome. Traditionally, CD69 is considered an early marker of NK activation; however, its constitutive expression by hepatic ILC1 suggests that they may be continuously held in an activated state, albeit naturally inhibited by the correlating high expression of the inhibitory receptor NKG2A.

To further investigate the role of NKG2A<sup>+</sup> ILC1 in controlling hepatic-resident DC activation and accumulation during Ad infection, we analyzed CD11b<sup>+</sup> and CD103<sup>+</sup> subsets at 0, 12, and 24 hpi. It was unexpected to find that hepatic DCs exhibit increased cell numbers in the NKG2A<sup>-/-</sup> livers at steady-state. The liver continually receives immunogenic antigens from the portal blood draining the gastrointestinal tract. Due to the high exposure to constituents derived from commensal organisms and other non-pathogenic oral antigens, it is possible that liver-resident DCs are in a continuous state of activation and proliferation. Without suppression of local DCs attempting to initiate pro-inflammatory immune responses, the liver would be held in a state of hyperactivation, tissue stress and overall organ failure. It is conceivable that liver-resident ILC1

perpetually assess the status of local DCs, having the power to eliminate unwarranted responses by regulating DC numbers and activation.

Using the expression of the costimulatory receptors CD80 and CD86 as a readout for DC activation, we demonstrate a marked increase in CD86 MFI in both CD11b<sup>+</sup> and CD103<sup>+</sup> DCs in the NKG2A<sup>-/-</sup> livers, but a selective upregulation of CD80 in NKG2A<sup>-/-</sup> CD103<sup>+</sup> DCs at 12 hpi. Furthermore, when we sorted CD11b<sup>+</sup> and CD103<sup>+</sup> DCs from B6 and NKG2A<sup>-/-</sup> livers at 12 hpi and set them, in equal ratios, against CSFE<sup>+</sup> OT-I T cells *in vitro* for 4 days, only the NKG2A<sup>-/-</sup> CD103<sup>+</sup> DCs were capable of inducing enhanced OT-I accumulation when compared to B6 CD103<sup>+</sup> DCs. It is possible that the enhanced expression of both CD80 and CD86 are required for the robust OT-I accumulation found in cultures with NKG2A<sup>-/-</sup> CD103<sup>+</sup> DCs. However, CD8a<sup>+</sup> and CD103<sup>+</sup> DCs are considered the primary APCs cross-presenting acquired antigen to naïve CD8<sup>+</sup> T cells, suggesting that it is also feasible that CD103<sup>+</sup> DCs in the NKG2A<sup>-/-</sup> livers are inherently better at antigen uptake and/or processing when compared to the CD11b<sup>+</sup> subset.

Liver-resident CD103<sup>+</sup> DCs are capable of priming anti-viral CD8<sup>+</sup> T cells *in situ*. Indeed, as naïve CD8<sup>+</sup> T cells only require initial Ag exposure to begin the process of their clonal expansion, it is possible that in addition to the intrinsically enhanced state of maturation by resident DCs, simply having more readable APCs available for Ag presentation during the OT-I T cell adoptive transfer model may be significantly contributing to the enhanced number of activated OT-I T cells found in the NKG2A<sup>-/-</sup> livers at 3 dpi (Fig. 5). Although we did not explore whether liver-resident ILC1 are

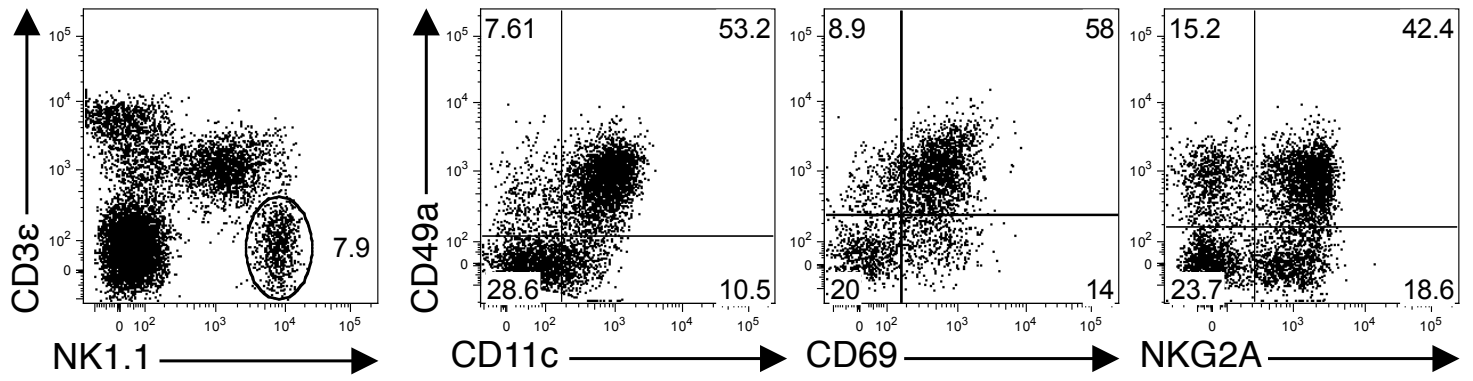
mediating OT-I T cell production of IFN $\gamma$  directly or through DC intermediates, the role of NKG2A<sup>+</sup> ILCs on global suppression of anti-viral immune responses in the liver is exciting for possible therapeutic applications.

It is thought that the concentration of inflammatory cytokines required to initiate a robust immune response in stressed tissues is not linear, but sigmoidal in nature, where a specific concentration of cytokine overcomes inhibition, leading to robust immune responses. The enhanced IFN $\gamma$  production via surface receptor signaling in NKG2A<sup>-/-</sup> CD49a<sup>+</sup> ILC1 suggests that NKG2A<sup>+</sup> ILC1 are naturally inhibited from producing high levels of IFN $\gamma$ , thereby limiting the concentration of IFN $\gamma$  required for local CD103<sup>+</sup> DC activation. Recent reports suggest that the induction of IFN $\gamma$  expression by surface receptor-ligand interaction on ILCs can be overridden by the presence of cytokines. Consistent with these findings, we demonstrate that the contribution of NKG2A mediated signaling in suppressing IFN $\gamma$  production is nullified by IL-12 and IL-18 restimulation (Fig. 4D). As we demonstrate increased IFN $\gamma$  message in whole liver homogenate and sorted CD49a<sup>+</sup> ILC1 from the NKG2A<sup>-/-</sup> mice early in Ad-OVA infection, it is likely that the contribution from cellular targets inducing ILC1 IFN $\gamma$  production is the primary mechanism controlling the levels of IFN $\gamma$  in the NKG2A<sup>-/-</sup> livers. However, the presence of higher levels of IL-12 and IL-18 in the NKG2A<sup>-/-</sup> livers driving IFN $\gamma$  expression has not been ruled out.

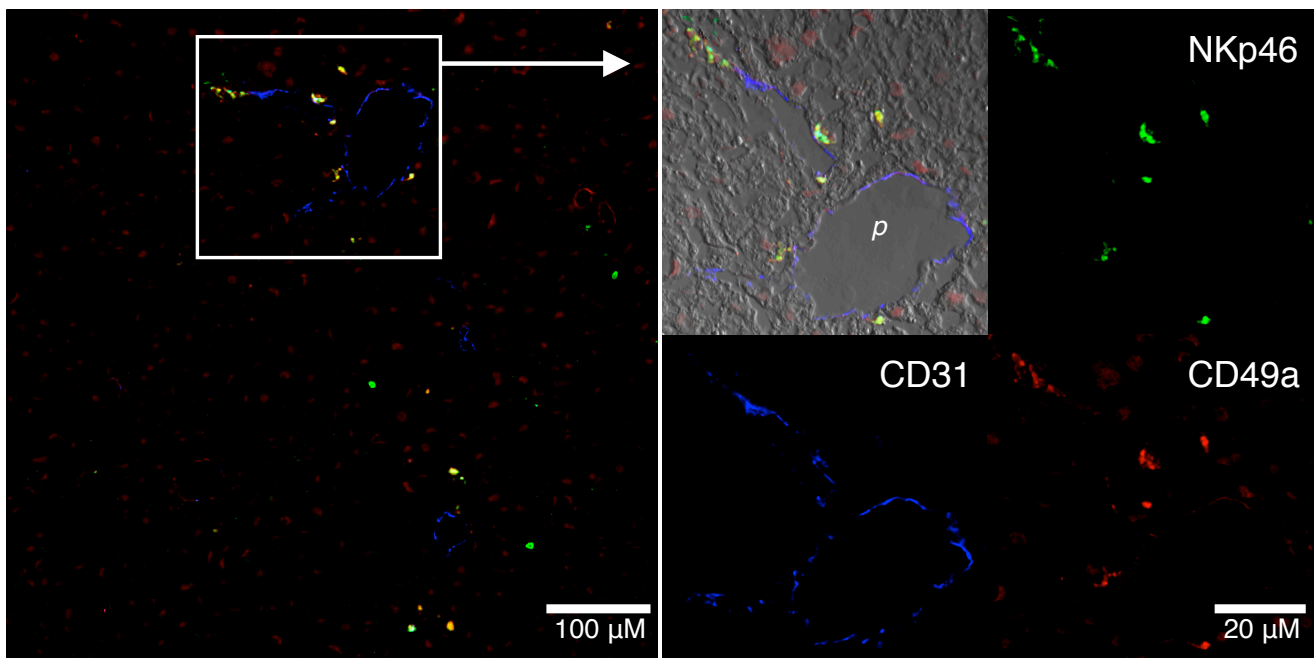
At present, there is an urgent need for vaccines capable of inducing robust and sustainable CD8<sup>+</sup> T cell responses to chronic or persistent hepatic infections. We

demonstrate enhanced endogenous CD8<sup>+</sup> T cell responses, which express significantly higher levels of IFN $\gamma$ , specifically in the NKG2A<sup>-/-</sup> livers starting at 6 dpi through 40 dpi. Recent literature has shown that CD11b<sup>+</sup> DCs play crucial roles in the production of memory anti-viral CD8<sup>+</sup> T cells. Although we find that CD103<sup>+</sup> DCs contribute to the activation and accumulation of CD8<sup>+</sup> T cells early in Ad-OVA infection, it is possible that CD11b<sup>+</sup> DCs are regulating the increased number of CD8<sup>+</sup> T cells seen at 40 dpi in the NKG2A<sup>-/-</sup> livers. Therefore, it is of interest to explore the nature of each liver-resident DC subset and their individual contribution to anti-viral CD8<sup>+</sup> T cells in the liver during to the course of hepatotropic viral infections. Lastly, blocking NKG2A on ILC1 in parallel with Ag delivery to hepatic resident DCs could significantly contribute to an effective vaccine that generates sustainable CD8<sup>+</sup> T cell responses required for the elimination of elusive hepatic pathogens.

**A**



**B**



**C**

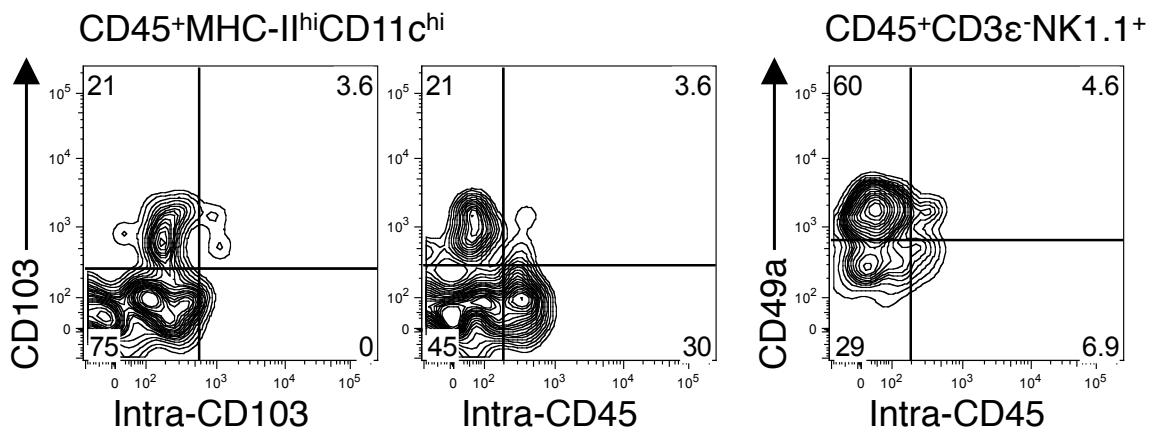
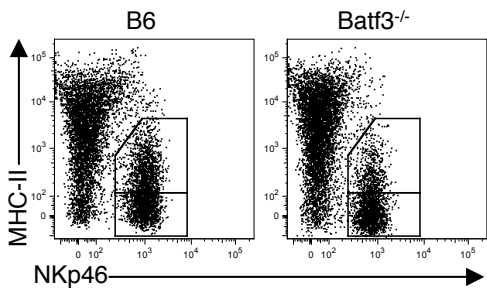


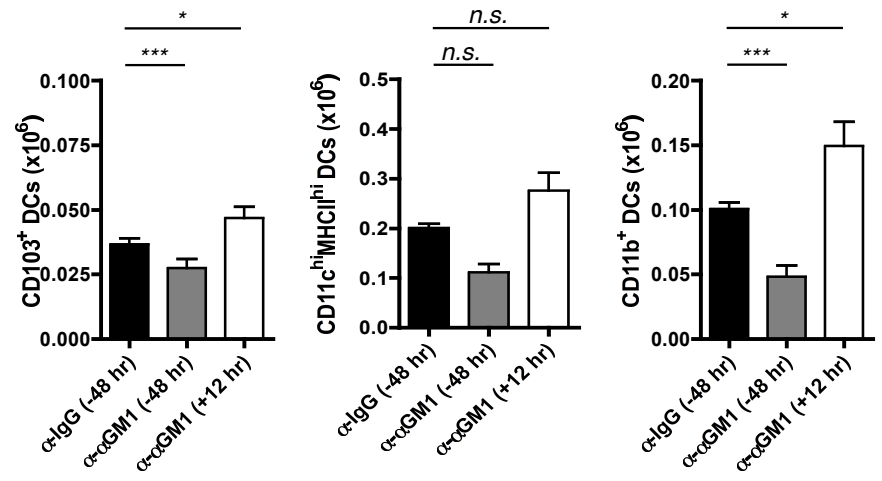
**Figure 4.1. CD49a<sup>+</sup> ILC1 are the major liver-resident ILC subset in the steady-state.**

(A – B) 8 – 12 week old C57BL/6 livers were perfused, digested for 0, 10, 20, or 30 min. in Collagenase IV at 37°C, and the mononuclear cells isolated by density gradient centrifugation. (A) Using flow cytometry, representative resident CD3ε<sup>-</sup>NK1.1<sup>+</sup> group 1 ILC populations, gated from debris and doublet excluded CD45<sup>+</sup> cells, are discriminated by CD49a and CD49b surface expression. (B) Fluorescence microscopy on a naïve liver section stained for CD49a<sup>+</sup> ILC1 using antibodies for CD31 (blue), CD49a (red) and NKp46 (green). (C) C57BL/6 livers with perfused with PBS followed by injection of anti-CD103 and anti-CD45 into the portal vein (x-axis). Representative flow plots of resident CD11c<sup>hi</sup>MHC-II<sup>hi</sup>CD103<sup>+</sup> DCs and CD3ε<sup>-</sup>NK1.1<sup>+</sup> group 1 ILCs gated from re-stained anti-CD45 population (tagged with a different fluorochrome) after mononuclear cell isolation via density gradient centrifugation. *Ex vivo* anti-CD103 staining was tagged with a different fluorochrome than *in situ* administered anti-CD103. (2 independent experiments, n = 4).

A



B



C

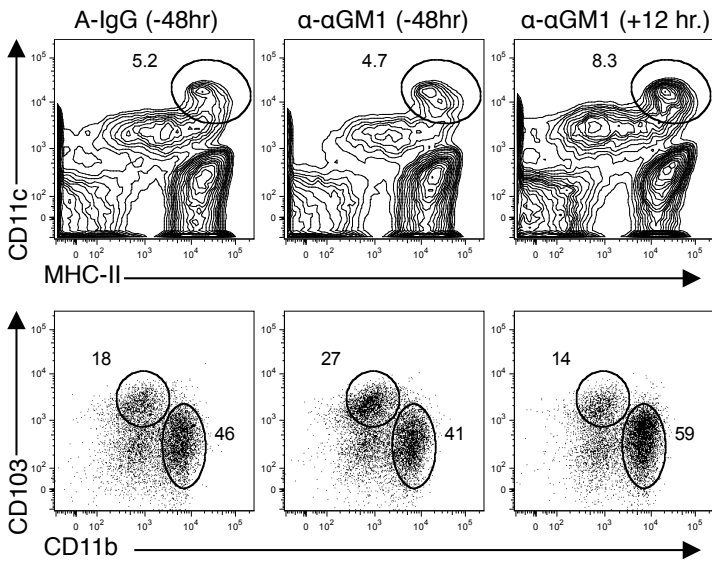
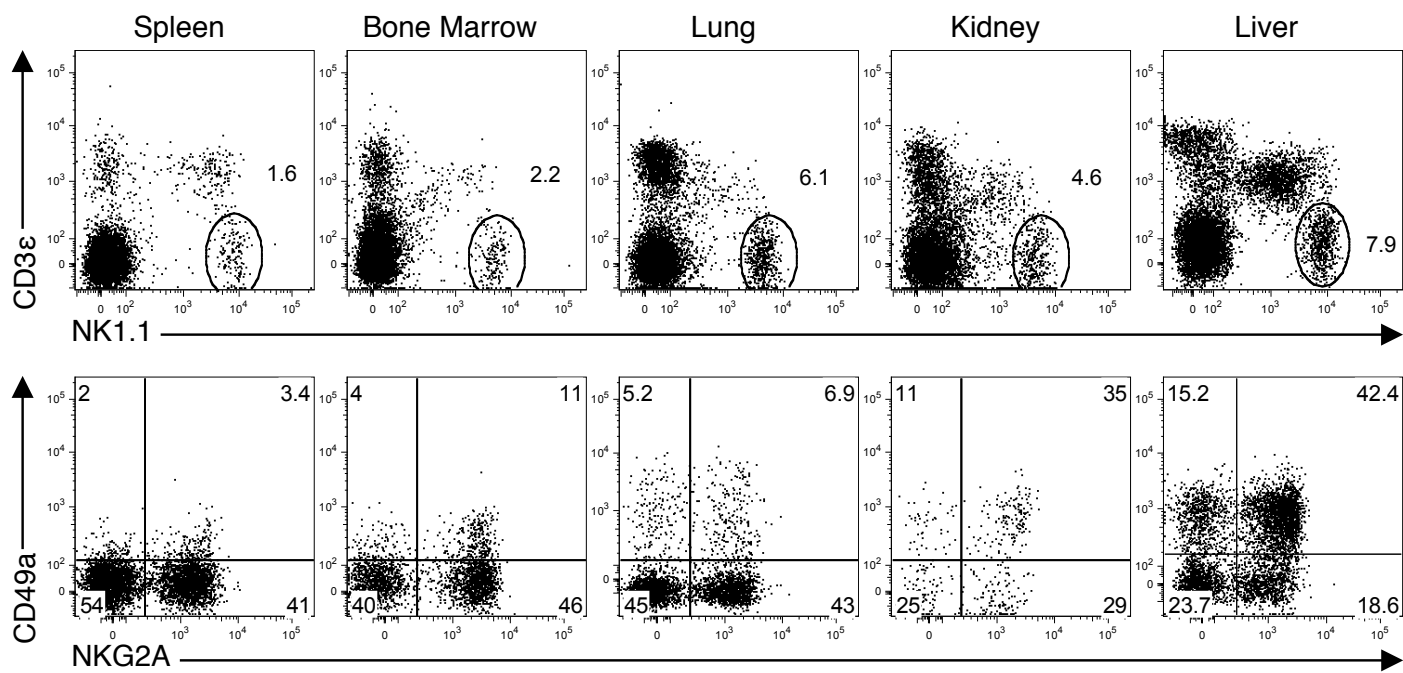


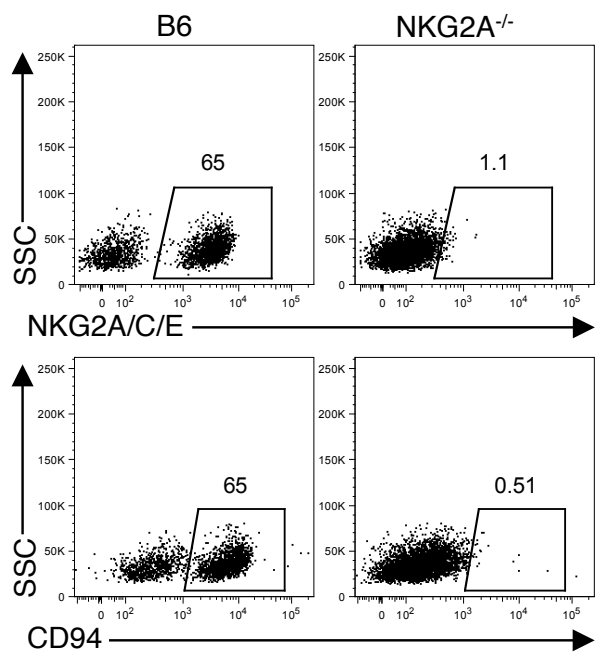
**Figure 4.2. Group 1 ILCs activate liver-resident DCs during Adenovirus infection.**

(A) Using flow cytometry, representative CD45<sup>+</sup> liver mononuclear cells stained for anti-MHC-II and anti-NKp46 from C57BL/6 or Batf3<sup>-/-</sup> livers. (3 independent experiments, n = 9). (B – C) Graphical representation(s) of (B) cellularity and (C) flow plots for total liver MHC-II<sup>hi</sup>CD11c<sup>hi</sup>, CD11b<sup>-</sup>CD103<sup>+</sup>, and CD103<sup>-</sup>CD11b<sup>+</sup> DCs from C57BL/6 mice that received 300µg anti-IgG (i.v.) or anti-αGM1 (i.v.) at -48 hours prior to, or 300µg anti-αGM1 (i.v.) at 12 hours post infection with 2.5 x 10<sup>7</sup> IU Ad-OVA (i.v.). (2 independent experiments, n = 6). Student's t test (two-tailed): \**p* < 0.05, \*\*\**p* < 0.001, n.s. not significant. Mean ± SEM.

A



B



C

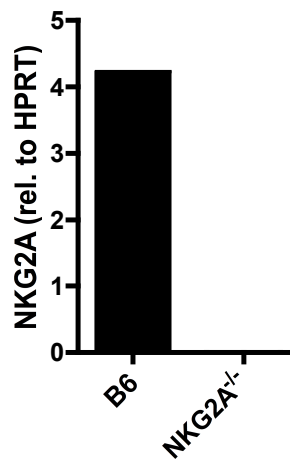
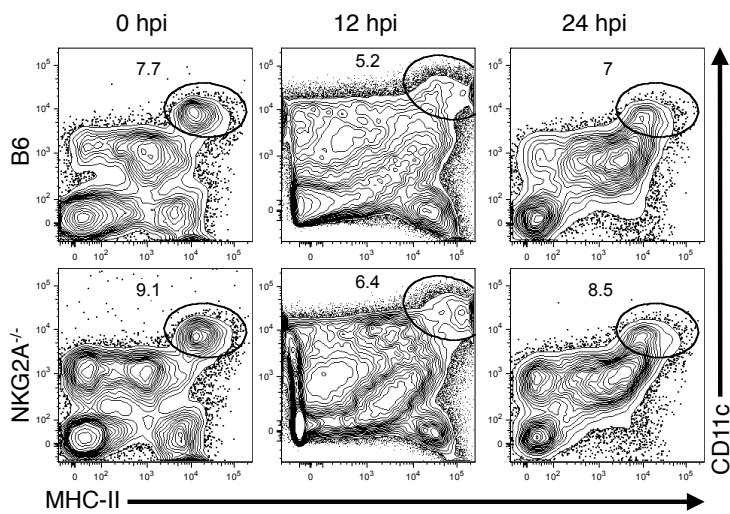


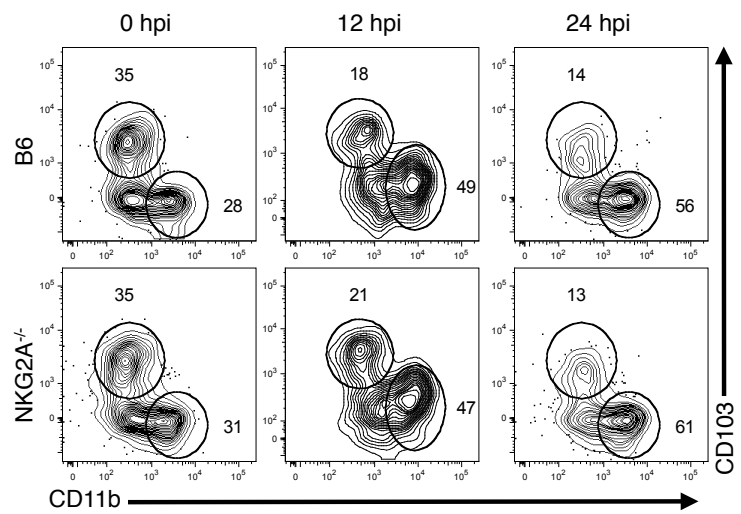
**Figure 4.3. Hepatic-resident CD49a<sup>+</sup> ILC1 express elevated NKG2A. (A)**

Representative CD45<sup>+</sup>CD3ε<sup>-</sup>NK1.1<sup>+</sup> group 1 ILC dot plots stained for NKG2A in C57BL/6 spleen, bone marrow, lung, kidney, and liver. (B) Representative CD45<sup>+</sup>CD3ε<sup>-</sup>NKp46<sup>+</sup> group 1 ILC dot plots stained for NKG2A/C/E and CD94 in C57Bl/6 and NKG2A<sup>-/-</sup> livers. (C) Relative qRT-PCR for NKG2A message from C57Bl/6 and NKG2A<sup>-/-</sup> sorted liver CD49a<sup>+</sup> ILC1. (2 independent experiments, n = 3 mice per experiment).

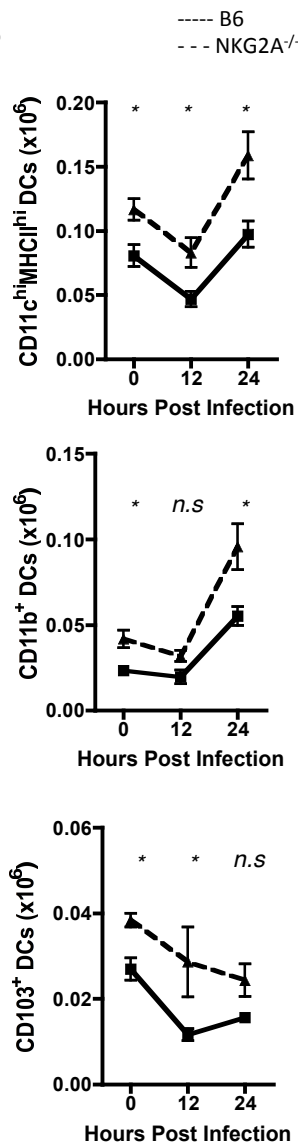
A



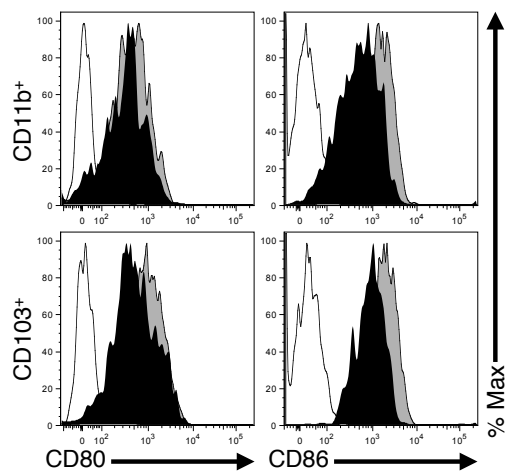
C



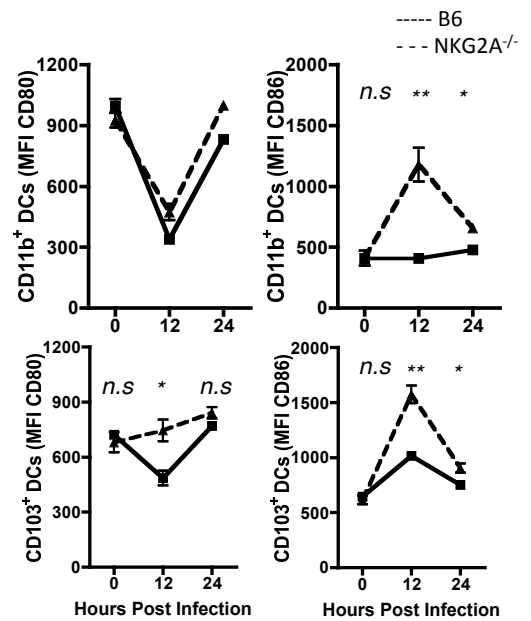
B



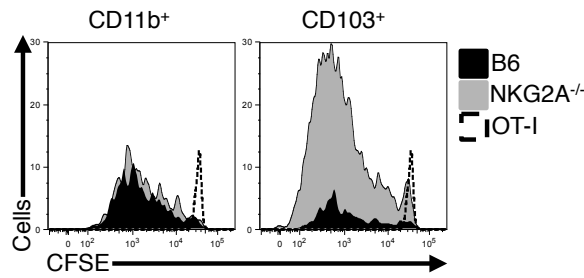
D



E



F



G

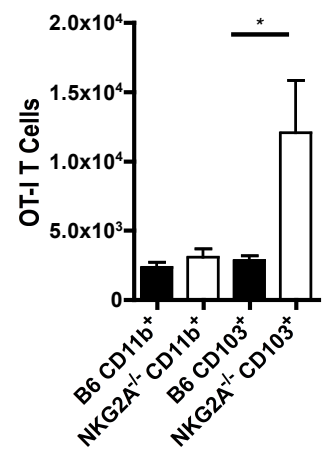
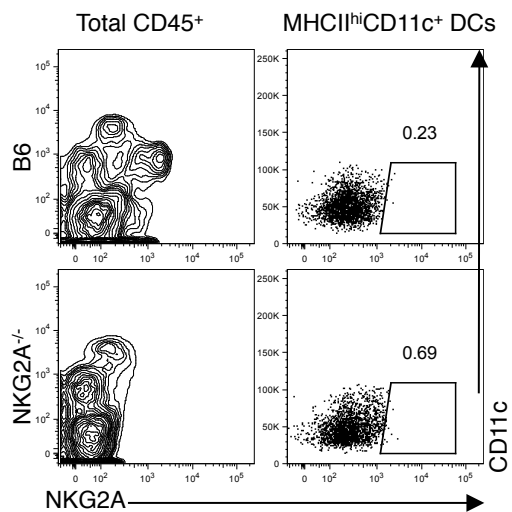
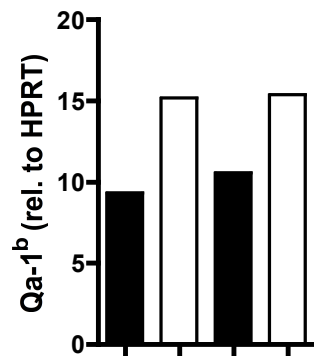


**Figure 4.4. Enhanced hepatic-resident DC numbers with enhanced priming by CD103<sup>+</sup> DCs in NKG2A<sup>-/-</sup> mice during Ad-OVA infection.** (A – E) CD45<sup>+</sup>MHC-II<sup>hi</sup>CD11c<sup>hi</sup> liver-resident DCs in naïve and 2.5 x 10<sup>7</sup> IU Ad-OVA (i.v.) infected C57Bl/6 and NKG2A<sup>-/-</sup> mice (representative of 2 independent experiments, n = 3 – 4 mice per experiment). (A – C) Representative (A) MHC-II<sup>hi</sup>CD11c<sup>hi</sup> and (C) CD11b<sup>+</sup> versus CD103<sup>+</sup> DC dot plots in C57Bl/6 and NKG2A<sup>-/-</sup> livers at 0, 12, and 24 hpi. (C) Graphical representation of total, CD11b<sup>+</sup>, and CD103<sup>+</sup> DC absolute numbers in C57Bl/6 (bold lines) and NKG2A<sup>-/-</sup> (dotted lines) livers at 0, 12, and 24 hpi. (D) Representative CD80 and CD86 histograms from CD11b<sup>+</sup> and CD103<sup>+</sup> C57Bl/6 (black) and NKG2A<sup>-/-</sup> (grey) liver DCs at 12h hpi. (E) Graphically quantified mean fluorescence intensity (MFI) of CD80 and CD86 from CD11b<sup>+</sup> and CD103<sup>+</sup> C57Bl/6 (black) and NKG2A<sup>-/-</sup> (grey) liver DCs at 0, 12, and 24 hpi. (F – G) Representative divided OT-I (F) CFSE dilution histograms and (G) quantified cell numbers (via counting beads, Spherotech<sup>inc</sup>) from cocultures of FACs sorted CD11b<sup>+</sup> and CD103<sup>+</sup> DCs, from 12 hours 2.5 x 10<sup>7</sup> IU Ad-OVA infected (i.v.) C57Bl/6 (black) and NKG2A<sup>-/-</sup> (white) livers, to OT-Is at a ratio of 2 x 10<sup>4</sup> : 2 x 10<sup>5</sup> for 4 days at 37°C (representative of 2 independent experiments done in triplicate). Student's t test (two-tailed): \**p* < 0.05, \*\**p* < 0.01, n.s. not significant. Mean ± SEM.

A



B



C

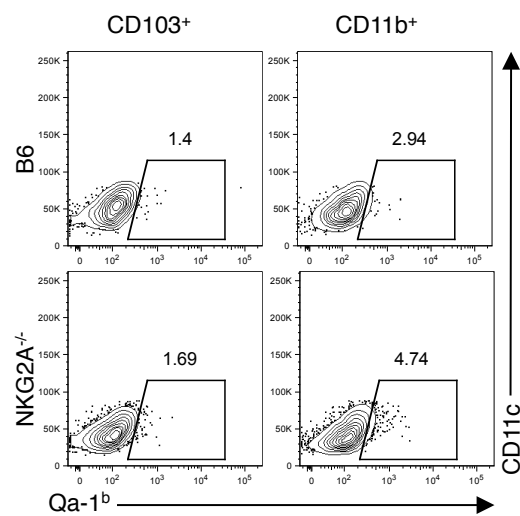
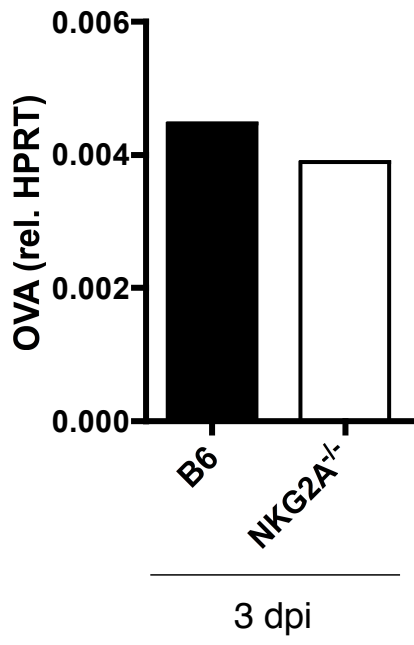
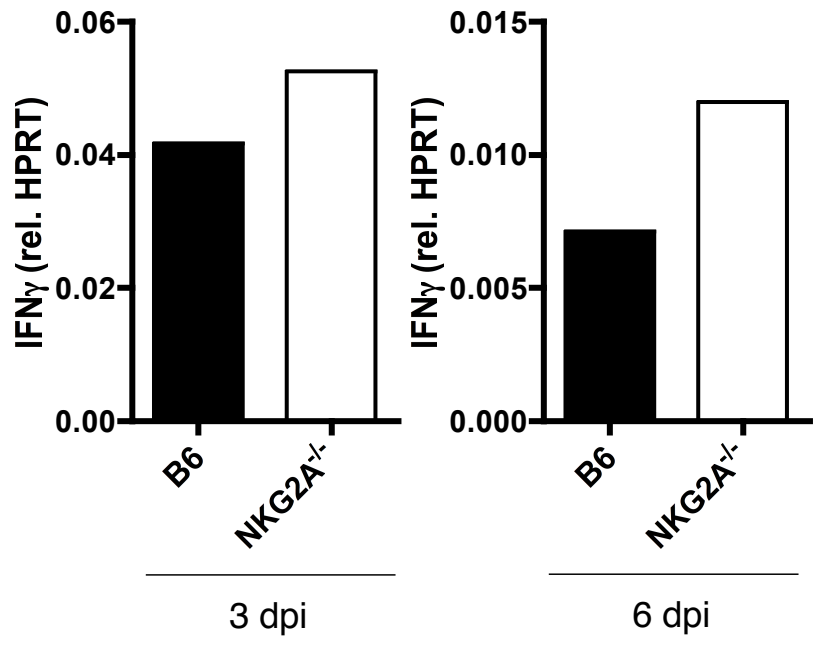


**Figure 4.5. Liver-resident DCs lack NKG2A but express Qa1b.** (A – C) C57Bl/6 and NKG2A<sup>-/-</sup> mice infected with  $2.5 \times 10^7$  IU Adenovirus-OVA (i.v.) (representative of 2 independent experiments, n = 3 mice per experiment). (A) Representative flow plots of total liver CD45<sup>+</sup> mononuclear cell and MHCII<sup>hi</sup>CD11c<sup>hi</sup> DC NKG2A expression at 2 dpi. (B) Relative qRT-PCR for Qa-1b message from 12 hpi sorted CD11b<sup>+</sup> and CD103<sup>+</sup> liver-resident DC subsets. (C) Representative flow plots of Qa1b expression on liver-resident CD11b<sup>+</sup> and CD103<sup>+</sup> DC subsets as 12 hpi.

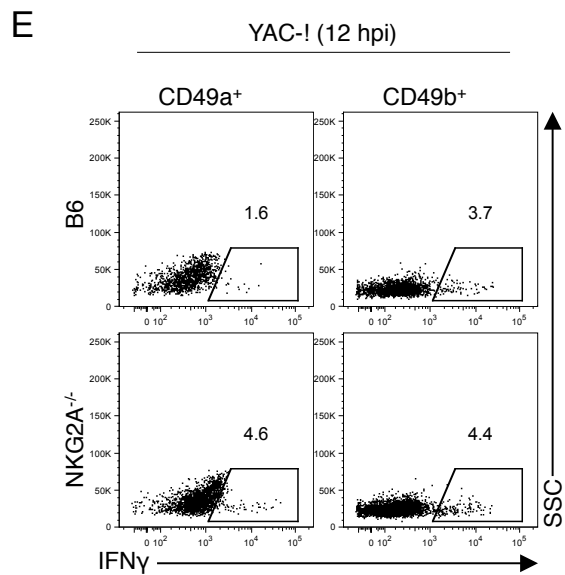
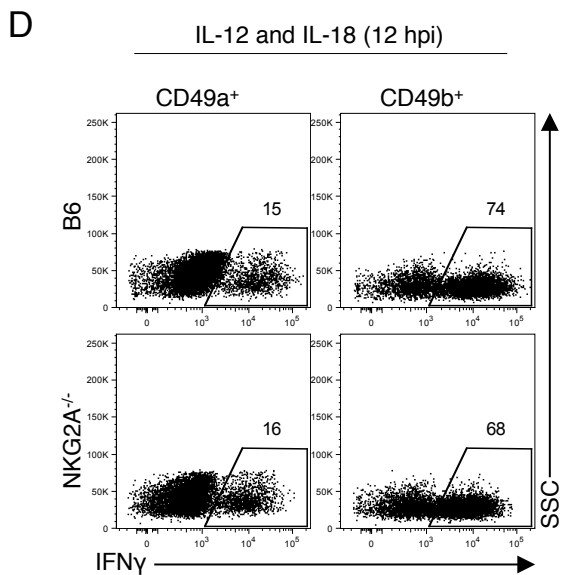
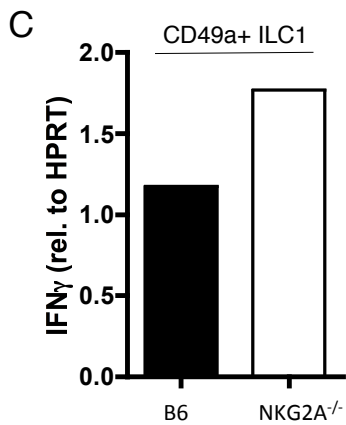
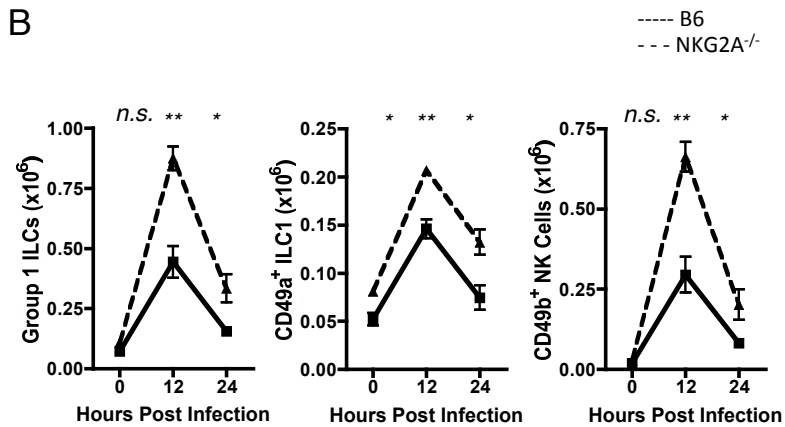
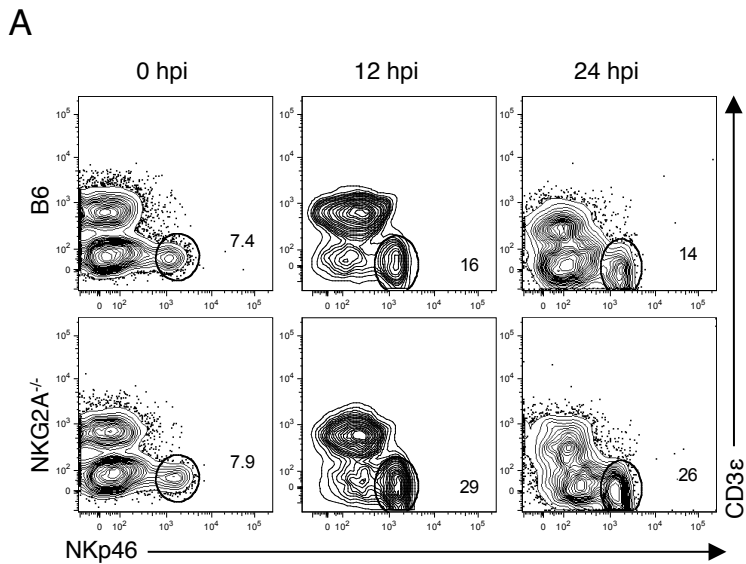
A



B



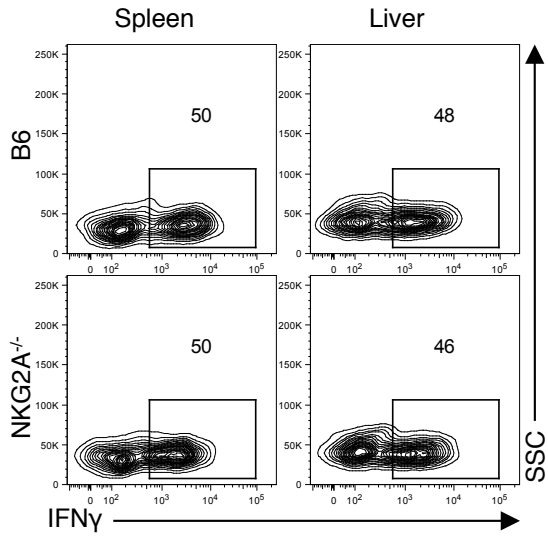
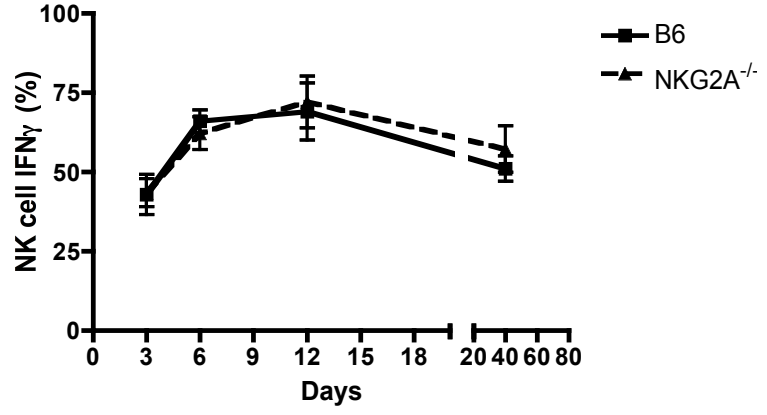
**Figure 4.6. Similar viral-load in NKG2A<sup>-/-</sup> livers at 3 dpi with Ad-OVA. (A – B)**  
C57BL/6 and NKG2A<sup>-/-</sup> mice infected with  $2.5 \times 10^7$  IU Adenovirus-OVA (i.v.)  
(representative of 4 independent experiments, n = 3 mice per experiment). (A) Relative  
qRT-PCR for OVA message from 1 gram of liver homogenate at 3 dpi. (B) Relative  
qRT-PCR for IFN $\gamma$  message from 1 gram of liver homogenate at 3 and 6 dpi.



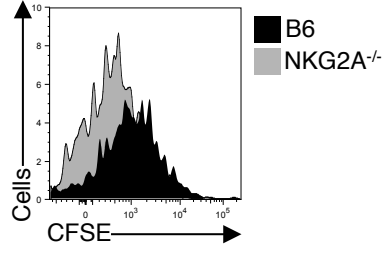
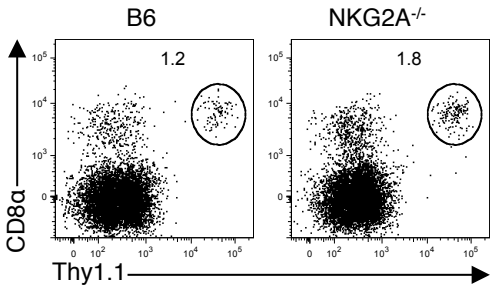
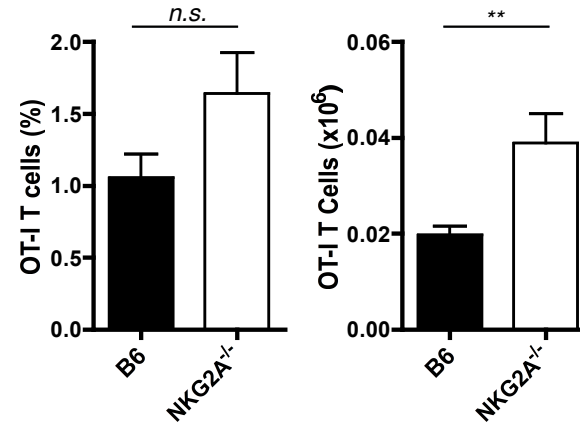
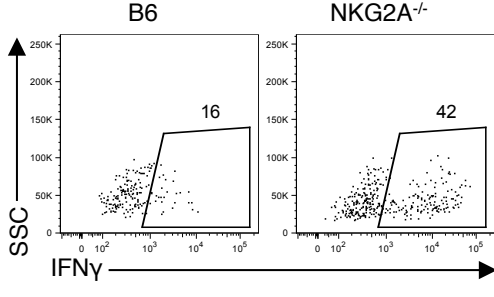
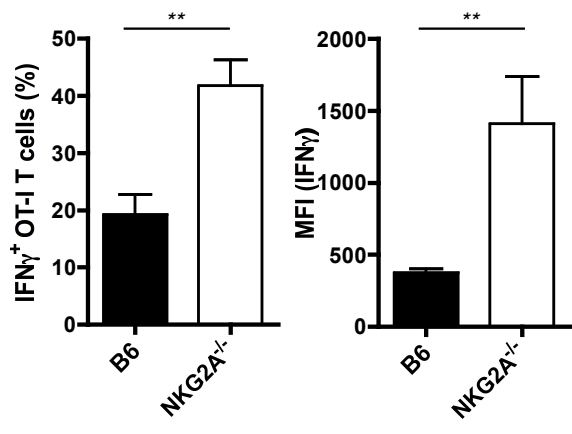
**Figure 4.7. Enhanced CD49a<sup>+</sup> ILC1 number and IFN $\gamma$  production in NKG2A<sup>-/-</sup> livers during Ad-OVA infection.** (A – B) Representative (A) CD45<sup>+</sup>CD3 $\epsilon$ <sup>-</sup>NKp46<sup>+</sup> liver-resident group 1 ILC dot plots and (B) quantified cellularity of total group 1 ILCs, CD49a<sup>+</sup> ILC1, and CD49b<sup>+</sup> NK cells from naïve and 2.5 x 10<sup>7</sup> IU Ad-OVA (i.v.) infected C57Bl/6 and NKG2A<sup>-/-</sup> livers (representative of 2 independent experiments, n = 3 – 4 mice per experiment). (C) Relative qRT-PCR for IFN $\gamma$  message from C57Bl/6 and NKG2A<sup>-/-</sup> sorted liver CD49a<sup>+</sup> ILC1 at 12 hpi with 2.5 x 10<sup>7</sup> IU Ad-OVA (i.v.). (D – E) Representative flow plots for IFN $\gamma$  from 12 hpi (2.5 x 10<sup>7</sup> IU Ad-OVA (i.v.)) C57BL/6 and NKG2A<sup>-/-</sup> liver CD49a<sup>+</sup> ILC1 and CD49b<sup>+</sup> NK cells restimulated with (D) 100ng IL-12/IL-18 or (E) 1:1 YAC-1 cells for 5 hr. at 37°C. (representative of 2 independent experiments, n = 3 mice per experiment). Student's t test (two-tailed): \**p* < 0.05, \*\**p* < 0.01, n.s. not significant. Mean  $\pm$  SEM.

**A**

3 dpi

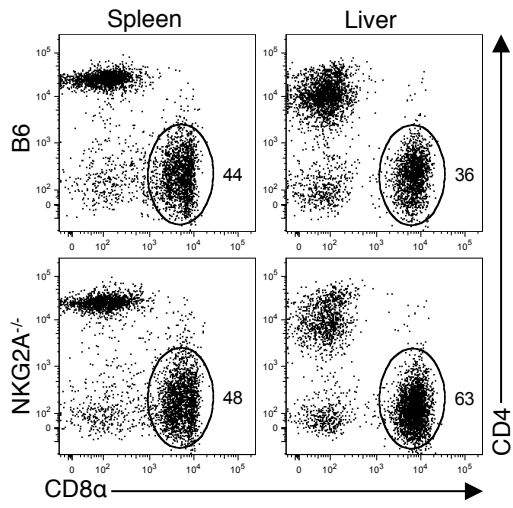
**B**

**Figure 4.8. NKG2A<sup>-/-</sup> liver-resident group 1 ILC exhibit no differences in IFN $\gamma$  production after IL-12 and IL-18 restimulation.** (A – B) Liver-resident group 1 ILC IFN $\gamma$  production after restimulation with 100ng IL-12/IL-18 for 5 hr. at 37°C from C57BL/6 and NKG2A<sup>-/-</sup> mice infected with 2.5 x 10<sup>7</sup> IU Adenovirus-OVA (i.v.) (representative of 3-4 independent experiments, n = 3 mice per experiment). (A) Representative flow plots of IFN $\gamma$  at 3 dpi. (B) Quantified frequencies of IFN $\gamma$  from 3 – 40 dpi.

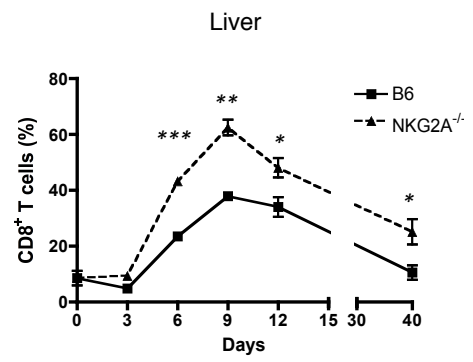
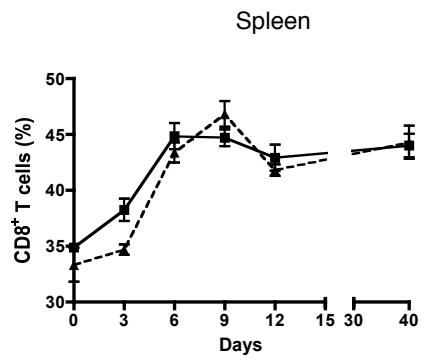
**A****B****C****D**

**Figure 4.9. Enhanced antigen-specific CD8<sup>+</sup> T cells in NKG2A<sup>-/-</sup> livers during Ad-OVA infection.** (A – D)  $2 \times 10^5$  naïve CFSE<sup>+</sup> OT-I cells were transferred via the tail vein into C57Bl/6 and NKG2A<sup>-/-</sup> mice 1 day prior to  $2.5 \times 10^7$  IU Ad-OVA infection (i.v.) (representative of 3 independent experiments, n = 3 mice per experiment). (A) Representative CD45<sup>+</sup>CD8 $\alpha$ <sup>+</sup>Thy1.1<sup>+</sup> OT-I flow plots and CFSE dilution histograms from C57BL/6 (black) and NKG2A<sup>-/-</sup> (grey) livers at 3 dpi. (B) Quantified OT-I CD8<sup>+</sup> T cell frequencies and cellularity from C57Bl/6 (black) and NKG2A<sup>-/-</sup> (white) livers at 3 dpi. (C – D) Representative IFN $\gamma$ <sup>+</sup> OT-I (C) flow plots and (D) frequencies and mean fluorescence intensity (MFI) from C57Bl/6 (black) and NKG2A<sup>-/-</sup> (white) livers at 3 dpi. Student's t test (two-tailed): \* $p < 0.05$ , \*\* $p < 0.01$ , n.s. not significant. Mean  $\pm$  SEM.

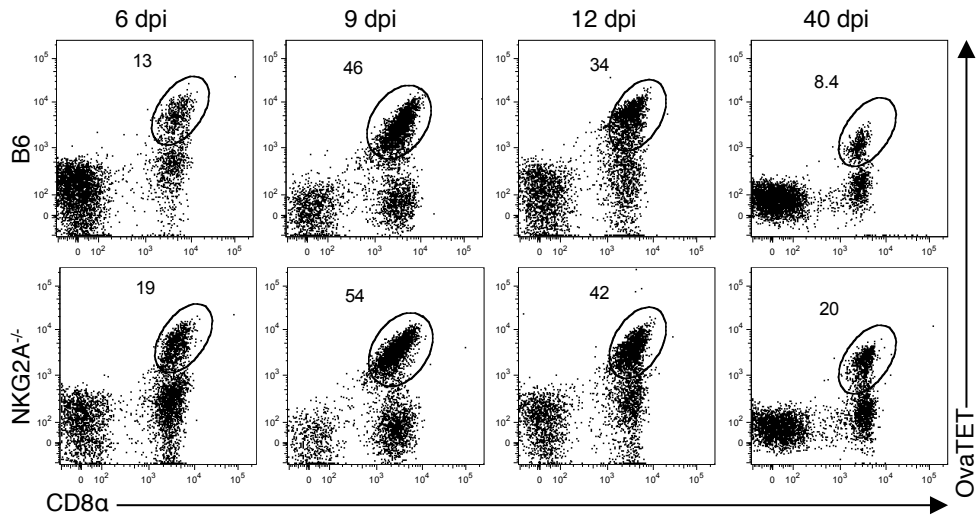
A



B



C



D

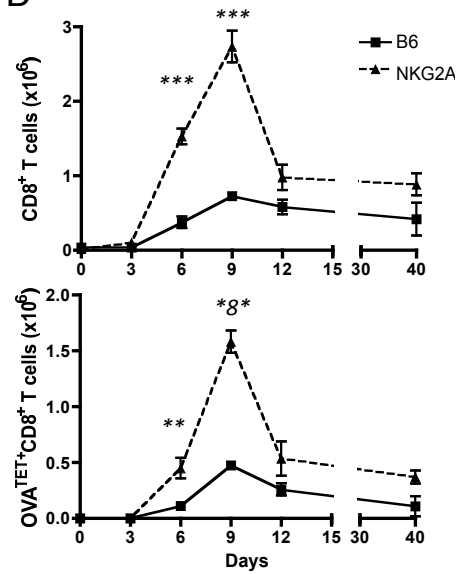
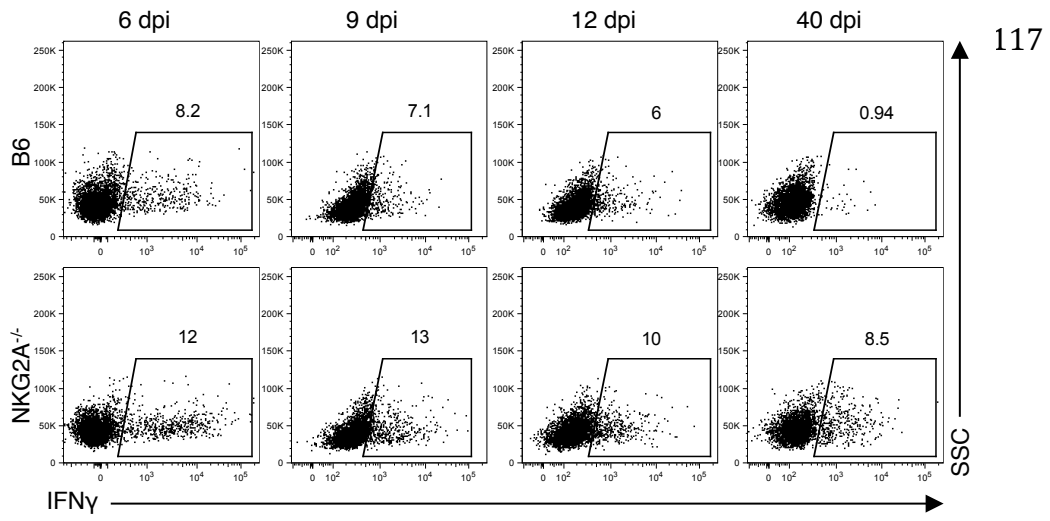
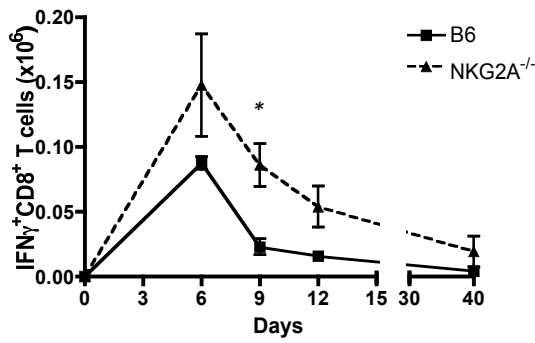


**Figure 4.10. NKG2A<sup>-/-</sup> mice exhibit increased hepatic CD8<sup>+</sup> T cells during Ad-OVA infection.** (A – G) C57Bl/6 and NKG2A<sup>-/-</sup> mice infected with  $2.5 \times 10^7$  IU Adenovirus-OVA (i.v.) (representative of 2 independent experiments, n = 3 – 4 mice per experiment). (A) Representative splenic and liver Thy1.2<sup>+</sup> T cell flow plots stained for CD4<sup>+</sup> and CD8<sup>+</sup> surface expression at 9 dpi. (B) Quantified frequencies from C57Bl/6 (bold lines) and NKG2A<sup>-/-</sup> (dotted lines) spleens and livers at 0, 3, 6, 9, and 40 dpi. (C) Representative liver OVA<sup>tet+</sup>CD8<sup>+</sup> T cell dot plots and (D) quantified total liver CD8<sup>+</sup> and OVA<sup>tet+</sup>CD8<sup>+</sup> T cell numbers at 6, 9, 12, and 40 dpi. Student's t test (two-tailed): \* $p < 0.05$ , \*\* $p < 0.01$ , \*\*\* $p < 0.001$ . Mean  $\pm$  SEM.

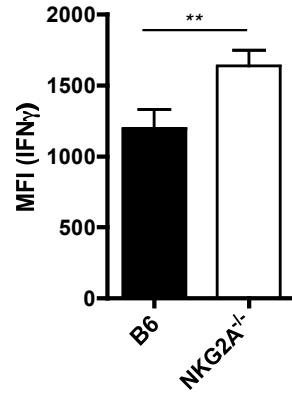
A



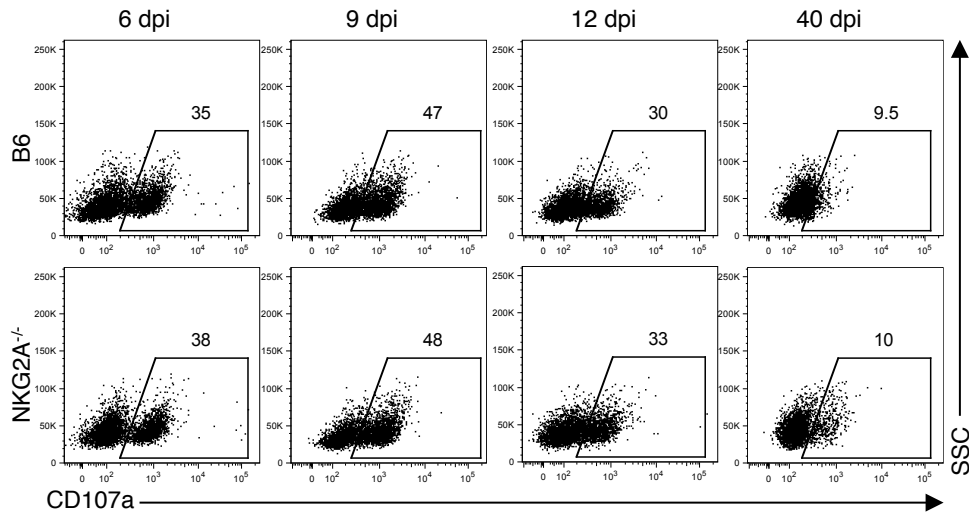
B



C



D



F

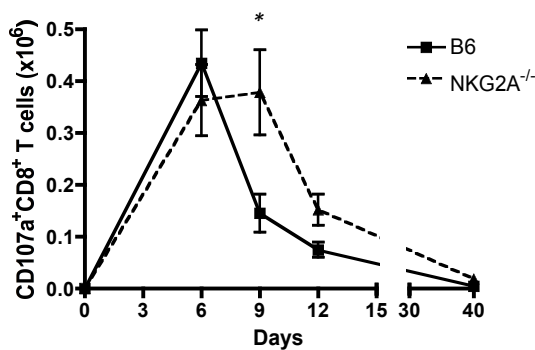
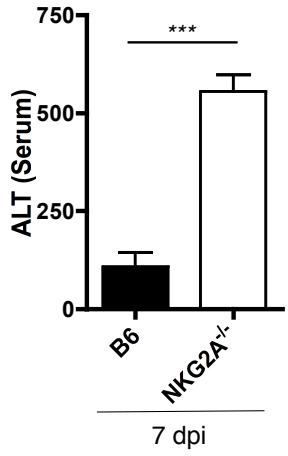
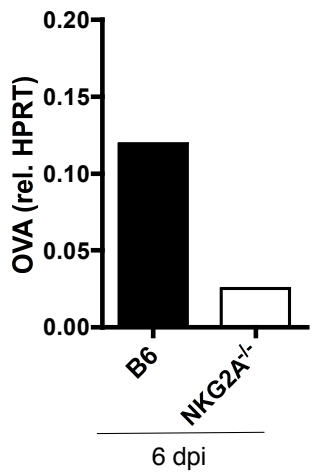


**Figure 4.11. NKG2A<sup>-/-</sup> mice exhibit increased hepatic IFN $\gamma$ <sup>+</sup> and CD107a<sup>+</sup> CD8<sup>+</sup> T cells during Ad-OVA infection.** (A – F) C57Bl/6 and NKG2A<sup>-/-</sup> mice infected with  $2.5 \times 10^7$  IU Adenovirus-OVA (i.v.) (representative of 2 independent experiments, n = 3 – 4 mice per experiment). (A – B) Representative liver IFN $\gamma$ <sup>+</sup>CD8<sup>+</sup> T cell (A) flow plots and (B) absolute numbers from total Thy1.2<sup>+</sup> cells at 6, 9, 12, and 40 dpi. (C) Quantified IFN $\gamma$  mean fluorescence intensity (MFI) at 6 dpi. (E – F) Representative liver CD107a<sup>+</sup>CD8<sup>+</sup> T cell (E) flow plots and (F) absolute numbers from total Thy1.2<sup>+</sup> cells at 6, 9, 12, and 40 dpi. Student's t test (two-tailed): \* $p < 0.05$ , \*\* $p < 0.01$ , Mean  $\pm$  SEM.

A



C



B

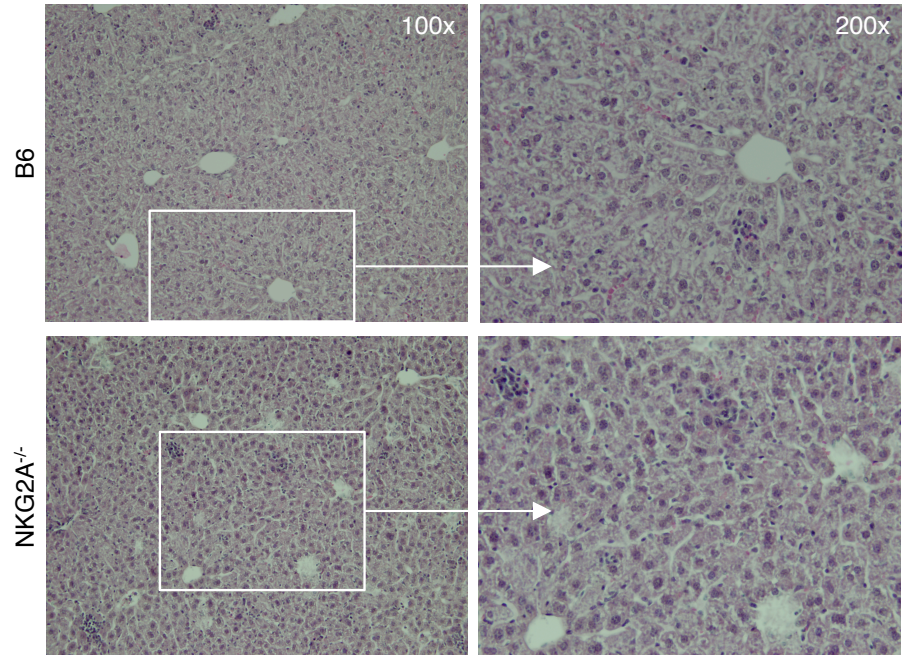


**Figure 4.12. Enhanced tissue damage and cellular infiltrate in NKG2A<sup>-/-</sup> livers during Ad-OVA infection.** (A – C) C57Bl/6 and NKG2A<sup>-/-</sup> mice infected with  $2.5 \times 10^7$  IU Adenovirus-OVA (i.v.) (representative of 2 independent experiments, n = 3 – 4 mice per experiment). (A) Alanine aminotransferase (ALT) levels from serum at 7 dpi. (B) H&E staining of liver tissue at 6 dpi. (C) Relative qRT-PCR for OVA message from 1 gram of liver homogenate at 6 dpi. Student's t test (two-tailed): \*\*\* $p < 0.001$ . Mean  $\pm$  SEM.

## **Chapter 5: Conclusions and Future Directions**

The molecular and cellular machinery controlling immunosuppression in the liver are of great interest to immunologists investigating potential therapeutic targets designed to disrupt the natural state of hyporesponsiveness, where the general strategy is to tip the immunologic balance away from tolerance. Although, the alternative approach has been gaining favor in recent years, where therapeutically enhancing the inherent potential for robust immune responses could prove successful. Next generation vaccine development seems to be moving in this direction, i.e. crosslinking specific TLR's to induce unique and regulated states of activation. Moreover, combinational therapies have recently proven to be incredibly successful in controlling chronic infections, including HIV and HCV, suggesting they are the logical next step in designing effective medicine for persistent hepatotropic pathogens. The rationale for my thesis work was to explore the early immunological events contributing to anti-viral responses in the liver. To do this I first probed the liver-resident APCs required for priming robust and sustainable anti-viral CD8<sup>+</sup> T cell responses (Chapter 3), and followed up by investigating how the liver has evolved to suppress the activation of those APCs (Chapter 4). In combination, future therapeutics directed from both angles could prove advantageous in driving robust immune responses required to eliminate or successfully vaccinate against deleterious hepatotropic pathogens. My data suggests targeting antigen to hepatic CD103<sup>+</sup> DCs while inhibiting ILC1 NKG2A signaling is a promising approach for inducing robust and sustainable anti-viral CD8<sup>+</sup> T cell responses in the liver.

### **Liver-resident DCs**

It is widely accepted that non-hematopoietic parenchymal cells prime unsustainable anti-viral CD8<sup>+</sup> T cells that lack strong effector profiles. However, the liver is able to mount robust anti-viral CD8<sup>+</sup> T cell responses, suggesting alternative APCs are required for effective anti-viral immunity. DCs exhibit the fundamental features necessary to induce sustained CD8<sup>+</sup> T effector cells, suggesting they are important APCs for successful anti-viral immunity in the liver. Previously published data demonstrating that hepatic DCs are poor APCs has discouraged further investigation into how these cells control anti-viral responses in the liver. However, recently developed genetically modified mouse models lacking specific DC subsets allow us to readdress the functional contribution of liver-resident DCs on anti-viral immunity. Using *Batf3*<sup>-/-</sup> and *CCR7*<sup>-/-</sup> mice, I demonstrate that CD103<sup>+</sup> DCs are highly immunogenic APCs capable of priming naïve CD8<sup>+</sup> T cells directly in the liver parenchyma during an Ad-OVA infection model.

Published reports suggest CD103<sup>+</sup> DCs are a minor population in naïve mouse livers. However, these findings failed to consider the importance of mononuclear cell isolation strategies in skewing the representation of intra-hepatic leukocyte profiles. For this reason I first optimized the isolation method to more accurately assess the DC repertoire, finding that disruption of liver tissue with digestion enzymes is necessary to efficiently dissociate all DC subsets. Comparing anti-CD45 magnetic cell sorting and histodenz gradient centrifugation after various digestion times with collagenase IV suggested that isolated DCs are best represented using flow cytometry after 30 min. digestion with gradient centrifugation, where there is optimal cellular dissociation with minimal death. I therefore used this isolation method for the duration of my investigations. As such we

fully characterize liver-resident DCs in the steady-state and found that the CD103<sup>+</sup> subset is indeed the dominant DC population by frequency and cellularity.

The hepatic DC profiles are merely ancillary data to whether diverse DC subsets exhibit unique functional capacity to present antigen to cognate naïve CD8<sup>+</sup> T cells. I therefore cell sorted liver-resident DC subsets and set them against naïve antigen-specific CD8<sup>+</sup> T cells *in vitro* for 4 days, after pulsing the DCs with peptide that can be presented to activate those T cells. The enhanced recovery of divided CD8<sup>+</sup> T cells from the CD103<sup>+</sup> DC cocultures, as compared to the CD11b<sup>+</sup> DCs or pDCs cocultures, suggest that liver-resident CD103<sup>+</sup> DCs exhibit superior potential to prime naïve CD8<sup>+</sup> T cells when compared to other liver DC subsets. However, this strategy for assessing hepatic DCs intrinsic ability to potentiate naïve CD8<sup>+</sup> T cell activation limits my interpretation of the results, where I am unable to address whether CD103<sup>+</sup> DCs are priming a greater number of naïve CD8<sup>+</sup> T cells early in activation, only merely sustainable CD8<sup>+</sup> T cells that can be recovered by 4-days in coculture. Furthermore, using the 4-day time point inhibits my ability to assess functional responses of the activated CD8<sup>+</sup> T cells, as it is unlikely these cells are receiving TCR stimulation due to the loss of available antigen. It would be interesting to kinetically assess CD8<sup>+</sup> T cell activation during the *in vitro* cocultures. If CD103<sup>+</sup> DCs are able to induce potent naïve CD8<sup>+</sup> T cell activation leading to increased accumulation at 1, 2, and 3 days in coculture, the data would support an enhanced ability by CD103<sup>+</sup> DCs to prime naïve CD8<sup>+</sup> T cells. In contrast, if CD11b<sup>+</sup> DCs lead to equal or increased accumulation at 1 day in coculture, the data would suggest that CD103<sup>+</sup> DC primed CD8<sup>+</sup> T cells exhibit superior survival when compared to CD11b<sup>+</sup> DC primed

CD8<sup>+</sup> T cells. Lastly, assessing the functional capacity of activated CD8<sup>+</sup> T cells, i.e. IFN $\gamma$  expression, at 1 or 2 day cocultures would be valuable information for understanding the different contributions of hepatic DC subsets on controlling activated CD8<sup>+</sup> T cell effector functions.

Indeed, the lack of functional differences, as qualified by IFN $\gamma$  and GrB expression, in activated CD8<sup>+</sup> T cells from Ad-OVA infected B6 or Batf3<sup>-/-</sup> livers makes it difficult to assess the *in vivo* contribution that CD103<sup>+</sup> DCs may impart on anti-viral CD8<sup>+</sup> T cells' effector status. There is discrepancy in the data, where I do see suppressed IFN $\gamma$ <sup>+</sup>CD8<sup>+</sup> T cells in the Batf3<sup>-/-</sup> livers during MCMV-OVA infection, suggesting CD103<sup>+</sup> DCs are indeed promoting robust and sustainable anti-viral CD8<sup>+</sup> T cells in this model. As Ad-OVA is a replication defective virus, it is possible that this discrepancy is due to lack of active viral replication. Furthermore, we have not probed for the effector status of CD8<sup>+</sup> T cells at 1 dpi during Ad-OVA infection, where we do not see any difference in CD8<sup>+</sup> T cell accumulation in the B6 or Batf3<sup>-/-</sup> livers. Therefore we cannot accurately speculate on the contribution of non-CD103<sup>+</sup> DC APCs on controlling CD8<sup>+</sup> T cell effector functions in the Batf3<sup>-/-</sup> early in infection. However, even though we see no differences in viral load, as assessed by qRT-PCR for Ad-Hexon, it is possible that the effector function of CD8<sup>+</sup> T cells primed by alternative APCs is enhanced in the Batf3<sup>-/-</sup> prior to 3 dpi. This is an intriguing notion, where it has recently been demonstrated that LSEC mediated priming of anti-viral CD8<sup>+</sup> T cells leads to high expression of GrB production via IL-6 cross presentation, albeit with survival limited to less than 18 hpi. It is also worth noting that CD103<sup>+</sup> and CD11b<sup>+</sup> DC subsets express unique TLR profiles, yet we

believe this bears no significance on the CD8<sup>+</sup> T cell effector status, as Ad virus has been demonstrated to activate DCs independently of TLR crosslinking. However, MCMV is highly sensitive to TLR stimulation, possibly accounting for the loss of IFN $\gamma$  by anti-viral CD8<sup>+</sup> T cells in the Batf3<sup>-/-</sup> livers during MCMV-OVA infection. Further investigation is necessary to more fully assess the capacity of hepatic CD103<sup>+</sup> DCs have on controlling CD8<sup>+</sup> T cell effector functions. We propose using a replication-competent Ad virus in the Batf3<sup>-/-</sup> to verify if active Ad production leads to decreased IFN $\gamma$  expression by activated CD8<sup>+</sup> T cells, as seen in the MCMV-OVA model, or if the Ad virus itself is overriding any differences in CD103<sup>+</sup> DC control on CD8<sup>+</sup> T cell function.

We believe that the lack of differences in activated CD8<sup>+</sup> T cell accumulation in the CCR7<sup>-/-</sup> mouse model is compelling evidence for *in situ* priming by liver-resident DCs. We further verified *in situ* priming by CD103<sup>+</sup> DCs by blocking naïve CD8<sup>+</sup> T cells from entering secondary LNs in splenectomized B6 and Batf3<sup>-/-</sup> mice. However, a better way to limit naïve CD8<sup>+</sup> T cells from entering secondary lymphoid sites is to use the LT $\beta$ R blockade model, in which pregnant mice administered anti-LT $\beta$ R birth pups lacking LNs. Using splenectomized and anti-LT $\beta$ R treated B6 and Batf3<sup>-/-</sup> mice would nicely verify that any differences in CD8<sup>+</sup> T cell accumulation are truly liver specific.

Although we attempted to assess the homing status of activated CD8<sup>+</sup> T cells in the Batf3<sup>-/-</sup> by investigating the status of various integrins and chemokine receptors, we were unable to detect any differences in homing potential at the time points analyzed. In addition to possible mediators of liver residency, we probed for CD103<sup>+</sup>CD8<sup>+</sup> T cells, the

common marker demarcating resident-memory (Trm), in the *Batf3*<sup>-/-</sup> during Ad-OVA infection. We were unable to detect CD103 expression on CD8<sup>+</sup> T cells during the first 3 days of infection. We propose investigating CD8<sup>+</sup> T cells at later times to determine if CD103<sup>+</sup> DCs are contributing to the formation of Trm anti-viral CD8<sup>+</sup> T cells, or induction of unique liver-specific homing receptors. These experiments could potentially enhance the significance of liver-resident CD103<sup>+</sup> mediated CD8<sup>+</sup> T cell priming, as it is possible vaccine strategies targeting DCs in the periphery induce poor liver specific homing.

It is also worthwhile to note that without the availability of a genetically modified mouse model specifically deficient in CD11b<sup>+</sup> DCs, it is currently difficult to assess the contribution that hepatic CD11b<sup>+</sup> DCs have on anti-viral CD8<sup>+</sup> T cell priming, accumulation, or effector function. When this mouse model, or other specific CD11b<sup>+</sup> DC depletion technique(s), becomes available in the future, it will be exciting to investigate their individual contribution to anti-viral CD8<sup>+</sup> T cell responses in the liver.

### **Liver-resident Group 1 ILCs**

Our lab recently published a beautifully detailed report on the phenotypic and functional features of liver-resident NK cells in the steady-state. Although the field had yet to establish the unique ILC1 subset in the liver, many of the key findings from that investigation introduced the possibility of hepatic specific NK cells. Most notably it suggested liver-resident NK cells exhibit unique requirements for liver homing, where adoptively transferred hepatic NK cells demonstrated significant preference for returning

to the liver. Indeed, the unique chemokine expression profile by liver-resident ILC1 satisfies our lab's previous findings. Furthermore, the enhanced expression of NKG2A, but limited Ly49 receptors expression by hepatic NK cells is now verified to specifically demarcate the ILC1 subset. Although liver ILC1 have been reported in multiple studies, their functional contribution to the anti-viral responses in the liver have yet to be explored. It is well established that NK cells are able to control DC fates via their ability to both express pro-inflammatory mediators used to activate immature DCs, and suppress DCs via direct killing. Therefore it was of interest to assess the functional contribution of liver-resident ILC1 on controlling hepatic DCs during Ad-OVA infection; where I demonstrate that NKG2A<sup>+</sup>ILC1<sup>+</sup> are inhibited in their ability to produce IFN $\gamma$  required to promote efficient CD103<sup>+</sup> DC activation and subsequent naïve anti-viral CD8<sup>+</sup> T cell priming.

As liver ILC1 have only recently been identified, their localization in the liver is not known. Using fluorescence microscopy I demonstrate that ILC1 preferentially localize near CD103<sup>+</sup> DCs in the marginal zones surrounding the portal triads. Moreover, ILC1 express high levels of CD69, CD44, and GrB, suggesting they are continuously activated and capable of immediate cellular target killing. As I demonstrate liver-resident CD103<sup>+</sup> DCs initiate a robust CD8<sup>+</sup> T cell response during Ad-OVA infection, the balance between immunogenic or tolerogenic responses in the liver may be determined by the outcome of ILC1-DC crosstalk, where CD103<sup>+</sup> DCs have to avoid ILC1 mediated cytotoxicity to promote anti-viral CD8<sup>+</sup> T cell activation. Although, upon group 1 ILC depletion, I demonstrate that liver-resident DCs exhibit dampened accumulation.

Therefore, it is possible that CD103<sup>+</sup> DCs also require ILC1 help to fully activate during viral infections. As ILC1 express high levels of NKG2A in the steady-state, it was of interest to assess the contribution of NKG2A signaling on controlling ILC1 function and subsequent DC activation during Ad-OVA infection.

NKG2A<sup>-/-</sup> infected with Ad-OVA exhibit enhanced adoptively transferred and endogenous anti-viral CD8<sup>+</sup> T cells in the liver. My data suggests that ILC1 signal through NKG2A to dampen IFN $\gamma$  production, where restimulation of NKG2A<sup>-/-</sup> ILC1 with cell targets enhances their ability to express IFN $\gamma$ . I hypothesize that heightened IFN $\gamma$  levels in the NKG2A<sup>-/-</sup> livers is promoting the capacity for CD103<sup>+</sup> DCs to prime naïve CD8<sup>+</sup> T cells during Ad-OVA infection. However, further experiments dissecting the role of IFN $\gamma$  levels on promoting DC activation are required. I propose exploring the requirement of IFN $\gamma$  on DC activation during Ad-OVA by first administering IFN $\gamma$  blocking antibodies in B6 mice prior to infection. If indeed IFN $\gamma$  is necessary for hepatic DC maturation, we should expect to see limited DC accumulation/activation in IFN $\gamma$  blocked mice. These data would suggest attempting the gain of function experiment, where administering exogenous IFN $\gamma$  to B6 mice should enhance DC activation during Ad-OVA infection. It then becomes imperative to determine that indeed the enhanced production of IFN $\gamma$  by NKG2A<sup>-/-</sup> ILC1 is alone contributing to DC activation. Utilizing ILC1 IFN $\gamma$ <sup>-/-</sup> is the ideal approach, however due to the lack of an ILC1 targeted Cre currently voids this strategy. Global IFN $\gamma$ <sup>-/-</sup> mice are known to exhibit multiple phenotypic concerns, including poor NK cell development, and will not help in determining ILC1 specific production of IFN $\gamma$ . However, *in vitro* experiments

investigating ILC1 mediated activation of hepatic DCs could help support my hypothesis, where blocking and/or adding exogenous IFN $\gamma$  in NK-DC cocultures may recapitulate the *in vivo* data. Lastly, assessing the IFN $\gamma$  signaling events in hepatic DCs may support that indeed increased IFN $\gamma$  is contributing to the NKG2A<sup>-/-</sup> DC phenotype. IFN $\gamma$  signals through the IFN $\gamma$ R via STAT1 homodimers to promote IFN $\gamma$  stimulated genes, where both targets should be analyzed in sorted DCs from the Ad-OVA infected B6 and NKG2A<sup>-/-</sup> mice.

There are additional caveats in my interpretation of NKG2A<sup>-/-</sup> data that must be addressed. One point of concern is that the NKG2A<sup>-/-</sup> mouse is on the B6 genetic background, but due to linkage disequilibrium, has retained the natural killer complex (NKC) from the 129/SvJ founder background. The NKC is a genetic region on Chromosome 6 that codes for the majority of NK cell receptors, including Ly49, NKG2A, and CD69. The Ly49 receptor profiles are diverse, including allelic differences, between the B6 and 129 backgrounds. As MHC-I binding Ly49 receptors are known to license NK cells, comparing the NKG2A<sup>-/-</sup> mice to the B6 background does not control for potential licensing differences. However, it is important to note that ILC1 express limited Ly49 receptors suggesting their contribution to ILC1 function may be inconsequential on DC activation in the NKG2A<sup>-/-</sup> livers. Nonetheless, to more carefully control for the NKC differences between the B6 and NKG2A<sup>-/-</sup> mice, further data verifying NKG2A's specific contribution is needed. I propose comparing Ad-OVA infection in the NKG2A<sup>-/-</sup> mice to a B6 mouse expressing the 129 or 129-like NKC.

Another important stipulation in my interpretation of the presented results is that I have not assessed the ability for NKG2A<sup>-/-</sup> group 1 ILCs to lyse cellular targets. NK cells are able to efficiently kill immature DCs during viral-infections. Furthermore, ILC1 express high levels of cytolytic granule proteins, including GrB. It is entirely possible that liver-resident NKG2A<sup>-/-</sup> ILC1 are unable to kill immature CD103<sup>+</sup> DCs. Previous reports have demonstrated that inhibitory NK receptors are important in polarizing lytic-protein containing granules. NKG2A may be required for targeting ILC1 lytic-proteins, where NKG2A<sup>-/-</sup> ILC1 are unable to polarize and degranulate. I propose two experiments to assess the capacity for NKG2A<sup>-/-</sup> ILC1 to kill; *in vitro*, and *in vivo* cytotoxicity assays. Cell sorting ILC1 from B6 and NKG2A<sup>-/-</sup> livers infected with Ad-OVA and setting them against varying concentrations of MHC-I deficient targets, i.e. YAC-1, will help determine if NKG2A<sup>-/-</sup> ILC1 exhibit cell killing differences. Lastly, transferring equal numbers of MHC-I competent RMA and MHC-I deficient RMA-S cells into B6 and NKG2A<sup>-/-</sup> mice will verify any potential killing differences group 1 ILCs may exhibit *in vivo*. If indeed there are intrinsic deficiencies in NKG2A<sup>-/-</sup> mice to kill MHC-I deficient targets, the recovered RMA-S cells will be fewer from the NKG2A<sup>-/-</sup> mice.

In conclusion, the data presented here demonstrate that hepatic CD103<sup>+</sup> DCs are contributing to the liver's ability to mount robust anti-viral CD8<sup>+</sup> T cell responses in an Ad-OVA infection model. It further suggests that hepatic ILC1 are actively suppressing CD103<sup>+</sup> DC activation via inhibited IFN $\gamma$  production mediated by NKG2A signaling. In sum, these data help elucidate not only how the liver suppresses anti-viral immune responses, but how it is able to switch away from an immunosuppressive environment to

a pro-inflammatory tissue required for successful hepatotropic viral clearance. Taken together, these data raises the possibility for an exciting therapeutic approach for developing next generation vaccines, i.e. targeting antigen to hepatic CD103<sup>+</sup> DCs while inhibiting ILC1 NKG2A signaling in order to induce a more robust and sustainable anti-viral CD8<sup>+</sup> T cell response.

## References

1. Klenerman, P., and R. Thimme. 2011. T cell responses in hepatitis C: the good, the bad and the unconventional. *Gut* 61:1226.
2. Claassen, M. A., H. L. Janssen, and A. Boonstra. 2013. Role of T cell immunity in hepatitis C virus infections. *Curr Opin Virol* 3:461.
3. Caetano, J., A. Martinho, A. Paiva, B. Pais, C. Valente, and C. Luxo. 2008. Differences in hepatitis C virus (HCV)-specific CD8 T-cell phenotype during pegylated alpha interferon and ribavirin treatment are related to response to antiviral therapy in patients chronically infected with HCV. *J Virol* 82:7567.
4. Schmidt, J., Blum, H.E., Thimme, R. 2013. T-cell responses in hepatitis B and C virus infection: similarities and differences. *Emerging Microbes and Infections* 2:1.
5. Grakoui, A., N. H. Shoukry, D. J. Woollard, J. H. Han, H. L. Hanson, J. Ghrayeb, K. K. Murthy, C. M. Rice, and C. M. Walker. 2003. HCV persistence and immune evasion in the absence of memory T cell help. *Science* 302:659.
6. Moskophidis, D., F. Lechner, H. Pircher, and R. M. Zinkernagel. 1993. Virus persistence in acutely infected immunocompetent mice by exhaustion of antiviral cytotoxic effector T cells. *Nature* 362:758.
7. Wherry, E. J. 2011. T cell exhaustion. *Nat Immunol* 12:492.
8. Nakamoto, N., D. E. Kaplan, J. Coleclough, Y. Li, M. E. Valiga, M. Kaminski, A. Shaked, K. Olthoff, E. Gostick, D. A. Price, G. J. Freeman, E. J. Wherry, and K. M. Chang. 2008. Functional restoration of HCV-specific CD8 T cells by PD-1 blockade is defined by PD-1 expression and compartmentalization. *Gastroenterology* 134:1927.
9. Golden-Mason, L., B. E. Palmer, N. Kassam, L. Townshend-Bulson, S. Livingston, B. J. McMahon, N. Castelblanco, V. Kuchroo, D. R. Gretch, and H. R. Rosen. 2009. Negative immune regulator Tim-3 is overexpressed on T cells in hepatitis C virus infection and its blockade rescues dysfunctional CD4+ and CD8+ T cells. *J Virol* 83:9122.

10. Berg, R. D. 1995. Bacterial translocation from the gastrointestinal tract. *Trends Microbiol* 3:149.
11. Lumsden, A. B., J. M. Henderson, and M. H. Kutner. 1988. Endotoxin levels measured by a chromogenic assay in portal, hepatic and peripheral venous blood in patients with cirrhosis. *Hepatology* 8:232.
12. Son, G., M. Kremer, and I. N. Hines. 2010. Contribution of gut bacteria to liver pathobiology. *Gastroenterol Res Pract* 2010.
13. Calne, R. Y., R. A. Sells, J. R. Pena, D. R. Davis, P. R. Millard, B. M. Herbertson, R. M. Binns, and D. A. Davies. 1969. Induction of immunological tolerance by porcine liver allografts. *Nature* 223:472.
14. Bishop, G. A., C. Wang, A. F. Sharland, and G. McCaughan. 2002. Spontaneous acceptance of liver transplants in rodents: evidence that liver leucocytes induce recipient T-cell death by neglect. *Immunol Cell Biol* 80:93.
15. Wisse, E., F. Braet, D. Luo, R. De Zanger, D. Jans, E. Crabbe, and A. Vermoesen. 1996. Structure and function of sinusoidal lining cells in the liver. *Toxicol Pathol* 24:100.
16. Crispe, I. N. 2011. Liver antigen-presenting cells. *J Hepatol* 54:357.
17. Oda, M., H. Yokomori, and J. Y. Han. 2003. Regulatory mechanisms of hepatic microcirculation. *Clin Hemorheol Microcirc* 29:167.
18. Bissell, D. M., S. S. Wang, W. R. Jarnagin, and F. J. Roll. 1995. Cell-specific expression of transforming growth factor-beta in rat liver. Evidence for autocrine regulation of hepatocyte proliferation. *J Clin Invest* 96:447.
19. Dolina, J. S., T. J. Braciale, and Y. S. Hahn. 2013. Liver-primed CD8+ T cells suppress antiviral adaptive immunity through galectin-9-independent T-cell immunoglobulin and mucin 3 engagement of high-mobility group box 1 in mice. *Hepatology* 59:1351.
20. Liblau, R. S., R. Tisch, K. Shokat, X. Yang, N. Dumont, C. C. Goodnow, and H. O. McDevitt. 1996. Intravenous injection of soluble antigen induces thymic and peripheral T-cells apoptosis. *Proc Natl Acad Sci U S A* 93:3031.

21. Gutgemann, I., A. M. Fahrner, J. D. Altman, M. M. Davis, and Y. H. Chien. 1998. Induction of rapid T cell activation and tolerance by systemic presentation of an orally administered antigen. *Immunity* 8:667.
22. Srinivasan, M., and K. A. Frauwirth. 2009. Peripheral tolerance in CD8+ T cells. *Cytokine* 46:147.
23. Redmond, W. L., and L. A. Sherman. 2005. Peripheral tolerance of CD8 T lymphocytes. *Immunity* 22:275.
24. Feuerer, M., P. Beckhove, N. Garbi, Y. Mahnke, A. Limmer, M. Hommel, G. J. Hammerling, B. Kyewski, A. Hamann, V. Umansky, and V. Schirmacher. 2003. Bone marrow as a priming site for T-cell responses to blood-borne antigen. *Nat Med* 9:1151.
25. Bertolino, P., D. G. Bowen, G. W. McCaughan, and B. Fazekas de St Groth. 2001. Antigen-specific primary activation of CD8+ T cells within the liver. *J Immunol* 166:5430.
26. Klein, I., and I. N. Crispe. 2006. Complete differentiation of CD8+ T cells activated locally within the transplanted liver. *J Exp Med* 203:437.
27. Rubinstein, D., A. K. Roska, and P. E. Lipsky. 1987. Antigen presentation by liver sinusoidal lining cells after antigen exposure in vivo. *J Immunol* 138:1377.
28. Limmer, A., J. Ohl, C. Kurts, H. G. Ljunggren, Y. Reiss, M. Groettrup, F. Momburg, B. Arnold, and P. A. Knolle. 2000. Efficient presentation of exogenous antigen by liver endothelial cells to CD8+ T cells results in antigen-specific T-cell tolerance. *Nat Med* 6:1348.
29. Limmer, A., J. Ohl, G. Wingender, M. Berg, F. Jungerkes, B. Schumak, D. Djandji, K. Scholz, A. Klevenz, S. Hegenbarth, F. Momburg, G. J. Hammerling, B. Arnold, and P. A. Knolle. 2005. Cross-presentation of oral antigens by liver sinusoidal endothelial cells leads to CD8 T cell tolerance. *Eur J Immunol* 35:2970.
30. Schildberg, F. A., A. Wojtalla, S. V. Siegmund, E. Endl, L. Diehl, Z. Abdullah, C. Kurts, and P. A. Knolle. Murine hepatic stellate cells veto CD8 T cell activation by a CD54-dependent mechanism. *Hepatology* 54:262.

31. von Oppen, N., A. Schurich, S. Hegenbarth, D. Stabenow, R. Tolba, R. Weiskirchen, A. Geerts, W. Kolanus, P. Knolle, and L. Diehl. 2009. Systemic antigen cross-presented by liver sinusoidal endothelial cells induces liver-specific CD8 T-cell retention and tolerization. *Hepatology* 49:1664.
32. Schurich, A., J. P. Bottcher, S. Burgdorf, P. Penzler, S. Hegenbarth, M. Kern, A. Dolf, E. Endl, J. Schultze, E. Wiertz, D. Stabenow, C. Kurts, and P. Knolle. 2009. Distinct kinetics and dynamics of cross-presentation in liver sinusoidal endothelial cells compared to dendritic cells. *Hepatology* 50:909.
33. Kern, M., A. Popov, K. Scholz, B. Schumak, D. Djandji, A. Limmer, D. Eggle, T. Sacher, R. Zawatzky, R. Holtappels, M. J. Reddehase, G. Hartmann, S. Debey-Pascher, L. Diehl, U. Kalinke, U. Koszinowski, J. Schultze, and P. A. Knolle. Virally infected mouse liver endothelial cells trigger CD8+ T-cell immunity. *Gastroenterology* 138:336.
34. Holz, L. E., V. Benseler, D. G. Bowen, P. Bouillet, A. Strasser, L. O'Reilly, W. M. d'Avigdor, A. G. Bishop, G. W. McCaughan, and P. Bertolino. 2008. Intrahepatic murine CD8 T-cell activation associates with a distinct phenotype leading to Bim-dependent death. *Gastroenterology* 135:989.
35. Bottcher, J. P., O. Schanz, C. Garbers, A. Zaremba, S. Hegenbarth, C. Kurts, M. Beyer, J. L. Schultze, W. Kastenmuller, S. Rose-John, and P. A. Knolle. IL-6 trans-signaling-dependent rapid development of cytotoxic CD8+ T cell function. *Cell Rep* 8:1318.
36. Bertolino, P., M. C. Trescol-Biemont, and C. Roubourdin-Combe. 1998. Hepatocytes induce functional activation of naive CD8+ T lymphocytes but fail to promote survival. *Eur J Immunol* 28:221.
37. Benseler, V., A. Warren, M. Vo, L. E. Holz, S. S. Tay, D. G. Le Couteur, E. Breen, A. C. Allison, N. van Rooijen, C. McGuffog, H. J. Schlitt, D. G. Bowen, G. W. McCaughan, and P. Bertolino. 2011. Hepatocyte entry leads to degradation of autoreactive CD8 T cells. *Proc Natl Acad Sci U S A* 108:16735.
38. Winau, F., G. Hegasy, R. Weiskirchen, S. Weber, C. Cassan, P. A. Sieling, R. L. Modlin, R. S. Liblau, A. M. Gressner, and S. H. Kaufmann. 2007. Ito cells are

- liver-resident antigen-presenting cells for activating T cell responses. *Immunity* 26:117.
39. Lechner, F., D. K. Wong, P. R. Dunbar, R. Chapman, R. T. Chung, P. Dohrenwend, G. Robbins, R. Phillips, P. Klenerman, and B. D. Walker. 2000. Analysis of successful immune responses in persons infected with hepatitis C virus. *J Exp Med* 191:1499.
  40. Thimme, R., D. Oldach, K. M. Chang, C. Steiger, S. C. Ray, and F. V. Chisari. 2001. Determinants of viral clearance and persistence during acute hepatitis C virus infection. *J Exp Med* 194:1395.
  41. Shoukry, N. H., A. Grakoui, M. Houghton, D. Y. Chien, J. Ghayeb, K. A. Reimann, and C. M. Walker. 2003. Memory CD8+ T cells are required for protection from persistent hepatitis C virus infection. *J Exp Med* 197:1645.
  42. Steinman, R. M., and Z. A. Cohn. 1973. Identification of a novel cell type in peripheral lymphoid organs of mice. I. Morphology, quantitation, tissue distribution. *J Exp Med* 137:1142.
  43. Shortman, K. 2012. Ralph Steinman and dendritic cells. *Immunol Cell Biol* 90:1.
  44. D'Amico, A., and L. Wu. 2003. The early progenitors of mouse dendritic cells and plasmacytoid predendritic cells are within the bone marrow hemopoietic precursors expressing Flt3. *J Exp Med* 198:293.
  45. Wu, L., A. D'Amico, H. Hochrein, M. O'Keeffe, K. Shortman, and K. Lucas. 2001. Development of thymic and splenic dendritic cell populations from different hemopoietic precursors. *Blood* 98:3376.
  46. Manz, M. G., D. Traver, K. Akashi, M. Merad, T. Miyamoto, E. G. Engleman, and I. L. Weissman. 2001. Dendritic cell development from common myeloid progenitors. *Ann N Y Acad Sci* 938:167.
  47. Karsunky, H., M. Merad, A. Cozzio, I. L. Weissman, and M. G. Manz. 2003. Flt3 ligand regulates dendritic cell development from Flt3+ lymphoid and myeloid-committed progenitors to Flt3+ dendritic cells in vivo. *J Exp Med* 198:305.

48. Traver, D., K. Akashi, M. Manz, M. Merad, T. Miyamoto, E. G. Engleman, and I. L. Weissman. 2000. Development of CD8alpha-positive dendritic cells from a common myeloid progenitor. *Science* 290:2152.
49. Shigematsu, H., B. Reizis, H. Iwasaki, S. Mizuno, D. Hu, D. Traver, P. Leder, N. Sakaguchi, and K. Akashi. 2004. Plasmacytoid dendritic cells activate lymphoid-specific genetic programs irrespective of their cellular origin. *Immunity* 21:43.
50. Fogg, D. K., C. Sibon, C. Miled, S. Jung, P. Aucouturier, D. R. Littman, A. Cumano, and F. Geissmann. 2006. A clonogenic bone marrow progenitor specific for macrophages and dendritic cells. *Science* 311:83.
51. Onai, N., A. Obata-Onai, M. A. Schmid, T. Ohteki, D. Jarrossay, and M. G. Manz. 2007. Identification of clonogenic common Flt3+M-CSFR+ plasmacytoid and conventional dendritic cell progenitors in mouse bone marrow. *Nat Immunol* 8:1207.
52. Naik, S. H., P. Sathe, H. Y. Park, D. Metcalf, A. I. Proietto, A. Dakic, S. Carotta, M. O'Keeffe, M. Bahlo, A. Papenfuss, J. Y. Kwak, L. Wu, and K. Shortman. 2007. Development of plasmacytoid and conventional dendritic cell subtypes from single precursor cells derived in vitro and in vivo. *Nat Immunol* 8:1217.
53. Reizis, B. 2010. Regulation of plasmacytoid dendritic cell development. *Curr Opin Immunol* 22:206.
54. Reizis, B., A. Bunin, H. S. Ghosh, K. L. Lewis, and V. Sisirak. 2011. Plasmacytoid dendritic cells: recent progress and open questions. *Annu Rev Immunol* 29:163.
55. Shortman, K., and W. R. Heath. 2010. The CD8+ dendritic cell subset. *Immunol Rev* 234:18.
56. Helft, J., F. Ginhoux, M. Bogunovic, and M. Merad. 2010. Origin and functional heterogeneity of non-lymphoid tissue dendritic cells in mice. *Immunol Rev* 234:55.
57. del Rio, M. L., G. Bernhardt, J. I. Rodriguez-Barbosa, and R. Forster. 2010. Development and functional specialization of CD103+ dendritic cells. *Immunol Rev* 234:268.

58. Idoyaga, J., N. Suda, K. Suda, C. G. Park, and R. M. Steinman. 2009. Antibody to Langerin/CD207 localizes large numbers of CD8alpha+ dendritic cells to the marginal zone of mouse spleen. *Proc Natl Acad Sci U S A* 106:1524.
59. Qiu, C. H., Y. Miyake, H. Kaise, H. Kitamura, O. Ohara, and M. Tanaka. 2009. Novel subset of CD8{alpha}+ dendritic cells localized in the marginal zone is responsible for tolerance to cell-associated antigens. *J Immunol* 182:4127.
60. Ginhoux, F., K. Liu, J. Helft, M. Bogunovic, M. Greter, D. Hashimoto, J. Price, N. Yin, J. Bromberg, S. A. Lira, E. R. Stanley, M. Nussenzweig, and M. Merad. 2009. The origin and development of nonlymphoid tissue CD103+ DCs. *J Exp Med* 206:3115.
61. Suzuki, S., K. Honma, T. Matsuyama, K. Suzuki, K. Toriyama, I. Akitoyo, K. Yamamoto, T. Suematsu, M. Nakamura, K. Yui, and A. Kumatori. 2004. Critical roles of interferon regulatory factor 4 in CD11bhighCD8alpha- dendritic cell development. *Proc Natl Acad Sci U S A* 101:8981.
62. Ichikawa, E., S. Hida, Y. Omatsu, S. Shimoyama, K. Takahara, S. Miyagawa, K. Inaba, and S. Taki. 2004. Defective development of splenic and epidermal CD4+ dendritic cells in mice deficient for IFN regulatory factor-2. *Proc Natl Acad Sci U S A* 101:3909.
63. Greter, M., J. Helft, A. Chow, D. Hashimoto, A. Mortha, J. Agudo-Cantero, M. Bogunovic, E. L. Gautier, J. Miller, M. Leboeuf, G. Lu, C. Aloman, B. D. Brown, J. W. Pollard, H. Xiong, G. J. Randolph, J. E. Chipuk, P. S. Frenette, and M. Merad. 2012. GM-CSF controls nonlymphoid tissue dendritic cell homeostasis but is dispensable for the differentiation of inflammatory dendritic cells. *Immunity* 36:1031.
64. Kingston, D., M. A. Schmid, N. Onai, A. Obata-Onai, D. Baumjohann, and M. G. Manz. 2009. The concerted action of GM-CSF and Flt3-ligand on in vivo dendritic cell homeostasis. *Blood* 114:835.
65. King, I. L., M. A. Kroenke, and B. M. Segal. 2010. GM-CSF-dependent, CD103+ dermal dendritic cells play a critical role in Th effector cell differentiation after subcutaneous immunization. *J Exp Med* 207:953.

66. Zhan, Y., E. M. Carrington, A. van Nieuwenhuijze, S. Bedoui, S. Seah, Y. Xu, N. Wang, J. D. Mintern, J. A. Villadangos, I. P. Wicks, and A. M. Lew. 2011. GM-CSF increases cross-presentation and CD103 expression by mouse CD8(+) spleen dendritic cells. *Eur J Immunol* 41:2585.
67. McKenna, H. J., K. L. Stocking, R. E. Miller, K. Brasel, T. De Smedt, E. Maraskovsky, C. R. Maliszewski, D. H. Lynch, J. Smith, B. Pulendran, E. R. Roux, M. Teepe, S. D. Lyman, and J. J. Peschon. 2000. Mice lacking flt3 ligand have deficient hematopoiesis affecting hematopoietic progenitor cells, dendritic cells, and natural killer cells. *Blood* 95:3489.
68. Waskow, C., K. Liu, G. Darrasse-Jeze, P. Guermonprez, F. Ginhoux, M. Merad, T. Shengelia, K. Yao, and M. Nussenzweig. 2008. The receptor tyrosine kinase Flt3 is required for dendritic cell development in peripheral lymphoid tissues. *Nat Immunol* 9:676.
69. Lewis, K. L., M. L. Caton, M. Bogunovic, M. Greter, L. T. Grajkowska, D. Ng, A. Klinakis, I. F. Charo, S. Jung, J. L. Gommerman, Ivanov, II, K. Liu, M. Merad, and B. Reizis. Notch2 receptor signaling controls functional differentiation of dendritic cells in the spleen and intestine. *Immunity* 35:780.
70. Wu, Q., Y. Wang, J. Wang, E. O. Hedgeman, J. L. Browning, and Y. X. Fu. 1999. The requirement of membrane lymphotoxin for the presence of dendritic cells in lymphoid tissues. *J Exp Med* 190:629.
71. Kabashima, K., T. A. Banks, K. M. Ansel, T. T. Lu, C. F. Ware, and J. G. Cyster. 2005. Intrinsic lymphotoxin-beta receptor requirement for homeostasis of lymphoid tissue dendritic cells. *Immunity* 22:439.
72. Wang, Y. G., K. D. Kim, J. Wang, P. Yu, and Y. X. Fu. 2005. Stimulating lymphotoxin beta receptor on the dendritic cells is critical for their homeostasis and expansion. *J Immunol* 175:6997.
73. Banchereau, J., and R. M. Steinman. 1998. Dendritic cells and the control of immunity. *Nature* 392:245.
74. Reis e Sousa, C. 2006. Dendritic cells in a mature age. *Nat Rev Immunol* 6:476.
75. Campbell, J. J., G. Haraldsen, J. Pan, J. Rottman, S. Qin, P. Ponath, D. P. Andrew, R. Warnke, N. Ruffing, N. Kassam, L. Wu, and E. C. Butcher. 1999. The

- chemokine receptor CCR4 in vascular recognition by cutaneous but not intestinal memory T cells. *Nature* 400:776.
76. Erdmann, I., E. P. Scheidegger, F. K. Koch, L. Heinzerling, B. Odermatt, G. Burg, J. B. Lowe, and T. M. Kundig. 2002. Fucosyltransferase VII-deficient mice with defective E-, P-, and L-selectin ligands show impaired CD4<sup>+</sup> and CD8<sup>+</sup> T cell migration into the skin, but normal extravasation into visceral organs. *J Immunol* 168:2139.
  77. Hudak, S., M. Hagen, Y. Liu, D. Catron, E. Oldham, L. M. McEvoy, and E. P. Bowman. 2002. Immune surveillance and effector functions of CCR10(+) skin homing T cells. *J Immunol* 169:1189.
  78. Morales, J., B. Homey, A. P. Vicari, S. Hudak, E. Oldham, J. Hedrick, R. Orozco, N. G. Copeland, N. A. Jenkins, L. M. McEvoy, and A. Zlotnik. 1999. CTACK, a skin-associated chemokine that preferentially attracts skin-homing memory T cells. *Proc Natl Acad Sci U S A* 96:14470.
  79. Tietz, W., Y. Allemand, E. Borges, D. von Laer, R. Hallmann, D. Vestweber, and A. Hamann. 1998. CD4<sup>+</sup> T cells migrate into inflamed skin only if they express ligands for E- and P-selectin. *J Immunol* 161:963.
  80. Martin-Fontecha, A., S. Sebastiani, U. E. Hopken, M. Uguccioni, M. Lipp, A. Lanzavecchia, and F. Sallusto. 2003. Regulation of dendritic cell migration to the draining lymph node: impact on T lymphocyte traffic and priming. *J Exp Med* 198:615.
  81. Sallusto, F., P. Schaerli, P. Loetscher, C. Schaniel, D. Lenig, C. R. Mackay, S. Qin, and A. Lanzavecchia. 1998. Rapid and coordinated switch in chemokine receptor expression during dendritic cell maturation. *Eur J Immunol* 28:2760.
  82. Edwards, A. D., S. S. Diebold, E. M. Slack, H. Tomizawa, H. Hemmi, T. Kaisho, S. Akira, and C. Reis e Sousa. 2003. Toll-like receptor expression in murine DC subsets: lack of TLR7 expression by CD8 alpha<sup>+</sup> DC correlates with unresponsiveness to imidazoquinolines. *Eur J Immunol* 33:827.
  83. Davey, G. M., M. Wojtasiak, A. I. Proietto, F. R. Carbone, W. R. Heath, and S. Bedoui. 2010. Cutting edge: priming of CD8 T cell immunity to herpes

- simplex virus type 1 requires cognate TLR3 expression in vivo. *J Immunol* 184:2243.
84. Yarovinsky, F., D. Zhang, J. F. Andersen, G. L. Bannenberg, C. N. Serhan, M. S. Hayden, S. Hieny, F. S. Sutterwala, R. A. Flavell, S. Ghosh, and A. Sher. 2005. TLR11 activation of dendritic cells by a protozoan profilin-like protein. *Science* 308:1626.
  85. Heath, W. R., and F. R. Carbone. 2009. Dendritic cell subsets in primary and secondary T cell responses at body surfaces. *Nat Immunol* 10:1237.
  86. Delamarre, L., M. Pack, H. Chang, I. Mellman, and E. S. Trombetta. 2005. Differential lysosomal proteolysis in antigen-presenting cells determines antigen fate. *Science* 307:1630.
  87. Lennon-Dumenil, A. M., A. H. Bakker, R. Maehr, E. Fiebiger, H. S. Overkleeft, M. Roseblatt, H. L. Ploegh, and C. Lagaudriere-Gesbert. 2002. Analysis of protease activity in live antigen-presenting cells shows regulation of the phagosomal proteolytic contents during dendritic cell activation. *J Exp Med* 196:529.
  88. Kovacsovics-Bankowski, M., and K. L. Rock. 1995. A phagosome-to-cytosol pathway for exogenous antigens presented on MHC class I molecules. *Science* 267:243.
  89. Hochrein, H., K. Shortman, D. Vremec, B. Scott, P. Hertzog, and M. O'Keeffe. 2001. Differential production of IL-12, IFN-alpha, and IFN-gamma by mouse dendritic cell subsets. *J Immunol* 166:5448.
  90. Dudziak, D., A. O. Kamphorst, G. F. Heidkamp, V. R. Buchholz, C. Trumpfheller, S. Yamazaki, C. Cheong, K. Liu, H. W. Lee, C. G. Park, R. M. Steinman, and M. C. Nussenzweig. 2007. Differential antigen processing by dendritic cell subsets in vivo. *Science* 315:107.
  91. Mattei, F., G. Schiavoni, F. Belardelli, and D. F. Tough. 2001. IL-15 is expressed by dendritic cells in response to type I IFN, double-stranded RNA, or lipopolysaccharide and promotes dendritic cell activation. *J Immunol* 167:1179.

92. Kim, T. S., S. A. Gorski, S. Hahn, K. M. Murphy, and T. J. Braciale. 2014. Distinct dendritic cell subsets dictate the fate decision between effector and memory CD8(+) T cell differentiation by a CD24-dependent mechanism. *Immunity* 40:400.
93. Jomantaite, I., N. Dikopoulos, A. Kroger, F. Leithauser, H. Hauser, R. Schirmbeck, and J. Reimann. 2004. Hepatic dendritic cell subsets in the mouse. *Eur J Immunol* 34:355.
94. Pillarisetty, V. G., A. B. Shah, G. Miller, J. I. Bleier, and R. P. DeMatteo. 2004. Liver dendritic cells are less immunogenic than spleen dendritic cells because of differences in subtype composition. *J Immunol* 172:1009.
95. Krueger, P. D., T. S. Kim, S. S. Sung, T. J. Braciale, and Y. S. Hahn. 2015. Liver-Resident CD103+ Dendritic Cells Prime Antiviral CD8+ T Cells In Situ. *J Immunol*.
96. Gao, X., S. Wang, Y. Fan, H. Bai, J. Yang, and X. Yang. CD8+ DC, but Not CD8(-)DC, isolated from BCG-infected mice reduces pathological reactions induced by mycobacterial challenge infection. *PLoS One* 5:e9281.
97. Sana, G., C. Lombard, O. Vosters, N. Jazouli, F. Andre, X. Stephenne, F. Smets, M. Najimi, and E. M. Sokal. Adult human hepatocytes promote CD4(+) T-cell hyporesponsiveness via interleukin-10-producing allogeneic dendritic cells. *Cell Transplant* 23:1127.
98. Tokita, D., T. L. Sumpter, G. Raimondi, A. F. Zahorchak, Z. Wang, A. Nakao, G. V. Mazariegos, M. Abe, and A. W. Thomson. 2008. Poor allostimulatory function of liver plasmacytoid DC is associated with pro-apoptotic activity, dependent on regulatory T cells. *J Hepatol* 49:1008.
99. Kingham, T. P., U. I. Chaudhry, G. Plitas, S. C. Katz, J. Raab, and R. P. DeMatteo. 2007. Murine liver plasmacytoid dendritic cells become potent immunostimulatory cells after Flt-3 ligand expansion. *Hepatology* 45:445.
100. Kudo, S., K. Matsuno, T. Ezaki, and M. Ogawa. 1997. A novel migration pathway for rat dendritic cells from the blood: hepatic sinusoids-lymph translocation. *J Exp Med* 185:777.

101. Zheng, M., J. Yu, and Z. Tian. 2012. Characterization of the liver-draining lymph nodes in mice and their role in mounting regional immunity to HBV. *Cell Mol Immunol* 10:143.
102. Barbier, L., S. S. Tay, C. McGuffog, J. A. Triccas, G. W. McCaughan, D. G. Bowen, and P. Bertolino. 2012. Two lymph nodes draining the mouse liver are the preferential site of DC migration and T cell activation. *J Hepatol* 57:352.
103. Abe, M., A. F. Zahorchak, B. L. Colvin, and A. W. Thomson. 2004. Migratory responses of murine hepatic myeloid, lymphoid-related, and plasmacytoid dendritic cells to CC chemokines. *Transplantation* 78:762.
104. Drakes, M. L., A. F. Zahorchak, T. Takayama, L. Lu, and A. W. Thomson. 2000. Chemokine and chemokine receptor expression by liver-derived dendritic cells: MIP-1alpha production is induced by bacterial lipopolysaccharide and interaction with allogeneic T cells. *Transpl Immunol* 8:17.
105. Yu, B., H. Ueta, Y. Kitazawa, T. Tanaka, K. Adachi, H. Kimura, M. Morita, Y. Sawanobori, H. X. Qian, T. Kodama, and K. Matsuno. 2012. Two immunogenic passenger dendritic cell subsets in the rat liver have distinct trafficking patterns and radiosensitivities. *Hepatology* 56:1532.
106. Tay, S. S., Y. C. Wong, B. Roediger, F. Sierro, B. Lu, D. M. McDonald, C. M. McGuffog, N. J. Meyer, I. E. Alexander, I. A. Parish, W. R. Heath, W. Weninger, G. A. Bishop, J. R. Gamble, G. W. McCaughan, P. Bertolino, and D. G. Bowen. 2014. Intrahepatic activation of naive CD4+ T cells by liver-resident phagocytic cells. *J Immunol* 193:2087.
107. Kanto, T., N. Hayashi, T. Takehara, T. Tatsumi, N. Kuzushita, A. Ito, Y. Sasaki, A. Kasahara, and M. Hori. 1999. Impaired allostimulatory capacity of peripheral blood dendritic cells recovered from hepatitis C virus-infected individuals. *J Immunol* 162:5584.
108. Galle, M. B., R. M. DeFranco, D. Kerjaschki, R. G. Romanelli, P. Montalto, P. Gentilini, M. Pinzani, and P. Romagnoli. 2001. Ordered array of dendritic cells and CD8+ lymphocytes in portal infiltrates in chronic hepatitis C. *Histopathology* 39:373.

109. Auffermann-Gretzinger, S., E. B. Keefe, and S. Levy. 2001. Impaired dendritic cell maturation in patients with chronic, but not resolved, hepatitis C virus infection. *Blood* 97:3171.
110. Miyagi, T., T. Tatsumi, T. Takehara, T. Kanto, N. Kuzushita, Y. Sugimoto, M. Jinushi, A. Kasahara, Y. Sasaki, M. Hori, and N. Hayashi. 2003. Impaired expression of proteasome subunits and human leukocyte antigens class I in human colon cancer cells. *J Gastroenterol Hepatol* 18:32.
111. Kwekkeboom, J., P. P. Boor, E. Sen, J. G. Kusters, H. A. Drexhage, E. C. de Jong, H. W. Tilanus, J. N. Ijzermans, and H. J. Metselaar. 2005. Human liver myeloid dendritic cells mature in vivo into effector DC with a poor allogeneic T-cell stimulatory capacity. *Transplant Proc* 37:15.
112. Abe, M., S. M. Akbar, N. Horiike, and M. Onji. 2003. Inability of liver dendritic cells from mouse with experimental hepatitis to process and present specific antigens. *Hepatol Res* 26:61.
113. McKenzie, A. N., H. Spits, and G. Eberl. 2014. Innate lymphoid cells in inflammation and immunity. *Immunity* 41:366.
114. Cella, M., H. Miller, and C. Song. 2014. Beyond NK cells: the expanding universe of innate lymphoid cells. *Front Immunol* 5:282.
115. Diefenbach, A., M. Colonna, and S. Koyasu. 2014. Development, differentiation, and diversity of innate lymphoid cells. *Immunity* 41:354.
116. Yu, X., Y. Wang, M. Deng, Y. Li, K. A. Ruhn, C. C. Zhang, and L. V. Hooper. 2014. The basic leucine zipper transcription factor NFIL3 directs the development of a common innate lymphoid cell precursor. *Elife* 3.
117. Robinette, M. L., A. Fuchs, V. S. Cortez, J. S. Lee, Y. Wang, S. K. Durum, S. Gilfillan, and M. Colonna. 2015. Transcriptional programs define molecular characteristics of innate lymphoid cell classes and subsets. *Nat Immunol* 16:306.
118. Sojka, D. K., B. Plougastel-Douglas, L. Yang, M. A. Pak-Wittel, M. N. Artyomov, Y. Ivanova, C. Zhong, J. M. Chase, P. B. Rothman, J. Yu, J. K. Riley, J. Zhu, Z. Tian, and W. M. Yokoyama. 2014. Tissue-resident natural killer (NK) cells are cell

- lineages distinct from thymic and conventional splenic NK cells. *Elife* 3:e01659.
119. Klose, C. S., M. Flach, L. Mohle, L. Rogell, T. Hoyler, K. Ebert, C. Fabiunke, D. Pfeifer, V. Sexl, D. Fonseca-Pereira, R. G. Domingues, H. Veiga-Fernandes, S. J. Arnold, M. Busslinger, I. R. Dunay, Y. Tanriver, and A. Diefenbach. 2014. Differentiation of type 1 ILCs from a common progenitor to all helper-like innate lymphoid cell lineages. *Cell* 157:340.
  120. Daussy, C., F. Faure, K. Mayol, S. Viel, G. Gasteiger, E. Charrier, J. Bienvenu, T. Henry, E. Debien, U. A. Hasan, J. Marvel, K. Yoh, S. Takahashi, I. Prinz, S. de Bernard, L. Buffat, and T. Walzer. 2014. T-bet and Eomes instruct the development of two distinct natural killer cell lineages in the liver and in the bone marrow. *J Exp Med* 211:563.
  121. Seillet, C., N. D. Huntington, P. Gangatirkar, E. Axelsson, M. Minnich, H. J. Brady, M. Busslinger, M. J. Smyth, G. T. Belz, and S. Carotta. 2014. Differential requirement for Nfil3 during NK cell development. *J Immunol* 192:2667.
  122. Crotta, S., A. Gkioka, V. Male, J. H. Duarte, S. Davidson, I. Nisoli, H. J. Brady, and A. Wack. 2014. The transcription factor E4BP4 is not required for extramedullary pathways of NK cell development. *J Immunol* 192:2677.
  123. Gonzaga, R., P. Matzinger, and A. Perez-Diez. 2011. Resident peritoneal NK cells. *J Immunol* 187:6235.
  124. Gordon, S. M., J. Chaix, L. J. Rupp, J. Wu, S. Madera, J. C. Sun, T. Lindsten, and S. L. Reiner. 2012. The transcription factors T-bet and Eomes control key checkpoints of natural killer cell maturation. *Immunity* 36:55.
  125. Di Santo, J. P. 2006. Natural killer cell developmental pathways: a question of balance. *Annu Rev Immunol* 24:257.
  126. Rosmaraki, E. E., I. Douagi, C. Roth, F. Colucci, A. Cumano, and J. P. Di Santo. 2001. Identification of committed NK cell progenitors in adult murine bone marrow. *Eur J Immunol* 31:1900.
  127. Hayakawa, Y., and M. J. Smyth. 2006. CD27 dissects mature NK cells into two subsets with distinct responsiveness and migratory capacity. *J Immunol* 176:1517.

128. Robbins, S. H., K. B. Nguyen, N. Takahashi, T. Mikayama, C. A. Biron, and L. Brossay. 2002. Cutting edge: inhibitory functions of the killer cell lectin-like receptor G1 molecule during the activation of mouse NK cells. *J Immunol* 168:2585.
129. Lassen, M. G., J. R. Lukens, J. S. Dolina, M. G. Brown, and Y. S. Hahn. Intrahepatic IL-10 maintains NKG2A+Ly49- liver NK cells in a functionally hyporesponsive state. *J Immunol* 184:2693.
130. Peng, H., X. Jiang, Y. Chen, D. K. Sojka, H. Wei, X. Gao, R. Sun, W. M. Yokoyama, and Z. Tian. 2013. Liver-resident NK cells confer adaptive immunity in skin-contact inflammation. *J Clin Invest* 123:1444.
131. Huntington, N. D., C. A. Vosshenrich, and J. P. Di Santo. 2007. Developmental pathways that generate natural-killer-cell diversity in mice and humans. *Nat Rev Immunol* 7:703.
132. Fernandez, N. C., E. Treiner, R. E. Vance, A. M. Jamieson, S. Lemieux, and D. H. Raulet. 2005. A subset of natural killer cells achieves self-tolerance without expressing inhibitory receptors specific for self-MHC molecules. *Blood* 105:4416.
133. Kim, S., J. Poursine-Laurent, S. M. Truscott, L. Lybarger, Y. J. Song, L. Yang, A. R. French, J. B. Sunwoo, S. Lemieux, T. H. Hansen, and W. M. Yokoyama. 2005. Licensing of natural killer cells by host major histocompatibility complex class I molecules. *Nature* 436:709.
134. Raulet, D. H., and R. E. Vance. 2006. Self-tolerance of natural killer cells. *Nat Rev Immunol* 6:520.
135. Yokoyama, W. M., and S. Kim. 2006. Licensing of natural killer cells by self-major histocompatibility complex class I. *Immunol Rev* 214:143.
136. Brodin, P., K. Karre, and P. Hoglund. 2009. NK cell education: not an on-off switch but a tunable rheostat. *Trends Immunol* 30:143.
137. Brown, M. G., and A. A. Scalzo. 2008. NK gene complex dynamics and selection for NK cell receptors. *Semin Immunol* 20:361.

138. Hanke, T., H. Takizawa, and D. H. Raulet. 2001. MHC-dependent shaping of the inhibitory Ly49 receptor repertoire on NK cells: evidence for a regulated sequential model. *Eur J Immunol* 31:3370.
139. Biassoni, R. 2009. Human natural killer receptors, co-receptors, and their ligands. *Curr Protoc Immunol Chapter 14:Unit 14 10*.
140. Long, E. O. 2008. Negative signaling by inhibitory receptors: the NK cell paradigm. *Immunol Rev* 224:70.
141. Gunturi, A., R. E. Berg, and J. Forman. 2004. The role of CD94/NKG2 in innate and adaptive immunity. *Immunol Res* 30:29.
142. Lanier, L. L. 2005. NK cell recognition. *Annu Rev Immunol* 23:225.
143. Le Drean, E., F. Vely, L. Olcese, A. Cambiaggi, S. Guia, G. Krystal, N. Gervois, A. Moretta, F. Jotereau, and E. Vivier. 1998. Inhibition of antigen-induced T cell response and antibody-induced NK cell cytotoxicity by NKG2A: association of NKG2A with SHP-1 and SHP-2 protein-tyrosine phosphatases. *Eur J Immunol* 28:264.
144. Vance, R. E., A. M. Jamieson, and D. H. Raulet. 1999. Recognition of the class Ib molecule Qa-1(b) by putative activating receptors CD94/NKG2C and CD94/NKG2E on mouse natural killer cells. *J Exp Med* 190:1801.
145. Vance, R. E., J. R. Kraft, J. D. Altman, P. E. Jensen, and D. H. Raulet. 1998. Mouse CD94/NKG2A is a natural killer cell receptor for the nonclassical major histocompatibility complex (MHC) class I molecule Qa-1(b). *J Exp Med* 188:1841.
146. Castriconi, R., C. Cantoni, M. Della Chiesa, M. Vitale, E. Marcenaro, R. Conte, R. Biassoni, C. Bottino, L. Moretta, and A. Moretta. 2003. Transforming growth factor beta 1 inhibits expression of Nkp30 and NKG2D receptors: consequences for the NK-mediated killing of dendritic cells. *Proc Natl Acad Sci U S A* 100:4120.
147. Sutherland, C. L., N. J. Chalupny, K. Schooley, T. VandenBos, M. Kubin, and D. Cosman. 2002. UL16-binding proteins, novel MHC class I-related proteins, bind to NKG2D and activate multiple signaling pathways in primary NK cells. *J Immunol* 168:671.

148. Roberts, A. I., L. Lee, E. Schwarz, V. Groh, T. Spies, E. C. Ebert, and B. Jabri. 2001. NKG2D receptors induced by IL-15 costimulate CD28-negative effector CTL in the tissue microenvironment. *J Immunol* 167:5527.
149. Jinushi, M., T. Takehara, T. Tatsumi, S. Yamaguchi, R. Sakamori, N. Hiramatsu, T. Kanto, K. Ohkawa, and N. Hayashi. 2007. Natural killer cell and hepatic cell interaction via NKG2A leads to dendritic cell-mediated induction of CD4 CD25 T cells with PD-1-dependent regulatory activities. *Immunology* 120:73.
150. Filtjens, J., S. Taveirne, A. Van Acker, E. Van Ammel, M. Vanhees, T. Kerre, T. Taghon, B. Vandekerckhove, J. Plum, and G. Leclercq. Abundant stage-dependent Ly49E expression by liver NK cells is not essential for their differentiation and function. *J Leukoc Biol* 93:699.
151. Wu, J., Y. Song, A. B. Bakker, S. Bauer, T. Spies, L. L. Lanier, and J. H. Phillips. 1999. An activating immunoreceptor complex formed by NKG2D and DAP10. *Science* 285:730.
152. Bauer, S., V. Groh, J. Wu, A. Steinle, J. H. Phillips, L. L. Lanier, and T. Spies. 1999. Activation of NK cells and T cells by NKG2D, a receptor for stress-inducible MICA. *Science* 285:727.
153. Mandelboim, O., and A. Porgador. 2001. NKp46. *Int J Biochem Cell Biol* 33:1147.
154. Walzer, T., M. Blery, J. Chaix, N. Fuseri, L. Chasson, S. H. Robbins, S. Jaeger, P. Andre, L. Gauthier, L. Daniel, K. Chemin, Y. Morel, M. Dalod, J. Imbert, M. Pierres, A. Moretta, F. Romagne, and E. Vivier. 2007. Identification, activation, and selective in vivo ablation of mouse NK cells via NKp46. *Proc Natl Acad Sci USA* 104:3384.
155. Moretta, L., C. Bottino, D. Pende, R. Castriconi, M. C. Mingari, and A. Moretta. 2006. Surface NK receptors and their ligands on tumor cells. *Semin Immunol* 18:151.
156. Mor-Vaknin, N., A. Punturieri, K. Sitwala, and D. M. Markovitz. 2003. Vimentin is secreted by activated macrophages. *Nat Cell Biol* 5:59.
157. Garg, A., P. F. Barnes, A. Porgador, S. Roy, S. Wu, J. S. Nanda, D. E. Griffith, W. M. Girard, N. Rawal, S. Shetty, and R. Vankayalapati. 2006. Vimentin

- expressed on Mycobacterium tuberculosis-infected human monocytes is involved in binding to the NKp46 receptor. *J Immunol* 177:6192.
158. Chong, W. P., J. Zhou, H. K. Law, W. Tu, and Y. L. Lau. Natural killer cells become tolerogenic after interaction with apoptotic cells. *Eur J Immunol* 40:1718.
  159. Bloushtain, N., U. Qimron, A. Bar-Ilan, O. Hershkovitz, R. Gazit, E. Fima, M. Korc, I. Vlodayevsky, N. V. Bovin, and A. Porgador. 2004. Membrane-associated heparan sulfate proteoglycans are involved in the recognition of cellular targets by NKp30 and NKp46. *J Immunol* 173:2392.
  160. Hamerman, J. A., K. Ogasawara, and L. L. Lanier. 2005. NK cells in innate immunity. *Curr Opin Immunol* 17:29.
  161. Takeda, K., Y. Hayakawa, M. J. Smyth, N. Kayagaki, N. Yamaguchi, S. Kakuta, Y. Iwakura, H. Yagita, and K. Okumura. 2001. Involvement of tumor necrosis factor-related apoptosis-inducing ligand in surveillance of tumor metastasis by liver natural killer cells. *Nat Med* 7:94.
  162. Martin-Fontecha, A., L. L. Thomsen, S. Brett, C. Gerard, M. Lipp, A. Lanzavecchia, and F. Sallusto. 2004. Induced recruitment of NK cells to lymph nodes provides IFN-gamma for T(H)1 priming. *Nat Immunol* 5:1260.
  163. Friedman, S. L. 2008. Mechanisms of hepatic fibrogenesis. *Gastroenterology* 134:1655.
  164. Mehal, W., and A. Imaeda. Cell death and fibrogenesis. *Semin Liver Dis* 30:226.
  165. Niki, T., M. Pekny, K. Hellemans, P. D. Bleser, K. V. Berg, F. Vaeyens, E. Quartier, F. Schuit, and A. Geerts. 1999. Class VI intermediate filament protein nestin is induced during activation of rat hepatic stellate cells. *Hepatology* 29:520.
  166. Andrews, D. M., A. A. Scalzo, W. M. Yokoyama, M. J. Smyth, and M. A. Degli-Esposti. 2003. Functional interactions between dendritic cells and NK cells during viral infection. *Nat Immunol* 4:175.
  167. Lu, L., K. Ikizawa, D. Hu, M. B. Werneck, K. W. Wucherpfennig, and H. Cantor. 2007. Regulation of activated CD4+ T cells by NK cells via the Qa-1-NKG2A inhibitory pathway. *Immunity* 26:593.

168. Moretta, A. 2002. Natural killer cells and dendritic cells: rendezvous in abused tissues. *Nat Rev Immunol* 2:957.
169. Roy, S., P. F. Barnes, A. Garg, S. Wu, D. Cosman, and R. Vankayalapati. 2008. NK cells lyse T regulatory cells that expand in response to an intracellular pathogen. *J Immunol* 180:1729.
170. Jinushi, M., T. Takehara, T. Tatsumi, T. Kanto, T. Miyagi, T. Suzuki, Y. Kanazawa, N. Hiramatsu, and N. Hayashi. 2004. Negative regulation of NK cell activities by inhibitory receptor CD94/NKG2A leads to altered NK cell-induced modulation of dendritic cell functions in chronic hepatitis C virus infection. *J Immunol* 173:6072.
171. Nattermann, J., G. Feldmann, G. Ahlenstiel, B. Langhans, T. Sauerbruch, and U. Spengler. 2006. Surface expression and cytolytic function of natural killer cell receptors is altered in chronic hepatitis C. *Gut* 55:869.
172. Golden-Mason, L., and H. R. Rosen. 2006. Natural killer cells: primary target for hepatitis C virus immune evasion strategies? *Liver Transpl* 12:363.
173. De Maria, A., M. Fogli, S. Mazza, M. Basso, A. Picciotto, P. Costa, S. Congia, M. C. Mingari, and L. Moretta. 2007. Increased natural cytotoxicity receptor expression and relevant IL-10 production in NK cells from chronically infected viremic HCV patients. *Eur J Immunol* 37:445.
174. Golden-Mason, L., A. L. Cox, J. A. Randall, L. Cheng, and H. R. Rosen. Increased natural killer cell cytotoxicity and NKp30 expression protects against hepatitis C virus infection in high-risk individuals and inhibits replication in vitro. *Hepatology*.
175. Rowe, W. P., R. J. Huebner, L. K. Gilmore, R. H. Parrott, and T. G. Ward. 1953. Isolation of a cytopathogenic agent from human adenoids undergoing spontaneous degeneration in tissue culture. *Proc Soc Exp Biol Med* 84:570.
176. Hilleman, M. R., and J. H. Werner. 1954. Recovery of new agent from patients with acute respiratory illness. *Proc Soc Exp Biol Med* 85:183.
177. Chen, R. F., and C. Y. Lee. Adenoviruses types, cell receptors and local innate cytokines in adenovirus infection. *Int Rev Immunol* 33:45.

178. Davison, A. J., M. Benko, and B. Harrach. 2003. Genetic content and evolution of adenoviruses. *J Gen Virol* 84:2895.
179. Morris, S. J., G. E. Scott, and K. N. Leppard. 2010. Adenovirus late-phase infection is controlled by a novel L4 promoter. *J Virol* 84:7096.
180. Cupelli, K., and T. Stehle. 2011. Viral attachment strategies: the many faces of adenoviruses. *Curr Opin Virol* 1:84.
181. Di Paolo, N. C., and D. M. Shayakhmetov. 2009. Adenovirus de-targeting from the liver. *Curr Opin Mol Ther* 11:523.
182. Di Paolo, N. C., N. van Rooijen, and D. M. Shayakhmetov. 2009. Redundant and synergistic mechanisms control the sequestration of blood-born adenovirus in the liver. *Mol Ther* 17:675.
183. Kalyuzhniy, O., N. C. Di Paolo, M. Silvestry, S. E. Hofherr, M. A. Barry, P. L. Stewart, and D. M. Shayakhmetov. 2008. Adenovirus serotype 5 hexon is critical for virus infection of hepatocytes in vivo. *Proc Natl Acad Sci U S A* 105:5483.
184. Waddington, S. N., J. H. McVey, D. Bhella, A. L. Parker, K. Barker, H. Atoda, R. Pink, S. M. Buckley, J. A. Greig, L. Denby, J. Custers, T. Morita, I. M. Francischetti, R. Q. Monteiro, D. H. Barouch, N. van Rooijen, C. Napoli, M. J. Havenga, S. A. Nicklin, and A. H. Baker. 2008. Adenovirus serotype 5 hexon mediates liver gene transfer. *Cell* 132:397.
185. Barnes, E., A. Folgori, S. Capone, L. Swadling, S. Aston, A. Kurioka, J. Meyer, R. Huddart, K. Smith, R. Townsend, A. Brown, R. Antrobus, V. Ammendola, M. Naddeo, G. O'Hara, C. Willberg, A. Harrison, F. Grazioli, M. L. Esposito, L. Siani, C. Traboni, Y. Oo, D. Adams, A. Hill, S. Colloca, A. Nicosia, R. Cortese, and P. Klenerman. 2012. Novel adenovirus-based vaccines induce broad and sustained T cell responses to HCV in man. *Sci Transl Med* 4:115ra1.
186. Kelly, C., L. Swadling, A. Brown, S. Capone, A. Folgori, M. Salio, P. Klenerman, and E. Barnes. 2014. Cross-reactivity of hepatitis C virus-specific vaccine induced T cells at immunodominant epitopes. *Eur J Immunol*.
187. Glasgow, J. N., M. Everts, and D. T. Curiel. 2006. Transductional targeting of adenovirus vectors for gene therapy. *Cancer Gene Ther* 13:830.

188. Jenne, C. N., and P. Kubes. 2013. Immune surveillance by the liver. *Nat Immunol* 14:996.
189. Horner, S. M. 2014. Activation and evasion of antiviral innate immunity by hepatitis C virus. *J Mol Biol* 426:1198.
190. Nieto, K., and A. Salvetti. 2014. AAV Vectors Vaccines Against Infectious Diseases. *Front Immunol* 5:5.
191. Zhang, N., and M. J. Bevan. 2011. CD8(+) T cells: foot soldiers of the immune system. *Immunity* 35:161.
192. Welten, S. P., C. J. Melief, and R. Arens. 2013. The distinct role of T cell costimulation in antiviral immunity. *Curr Opin Virol* 3:475.
193. Bousso, P., and E. Robey. 2003. Dynamics of CD8+ T cell priming by dendritic cells in intact lymph nodes. *Nat Immunol* 4:579.
194. Desmet, V. J. 1991. Immunopathology of chronic viral hepatitis. *Hepatology* 38:14.
195. Butz, E. A., and M. J. Bevan. 1998. Massive expansion of antigen-specific CD8+ T cells during an acute virus infection. *Immunity* 8:167.
196. Villadangos, J. A., and P. Schnorrer. 2007. Intrinsic and cooperative antigen-presenting functions of dendritic-cell subsets in vivo. *Nat Rev Immunol* 7:543.
197. Trombetta, E. S., and I. Mellman. 2005. Cell biology of antigen processing in vitro and in vivo. *Annu Rev Immunol* 23:975.
198. Mandraju, R., S. Murray, J. Forman, and C. Pasare. 2014. Differential ability of surface and endosomal TLRs to induce CD8 T cell responses in vivo. *J Immunol* 192:4303.
199. Iwasaki, A., and R. Medzhitov. 2004. Toll-like receptor control of the adaptive immune responses. *Nat Immunol* 5:987.
200. Zhu, Q., C. Egelston, A. Vivekanandhan, S. Uematsu, S. Akira, D. M. Klinman, I. M. Belyakov, and J. A. Berzofsky. 2008. Toll-like receptor ligands synergize through distinct dendritic cell pathways to induce T cell responses: implications for vaccines. *Proc Natl Acad Sci U S A* 105:16260.
201. Nielsen, K. N., M. A. Steffensen, J. P. Christensen, and A. R. Thomsen. 2014. Priming of CD8 T cells by adenoviral vectors is critically dependent on B7

- and dendritic cells but only partially dependent on CD28 ligation on CD8 T cells. *J Immunol* 193:1223.
202. Belz, G. T., C. M. Smith, D. Eichner, K. Shortman, G. Karupiah, F. R. Carbone, and W. R. Heath. 2004. Cutting edge: conventional CD8 alpha+ dendritic cells are generally involved in priming CTL immunity to viruses. *J Immunol* 172:1996.
  203. Martin-Fontecha, A., A. Lanzavecchia, and F. Sallusto. 2009. Dendritic cell migration to peripheral lymph nodes. *Handb Exp Pharmacol*:31.
  204. den Haan, J. M., S. M. Lehar, and M. J. Bevan. 2000. CD8(+) but not CD8(-) dendritic cells cross-prime cytotoxic T cells in vivo. *J Exp Med* 192:1685.
  205. Bedoui, S., P. G. Whitney, J. Waithman, L. Eidsmo, L. Wakim, I. Caminschi, R. S. Allan, M. Wojtasiak, K. Shortman, F. R. Carbone, A. G. Brooks, and W. R. Heath. 2009. Cross-presentation of viral and self antigens by skin-derived CD103+ dendritic cells. *Nat Immunol* 10:488.
  206. Edelson, B. T., W. Kc, R. Juang, M. Kohyama, L. A. Benoit, P. A. Klekotka, C. Moon, J. C. Albring, W. Ise, D. G. Michael, D. Bhattacharya, T. S. Stappenbeck, M. J. Holtzman, S. S. Sung, T. L. Murphy, K. Hildner, and K. M. Murphy. 2010. Peripheral CD103+ dendritic cells form a unified subset developmentally related to CD8alpha+ conventional dendritic cells. *J Exp Med* 207:823.
  207. Schuldt, N. J., and A. Amalfitano. 2012. Malaria vaccines: focus on adenovirus based vectors. *Vaccine* 30:5191.
  208. Witmer-Pack, M. D., M. T. Crowley, K. Inaba, and R. M. Steinman. 1993. Macrophages, but not dendritic cells, accumulate colloidal carbon following administration in situ. *J Cell Sci* 105 ( Pt 4):965.
  209. Prickett, T. C., J. L. McKenzie, and D. N. Hart. 1988. Characterization of interstitial dendritic cells in human liver. *Transplantation* 46:754.
  210. Sumpter, T. L., and A. W. Thomson. 2011. The STATus of PD-L1 (B7-H1) on tolerogenic APCs. *Eur J Immunol* 41:286.
  211. Lukens, J. R., J. S. Dolina, T. S. Kim, R. S. Tacke, and Y. S. Hahn. 2009. Liver is able to activate naive CD8+ T cells with dysfunctional anti-viral activity in the murine system. *PLoS One* 4:e7619.

212. Forster, R., A. Schubel, D. Breitfeld, E. Kremmer, I. Renner-Muller, E. Wolf, and M. Lipp. 1999. CCR7 coordinates the primary immune response by establishing functional microenvironments in secondary lymphoid organs. *Cell* 99:23.
213. Kim, T. S., and T. J. Braciale. 2009. Respiratory dendritic cell subsets differ in their capacity to support the induction of virus-specific cytotoxic CD8<sup>+</sup> T cell responses. *PLoS One* 4:e4204.
214. Lukens, J. R., M. W. Cruise, M. G. Lassen, and Y. S. Hahn. 2008. Blockade of PD-1/B7-H1 interaction restores effector CD8<sup>+</sup> T cell responses in a hepatitis C virus core murine model. *J Immunol* 180:4875.
215. Goldszmid, R. S., P. Caspar, A. Rivollier, S. White, A. Dzutsev, S. Hieny, B. Kelsall, G. Trinchieri, and A. Sher. NK cell-derived interferon-gamma orchestrates cellular dynamics and the differentiation of monocytes into dendritic cells at the site of infection. *Immunity* 36:1047.
216. Borrego, F., M. J. Robertson, J. Ritz, J. Pena, and R. Solana. 1999. CD69 is a stimulatory receptor for natural killer cell and its cytotoxic effect is blocked by CD94 inhibitory receptor. *Immunology* 97:159.
217. Wu, X., Y. Chen, R. Sun, H. Wei, and Z. Tian. Impairment of hepatic NK cell development in IFN-gamma deficient mice. *Cytokine* 60:616.
218. Keppel, M. P., N. Saucier, A. Y. Mah, T. P. Vogel, and M. A. Cooper. Activation-Specific Metabolic Requirements for NK Cell IFN-gamma Production. *J Immunol* 194:1954.
219. Xu, H. C., M. Grusdat, A. A. Pandyra, R. Polz, J. Huang, P. Sharma, R. Deenen, K. Kohrer, R. Rahbar, A. Diefenbach, K. Gibbert, M. Lohning, L. Hocker, Z. Waibler, D. Haussinger, T. W. Mak, P. S. Ohashi, K. S. Lang, and P. A. Lang. Type I interferon protects antiviral CD8<sup>+</sup> T cells from NK cell cytotoxicity. *Immunity* 40:949.
220. Crouse, J., G. Bedenikovic, M. Wiesel, M. Ibberson, I. Xenarios, D. Von Laer, U. Kalinke, E. Vivier, S. Jonjic, and A. Oxenius. Type I interferons protect T cells against NK cell attack mediated by the activating receptor NCR1. *Immunity* 40:961.

221. Masilamani, M., C. Nguyen, J. Kabat, F. Borrego, and J. E. Coligan. 2006. CD94/NKG2A inhibits NK cell activation by disrupting the actin network at the immunological synapse. *J Immunol* 177:3590.
222. Das, A., and E. O. Long. Lytic granule polarization, rather than degranulation, is the preferred target of inhibitory receptors in NK cells. *J Immunol* 185:4698.
223. Jenkins, M. R., J. A. Rudd-Schmidt, J. A. Lopez, K. M. Ramsbottom, S. I. Mannering, D. M. Andrews, I. Voskoboinik, and J. A. Trapani. Failed CTL/NK cell killing and cytokine hypersecretion are directly linked through prolonged synapse time. *J Exp Med*.
224. Cooper, M. A., T. A. Fehniger, A. Fuchs, M. Colonna, and M. A. Caligiuri. 2004. NK cell and DC interactions. *Trends Immunol* 25:47.
225. Nakayama, M., K. Takeda, M. Kawano, T. Takai, N. Ishii, and K. Ogasawara. Natural killer (NK)-dendritic cell interactions generate MHC class II-dressed NK cells that regulate CD4<sup>+</sup> T cells. *Proc Natl Acad Sci U S A* 108:18360.
226. Schenkel, J. M., K. A. Fraser, L. K. Beura, K. E. Pauken, V. Vezyts, and D. Masopust. T cell memory. Resident memory CD8 T cells trigger protective innate and adaptive immune responses. *Science* 346:98.
227. Balmer, M. L., E. Slack, A. de Gottardi, M. A. Lawson, S. Hapfelmeier, L. Miele, A. Grieco, H. Van Vlierberghe, R. Fahrner, N. Patuto, C. Bernsmeier, F. Ronchi, M. Wyss, D. Stroka, N. Dickgreber, M. H. Heim, K. D. McCoy, and A. J. Macpherson. The liver may act as a firewall mediating mutualism between the host and its gut commensal microbiota. *Sci Transl Med* 6:237ra66.